AD-A097 416 OHIO STATE UNIV COLUMBUS ELECTROSCIENCE LAB F/G 20/14
NUMERICAL ELECTROMAGNETIC CODE (NEC)-BASIC SCATTERING CODE. PAR--ETC(U)
SEP 79 R J MARHEFKA, W D BURNSIDE N00123-76-C-1371
UNCLASSIFIED ESL-784508-18 NL

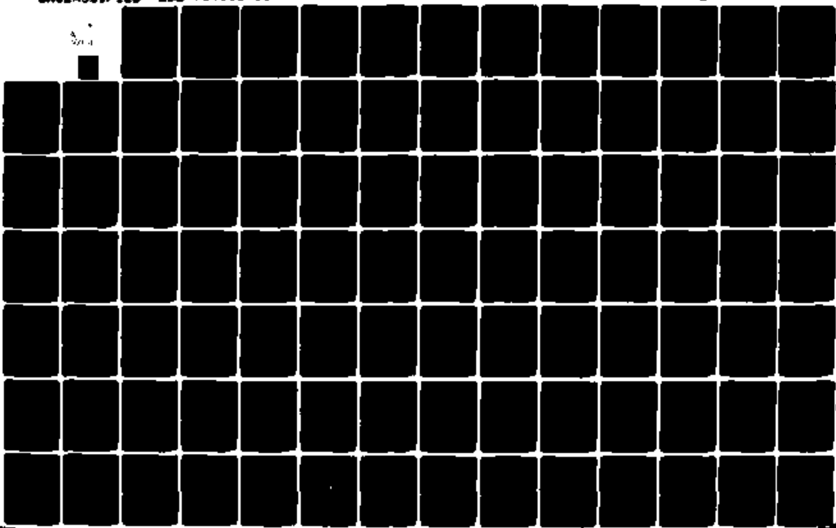

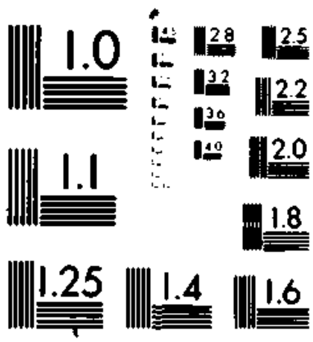

MICROCOPY RESOLUTION TEST CHART
NATIONAL BUREAU OF STANDARDS 1963 A

4

LEVEL IV

OSU

NUMERICAL ELECTROMAGNETIC CODE (NEC) - BASIC SCATTERING CODE
PART I: USER'S MANUAL

The Ohio State University

R. J. Marhefka and W. D. Burnside

AD A097416

The Ohio State University

ElectroScience Laboratory

Department of Electrical Engineering
Columbus, Ohio 43212

Technical Report 784508-18

September 1979

Contract N00123-76-C-1371

Naval Regional Procurement Office
Long Beach, California 90822

Approved for public release;
distribution unlimited.

NOTICES

When Government drawings, specifications, or other data are used for any purpose other than in connection with a definitely related Government procurement operation, the United States Government thereby incurs no responsibility nor any obligation whatsoever, and the fact that the Government may have formulated, furnished, or in any way supplied the said drawings, specifications, or other data, is not to be regarded by implication or otherwise as in any manner licensing the holder or any other person or corporation, or conveying any rights or permission to manufacture, use, or sell any patented invention that may in any way be related thereto.

SECURITY CLASSIFICATION OF THIS PAGE (When Data Entered)

REPORT DOCUMENTATION PAGE

READ INSTRUCTIONS BEFORE COMPLETING FORM

1. REPORT NUMBER	
2. GOVT ACCESSION NO.	AD-A097416
3. RECIPIENT'S CATALOG NUMBER	
4. TITLE (and Subtitle)	NUMERICAL ELECTROMAGNETIC CODE (NEC) - BASIC SCATTERING CODE. PART I. USER'S MANUAL.
5. TYPE OF REPORT & PERIOD COVERED	Technical Report
6. PERFORMING ORG. REPORT NUMBER	ESL-784508-18
7. AUTHOR(s)	R. J. Marhefka [redacted] W. D. Burnside
8. CONTRACT OR GRANT NUMBER(s)	N00123-76-C-1371
9. PERFORMING ORGANIZATION NAME AND ADDRESS	The Ohio State University ElectroScience Laboratory, Department of Electrical Engineering Columbus, Ohio 43212
10. PROGRAM ELEMENT, PROJECT, TASK AREA & WORK UNIT NUMBERS	Project N00953/6/009121
11. CONTROLLING OFFICE NAME AND ADDRESS	Naval Regional Procurement Office Long Beach, California 90822
12. REPORT DATE	September 1979
13. NUMBER OF PAGES	131
14. MONITORING AGENCY NAME & ADDRESS (if different from Controlling Office)	
15. SECURITY CLASS. (of this report)	Unclassified
15a. DECLASSIFICATION/DOWNGRADING SCHEDULE	

16. DISTRIBUTION STATEMENT (of this Report)

17. DISTRIBUTION STATEMENT (of the abstract entered in Block 20, if different from Report)

18. SUPPLEMENTARY NOTES

19. KEY WORDS (Continue on reverse side if necessary and identify by block number)

Geometrical Theory of Diffraction
Uniform asymptotic solutions
Plate models
Cylinder model
Far field pattern
Computer code

20. ABSTRACT (Continue on reverse side if necessary and identify by block number)

The Numerical Electromagnetic Code - Basic Scattering Code is a user-oriented computed code for the analysis of the far field patterns of antennas in the presence of perfectly conducting metal structures at UHF and above. The analysis is based on uniform asymptotic techniques formulated in terms of the Geometrical Theory of Diffraction (GTD). Complicated structures can be simulated by arbitrarily oriented flat plates, an infinite ground plane, and a finite elliptic cylinder.

DD FORM 1 JAN 73 1473 EDITION OF 1 NOV 65 IS OBSOLETE

4

SECURITY CLASSIFICATION OF THIS PAGE (When Data Entered)

20.

A wide range of practical problems can be simulated using these shapes. For example, flat plates can be used to model the superstructure of a ship, the body of a truck, or the wings and stores of an aircraft. The finite elliptic cylinder can be used to model a mast or smoke stack of a ship, or the fuselage and engines of an aircraft.

This document is designed to give an overall view of the operation of the computer code, to instruct a user in how to model structures, and to show the validity of the code by comparing various computed results against measured data whenever available. It, also, describes in detail the input and output data for the code. This information should be sufficient for most user's to learn how to effectively operate the code.

CONTENTS

CHAPTER I
INTRODUCTION

The Numerical Electromagnetic Code - Basic Scattering Code is a user-oriented computer code for the analysis of the far field patterns of antennas in the presence of perfectly conducting metal structures at UHF and above. Complicated structures can be simulated by arbitrarily oriented flat plates, an infinite ground plane, and a finite elliptic cylinder. This type of analysis has been used very successfully in the past to model aircraft shapes [1,2,3]. The present solution has been extended to include a wide range of problems. For example, flat plates can be used to model the superstructure of a ship, the body of a truck, or the wings and stores of an aircraft. The finite elliptic cylinder can be used to model a mast or smoke stack of a ship, or the fuselage and engines of an aircraft.

The analysis is based on uniform asymptotic techniques formulated in terms of the Geometrical Theory of Diffraction (GTD) [4,5,6]. The GTD approach is ideal for a general high frequency study of antennas in a complex environment in that only the most basic structural features of an otherwise very complicated structure need to be modeled. This is because ray optical techniques are used to determine components of the field incident on and diffracted by the various sttuctures. Components of the diffracted fields are found using the GTD solutions in terms of the individual rays which are summed with the geometrical optics terms in the far field. The rays from a given scatterer tend to interact with other structures causing various higher-order terms. In this way one can trace out the various possible combinations of rays that interact between scatterers and determine and include only the dominant terms. Thus, one need only be concerned with the important scattering components and neglect all other higher-order terms. This method leads to accurate and efficient computer codes that can be systematically written and tested. Complex problems can be built up from simpler problems in manageable pieces.

The limitations associated with the computer code result from the basic nature of the analyses. The solution is derived using the GTD which is a high frequency approach. In terms of the scattering from plate structures this means that each plate should have edges at least a wavelength long. In terms of the cylinder structure its major and minor radii and length should be a wavelength in extent. In addition, each antenna element should be at least a wavelength from all edges and the curved surface. In many cases, the wavelength limit can be reduced to a quarter wavelength for engineering purposes.

Modeling small structures and antennas can be better accomplished using an integral equation solution such as NEC-Moment Methods[7]. The Basic Scattering Code has been interfaced with the Moment Method code so that the capabilities of both methods can be used to the fullest. For example, the Moment Method code can be used to analyze the currents and impedance of an antenna. The magnitude and phase of the current weights can then be used in the Basic Scattering Code to predict the far field patterns of the antennas in arbitrary pattern cuts.

There are two documents describing the NEC-Basic Scattering Code. The present document in known as Part I. Part II is a Code Manual[8] that describes the FORTRAN coding in detail. The Code Manual, first, gives background on practical aspects of the GTD. Several examples are shown to illustrate how the various GTD fields superimpose to give a total solution. Next, a particular GTD term is discussed in more detail to show the general concepts involved throughout the code. An overview on how the code is organized is discussed along with a description of the various coordinate systems involved, how a general subroutine is organized, and how the various subroutines are interrelated. The Code Manual also contains for each subroutine: (1) a statement of purpose, (2) an illustration showing the geometry involved, (3) a brief narrative on the method used, (4) a flow diagram, (5) a dictionary of major variables, and (6) a listing of the code. Finally, it defines the common blocks and lists the system library functions used by the code. The information in the Code Manual will be of primary interest to someone attempting to modify the code. It will also be helpful when the code is being implemented on a computer system on which the coding may not be compatible.

This document is designed to give an overall view of the operation of the computer code, to instruct a user in how to use it to model structures, and to show the validity of the code by comparing various computed results against measured data whenever available. Chapter II describes an overall view of the organization of the code. A detailed description of the input command words and their associated input parameters is given in Chapter III. How to apply the capabilites of this input data to a practical structure is briefly discussed in Chapter IV. This includes a clarification of the subtle points of interpreting the input data. The representation of the output is discussed in Chapter V. Various sample problems are presented in Chapter VI to illustrate the operation, versatility, and validity of the code. Most users of the code should find that the User's Manual is sufficient to learn how to effectively operate the code.

CHAPTER II

PRINCIPLES OF OPERATION

The NEC-Basic Scattering Code is designed to be a user oriented computer code. The necessary data to describe a problem can be input and the resulting answers can be obtained with a minimum amount of knowledge by the user on how the code operates. As with most codes, however, it is necessary to have at least a basic knowledge of the key points in order to be able to intelligently use it and interpret its results. This section is designed to give just a brief description of the code for this purpose. The Code Manual, which is the second part of the Basic Scattering Code documentation, gives more in depth information about the FORTRAN coding. Thus, this information will not be repeated here.

The NEC-Basic Scattering Code is constructed in a systematic way, such that the various operations of the code are set up in modular sections. The flow diagram shown below illustrates the major divisions of the main program. The first part of the main program is the input section where the geometry of the problem is described. The method used to input data into the computer code is based on a command word system. Details of the available commands and the ways to use them are given in the next chapter.

Once the necessary information to describe a problem is input into the code, the program analyzes the data and puts it into the correct form so that the electric fields can be calculated. This includes normalizing the geometry to wavelengths, organizing the data into the optimum coordinate system for computations, and defining the fixed geometry bounds for a given source. Of course, all of these operations and the ones to follow are done opaque to the user.

FLOW DIAGRAM OF THE MAIN PROGRAM

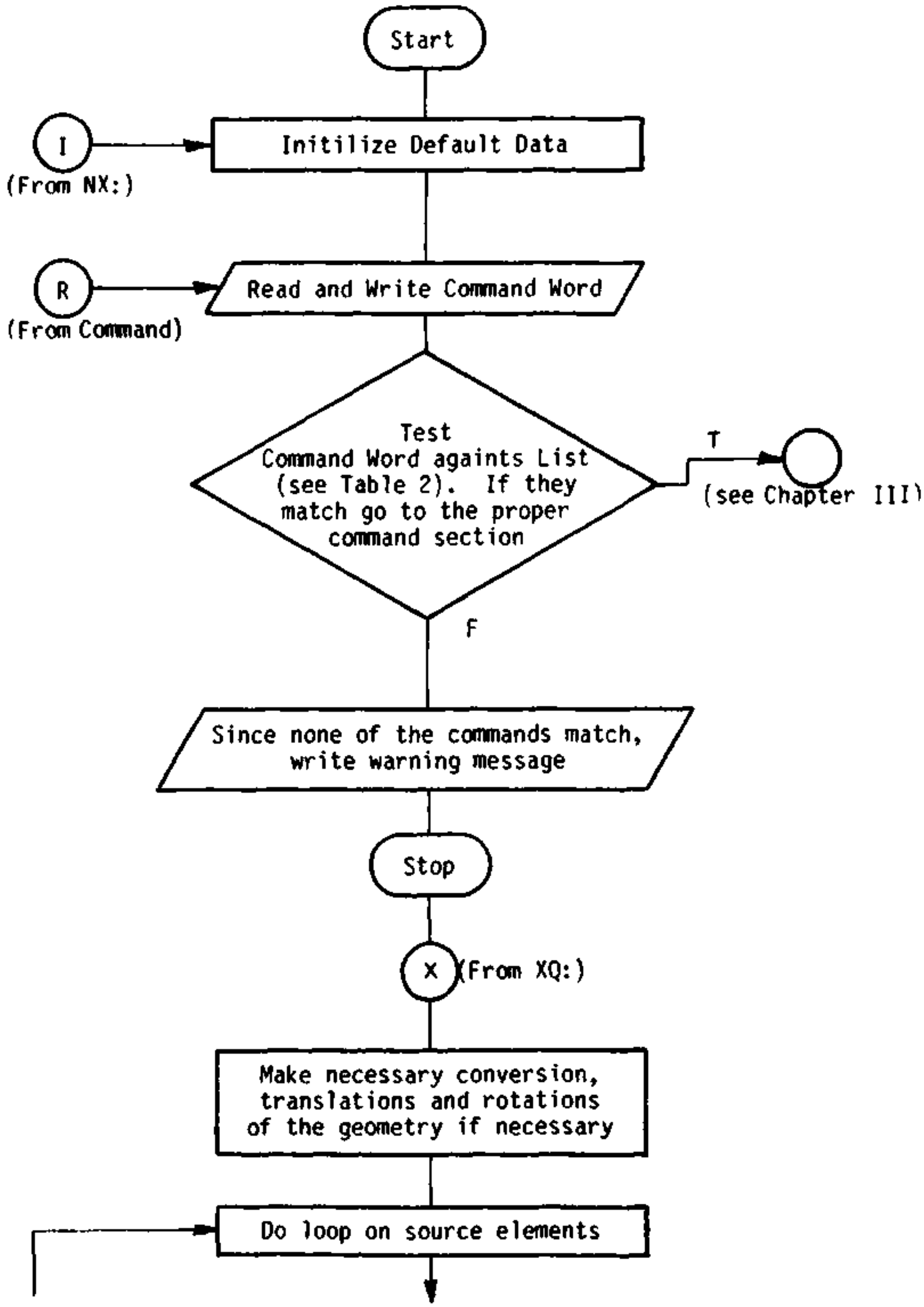

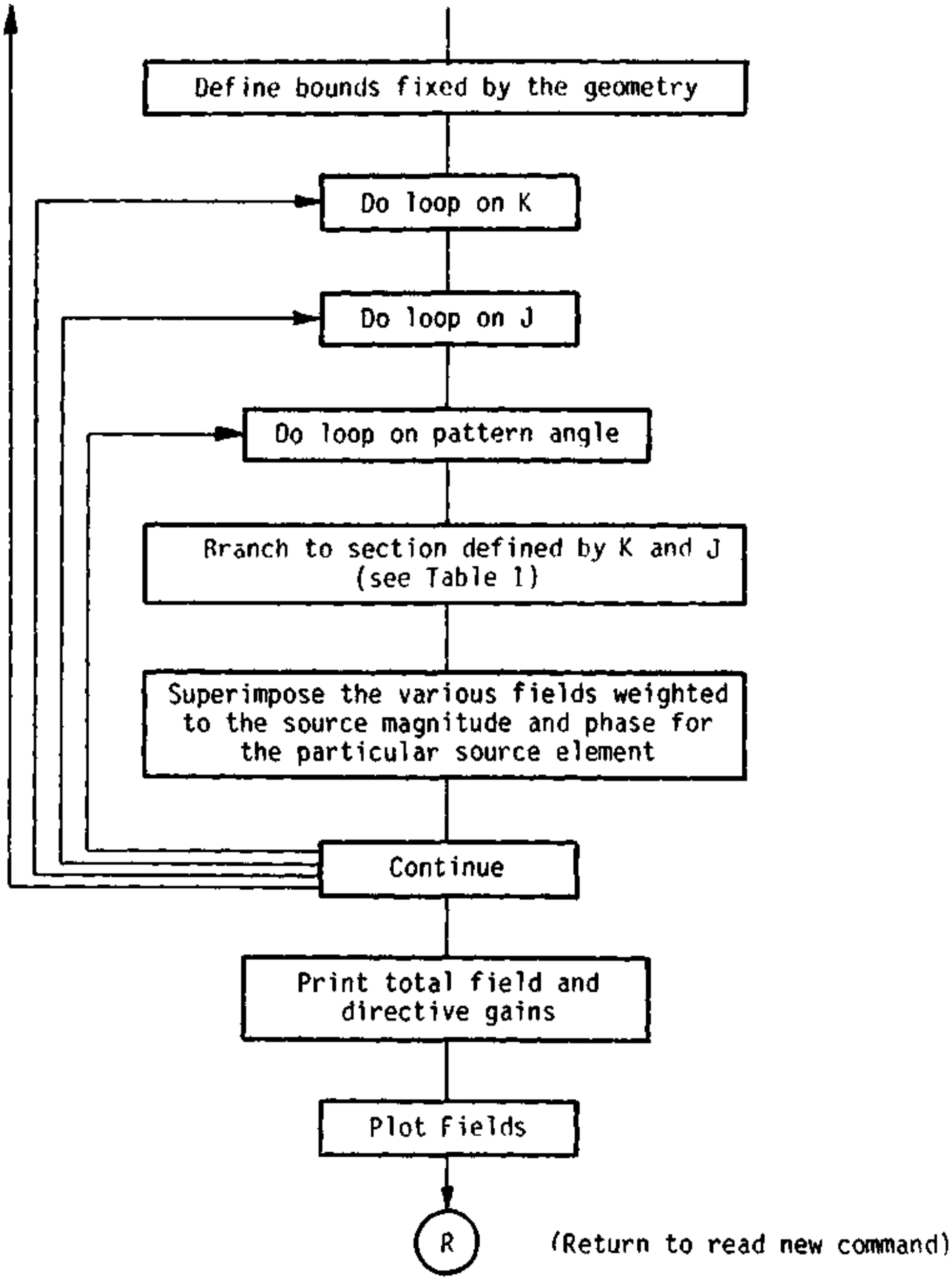

Define bounds fixed by the geometry
Do loop on K
Do loop on J
Do loop on pattern angle
Branch to section defined by K and J (see Table 1)
Superimpose the various fields weighted to the source magnitude and phase for the particular source element
Continue
Print total field and directive gains
Plot Fields
R
(Return to read new command)

Table 1

List of Field Subroutines

Plate Field Subroutines K=1

J=1	INCFLD -	direct field
J=2	REFPLA -	field reflected from a plate
J=3	RPLRPL -	field doubly reflected by plates
J=4	DIFPLT -	field diffracted by a plate
J=5	RPLDPL -	field reflected by a plate then diffracted by a plate
J=6	DPLRPL -	field diffracted by a plate then reflected by a plate

Cylinder Field Subroutines K=2

J=1	SCTCYL -	field scattered by a cylinder
J=2	REFCAP -	field reflected by an end cap
J=3	ENDIF -	field diffracted by an end cap rim

Plate-Cylinder Interaction Field Subroutines K=3

J=1	RPLSCL -	field reflected by a plate then scattered by a cylinder
J=2	SCLRPL -	field scattered by a cylinder then reflected by a plate
J=3	RCLDPL -	field reflected by a cylinder then diffracted by a plate
J=4	DPLRCL -	field diffracted by a plate then reflected by a cylinder.

The scattering code then computes the electric fields for each individual source in succession. Each GTD scattered field type is broken up into a separate subroutine. As can be seen from the flow chart, the code is structured so that all of one type of scattered field is computed at one time for the complete pattern cut so that the amount of core swapping is minimized thereby reducing overlaying and increasing efficiency. This also is an important feature that allows the code to be used on small computers that are not large enough to accept the entire code at one time. The code can be broken into smaller overlay segments which will individually fit in the machine. The results are, then, superimposed in the main program as the various segments are executed.

The field computation part of the code is divided into three large sections (the K=1,2,3 loop). The first section (K=1) contains the major scattered fields associated with the individual flat plates and the interactions between the different plates. These include the direct field. the singly reflected fields, doubly reflected fields, the singly diffracted fields, the reflected-diffracted fields, and the diffracted-reflected fields. The diffracted fields include the normal diffracted fields as well as slope diffraction, a newly developed heuristic corner diffracted field and slope-corner diffracted field. The double diffracted fields are not included at present, but a warning is provided wherever this field component might be important. This is usually only a small angular section of space. This field may be included later whenever time and effort permit. The second section (K=2) contains the major scattered fields associated with the finite elliptic cylinder. This includes the direct field, if not already computed in the plate section, the reflected field the transition field, the deep shadow fields, the reflected field from the end caps, and the diffracted field from the end cap rims. The diffracted field from the end cap rim is not at present corrected in the pseudo caustic regions. This is where three diffraction points on the rim coalesce into one. This is only important in small angular regions in space and is not deemed appropriate to be included at the present time. An equivalent current method could be used for this small region but it is rather time consuming to use for the benefits derived from it for such a general code. The third section (K=3) contains the major scattered fields associated with the interactions between the plates and cylinder. This includes, at present, the fields reflected from the plates then reflected or diffracted from the cylinder, the fields reflected from the cylinder then reflected from the plates, the fields reflected from the cylinder then diffracted from the plates, and the fields diffracted from the plates then reflected from the cylinder. These terms have been found to be sufficient for engineering purposes when analyzing most structures.

The subroutines for each of the scattered field components are all structured in the same basic way. First, the ray path is traced backward from the chosen observation direction to a particular scatterer and subsequently to the source using either the laws of reflection or diffraction. Each ray path, assuming one is possible, is then checked to see if it is shadowed by any structure along the complete ray path. If it is shadowed the field is not computed and the code proceeds to the next scatterer or observation direction. If the path is not interrupted the scattered field is computed using the appropriate GTD solutions. The fields are then superimposed in the main program. This shadowing process is often speeded up by making various decisions based on bounds associated with the geometry of the structure. This type of knowledge is used wherever possible.

The shadowing of rays is a very important part of the scattering code. It is obvious that this approach should lead to various discontinuities in the resulting pattern. However, the GTD diffraction coefficients are designed to smooth out the discontinuities in the fields such that a continuous field is obtained. When a scattered field is not included in the result, therefore, the lack of its presence is apparent. This can be used to advantage in analyzing complicated problems. Obviously in a complex problem not all the possible scattered fields can be included. In the GTD scattering code the importance of the neglected terms are determined by the size of the so-called gliches or jumps in the pattern trace. If the gliches are small no additional terms are needed for a good engineering solution. If the gliches are large if may be necessary to include more terms in the solution. In any case the user has a gauge with which he can examine the accuracy of the results and is not falsely led into believing a result is correct when in fact there could be an error. The examples in Chapter VI illustrate these points and confirm the validity of the solution.

The source presently considered in the computer code is an electric or magnetic radiator with a cosine distribution in one dimension and either a zero width or a uniform distribution in the other. It has arbitrary length and width, arbitrary magnitude and phase, and arbitrary orientation. The source distribution is given as follows

dipole source: $$\left.\begin{matrix} I(z_p) \\ K(z_p) \end{matrix}\right\} = \left\{\begin{matrix} I_m \\ K_m \end{matrix}\right\} \cos\left(\frac{\pi z_p}{HS}\right), \quad x_p=0,\ y_p=0,\ \frac{-HS}{2} \le z_p \le \frac{HS}{2}$$

aperture source: $$\left.\begin{matrix} J(z_p,x_p) \\ M(z_p,x_p) \end{matrix}\right\} = \left\{\begin{matrix} J_m \\ M_m \end{matrix}\right\} \cos\left(\frac{\pi z_p}{HS}\right), \quad y_p=0,\ \frac{-HAWS}{2} \le x_p \le \frac{HAWS}{2},$$

$$\frac{-HS}{2} \le z_p \le \frac{HS}{2}$$

where the x_p dimension is oriented in the THOX and PHOX direction and the z_p dimension is oriented in the THOZ and PHOZ direction, as illustrated in Figure 5. The far-zone electric field is given by

$$\bar{E}(\theta_p,\phi_p) = \bar{E}_o F_z(\theta_p) F_x(\theta_p,\phi_p) \frac{e^{-jkr'}}{r'}$$

where for an electric source

$$\bar{E}_o = \begin{cases} \hat{\theta}_p \dfrac{j\eta}{\pi} I_m HS, & \text{dipole source} \\ \hat{\theta}_p \dfrac{j\eta}{\pi} J_m HS\ HAWS, & \text{aperture source,} \end{cases}$$

and for a magnetic source,

$$\bar{E}_o = \begin{cases} -\hat{\phi}_p \frac{j}{\pi} HS, & \text{dipole source} \\ -\hat{\phi}_p \frac{j}{\pi} M_m \, HS \, HAWS, & \text{aperture source,} \end{cases}$$

and where

$$F_z(\theta_p) = \frac{\sin\theta_p \cos(\pi HS \cos\theta_p)}{(1-4HS^2 \cos^2\theta_p)}$$

$$F_x(\theta_p,\phi_p) = \begin{cases} 1 & \text{, dipole source} \\ \dfrac{\sin(\pi \, HAWS \sin\theta_p \cos\phi_p)}{HAWS \sin\theta_p \cos\phi_p} & \text{, aperture source.} \end{cases}$$

Any arbitrary antenna can be simulated by superposition of the elements by making the length HS small ($HS \approx 0.1\lambda$) and HAWS=0, spacing the elements less than a quarter wavelength, and then weighting their magnitudes and phases to simulate the current distribution of the desired antenna[9]. Since the radiation pattern is relatively insensitive to the current distribution this method works very well. This current distribution information can be obtained using the NEC-Moment Method Code. Using that approach the field from an individual element in the moment method interface section, assuming HS is small, is given by

$$E_{\theta'} = \frac{j\eta_o HS \, I_m}{2\lambda} \sin\theta' \frac{e^{-jkr'}}{r'} \; .$$

This shows consistent resultant fields between the Moment Method and Basic Scattering Codes. It should be emphasized that the time required to calculate a radiation pattern increases by a factor N where N is the number of elemental radiators specified.

Even though the present code is based on the above source model it can be easily changed by modifying the SOURCE subroutine and the SOURCP subroutine, which contains the derivative of the pattern for the slope diffracted fields. This information is given in more detail in the Code Manual.

The brief discussion of the operation of the scattering code given above should help the user get a feel for the overall code so he might better understand the codes capabilities and interpret its results. The code is designed, however, so that the general user can run the code without knowing all the details of its operation. Yet, he must become familiar with the input/output details which will be discussed in the next three chapters.

CHAPTER III

DEFINITION OF INPUT DATA

The method used to input data into the computer code is presently based on a command word system. This is especially convenient when more than one problem is to be analyzed during a computer run. The code stores the previous input data such that one need only input that data which needs to be changed from the previous execution. Also, there is a default list of data so for any given problem the amount of data that needs to be input has been shortened. The command word options presently available are listed in Table 2.

Table 2
Input Command Options

Command	Description	Page
AM:	NEC or AMP Input	44
CE:	Last or Only Comment Card	15
CG:	Cylinder Geometry Input	36
CM:	Comment Card	15
EN:	End of Execution	57
FR:	Frequency	24
GP:	Infinite Ground Plane	35
LP:	Line Printer Listing of Results	54
NC:	No Cylinder	51
NG:	No Ground Plane	50
NP:	Next Set of Plates	49
NS:	Next Set of Sources	52
NX:	Next Problem	53
PD:	Pattern Data Desired	25
PG:	Plate Geometry Input	32
PP:	Pen Plot Results	55
PR:	Power Radiated Input	48
RG:	Far Field Range Input	28
RT:	Translate and/or Rotate Coordinates	29
SG:	Source Geometry Input	39
TO:	Test Data Generation Options	17
UN:	Units of Input	21
US:	Units of HS and HAWS in SG:	22
XQ:	Execute Program	56

In this system, all linear dimensions may be specified in either meters, inches, or feet and all angular dimensions are in degrees. All the dimensions are eventually referred to a fixed cartesian coordinate system used as a common reference for the source and scattering structures. There is, however, a geometry definition coordinate system that may be defined using the "RT:" command. This command enables the user to rotate and translate the coordinate system to be used to input any selected data set into the best coordinate system for that particular geometry. Once the "RT:" command is used all the input following the command will be in that rotated and translated coordinate system until the "RT:" command is called again. See below for more details. There is also a separate coordinate system that can be used to define a pattern coordinate system. This is discussed in more detail below in terms of the "PD:" command.

It is felt that the maximum usefulness of the computer code can be achieved using it on an interactive computer system. As a consequence, all input data are defined in free format such that the operator need only put commas between the various inputs. This allows the user on an interactive terminal to avoid the problems associated with typing in the field length associated with a fixed format. This method also is useful on batch processing computers. Note that all read statements are made on unit #5, i.e., READ (5,*), where the "*" symbol refers to free format. Other machines, however, may have different symbols representing free format.

In all the following discussions associated with logical variables a "T" will imply true, and an "F" will imply false. The complete words true and false need not be input since most compilers just consider the first character in determining the state of the logical variable.

The following list defines in detail each command word and the variables associated with them. Chapter VI will give specific examples using this input method.

A. Commands CM: and CE:

These commands enable the user to place comment cards in the input and output data in order to help identify the computer runs for present and future reference.

1. READ: (IR(I), I=1,24)

a) IR(I): This is an integer dimensioned array used to store the command word and comments. Each card should have CM: or CE: on them followed by an alphanumeric string of characters. The CM: command implies that there will be another comment card following it. The last comment card must have the CE: command on it. If there is only one comment card the CE: command must be used.

Note: It is possible to place comments to the right of all the command words, if desired.

FLOW DIAGRAM FOR CE:

FLOW DIAGRAM FOR CM:

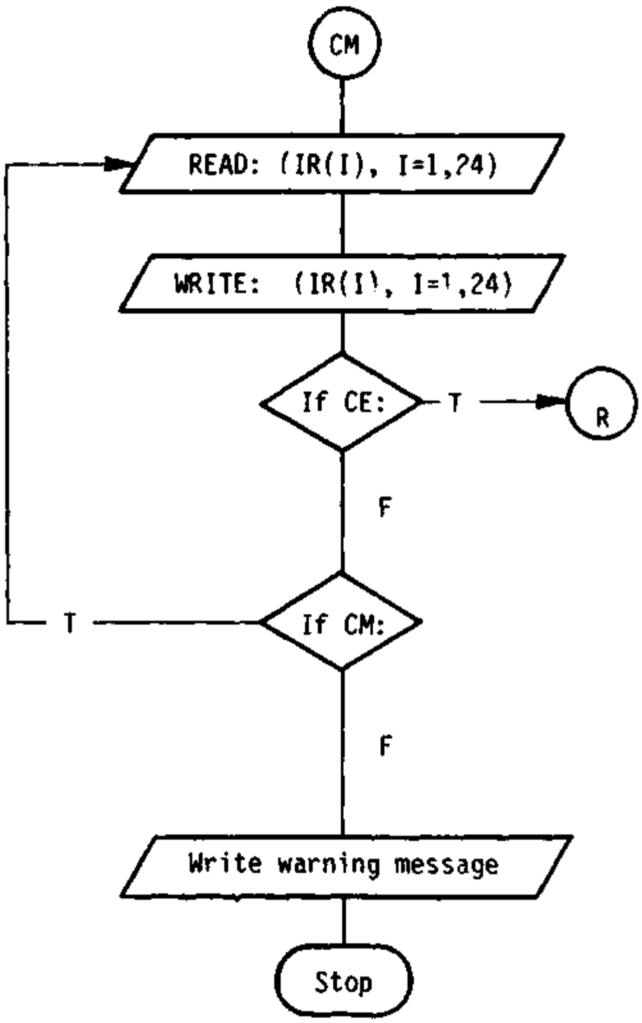

B. Command TO:

This command enables the user to obtain an extended output of various intermediate quantities in the computer code. This is useful in testing the program or in analyzing the contributions from various scattering mechanisms in terms of the total solution.

1. READ: LDEBUG, LTEST, LOUT

a) LDEBUG: This is a logical variable defined by T or F. It is used to debug the program if errors are suspected within the program. If set true, the program prints out data on unit #6 associated with each of its internal operations. These data can, then be compared with previous data which are known to be correct. It is, also, used to insure initial operation of the code. Only one pattern angle is considered. (normally set false)

b) LTEST: This is a logical variable defined by T or F. It is used to test the input/output associated with each subroutine. The data written out on unit #6 are associated with the data in the window of the subroutine. They are written out each time the subroutine is called. It is, also, used to insure initial operation of the code. Only one pattern angle is considered.
(normally set false)

c) LOUT: This is a logical variable defined by T or F. It is used to output data on unit #6 associated with the main program. It too is used to initially insure proper operation. It can, also, be used to examine the various components of the pattern. This is expecially useful to someone interested in analvzing which scattering center contributed in a particular direction. See Table 3 for a list of the fields and their identifiers.

2. READ: LSLOPE, LCORNR, LSOR

a) LSLOPE: This is a logical variable defined by T or F. It is used to tell the code whether or not slope diffraction is desired during the computation.
(normally set true)

b) LCORNR: This is a logical variable defined by T or F. It is used to tell the code whether or not corner diffraction is desired during the computation.
(normally set true)

c) LSOR: This is a logical variable which is defined by T or F. It is used to specify whether or not the operator wants simply the antenna pattern alone.
(normally set false)

3. READ: JMN(1), JMX(1), JMN(2), JMX(2), JMN(3), JMX(3)

a) JMN(1), JMX(1): These are integer variables used to specify a set of individual scattering components that are to be included in the scattered field computation for the plate structures alone. JMN(1) is the minimum component number and JMX(1) is the maximum component number for the range of the set where the components are defined by the following number designations:
0 = skip the plates section
1 = incident field
2 = single reflected fields
3 = double reflected fields
4 = single diffracted fields
5 = reflected-diffracted fields
6 = diffracted-reflected fields
7 = identifies double diffracted problem areas (double diffracted fields are not computed at present).
Normally JMN(1)=1 and JMX(1)=7. This would compute all the available field values for a convex or concave plate structure.

b) JMN(2), JMX(2): These are integer variables used to specify a set of individual scattering components that are to be included in the scattered field computation for the finite elliptic cylinder structure alone. JMN(2) is the minimum component number and JMX(2) is the maximum component number for the range of the set where the components are defined by the following number designations:
0 = skip the cylinder section
1 = incident, reflected, transition and creeping wave fields.
2 = single reflected fields from the end caps.

3 = single diffracted fields from the end cap rims.

Normally JMN(2)=1 and JMX(2)=3. This would compute all the field values for a finite elliptic cylinder structure.

c) JMN(3), JMX(3): These are integer variables used to specify a set of individual scattering components that are to be included in the scattered field computation for the interactions between the plate and cylinder structures. JMN(3) is the minimum component number and JMX(3) is the maximum component number for the range of the set where the components are defined by the following number designations:

0 = skip the plate-cylinder interaction section.

1 = fields reflected from the plates then reflected or diffracted from the cylinder.

2 = fields reflected or diffracted from the cylinder then reflected from the plates.

3 = fields reflected from the cylinder then diffracted from the plates.

4 = fields diffracted from the plates then reflected from the cylinder.

Normally JMN(3)=1 and JMX(3)=4.

FLOW DIAGRAM FOR TO:

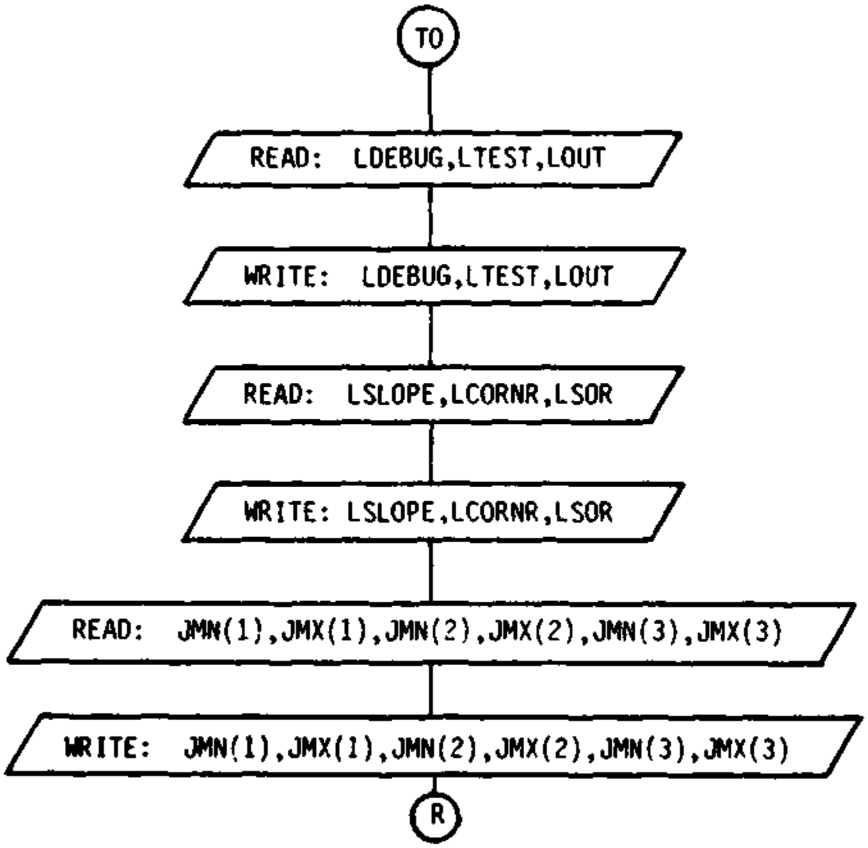

Table 3
Individual Field Types Printed when LOUT=.TRUE.

L	K	J	I	Field Type
100	0	0	0	Direct field when plates are present
200	MP	0	0	Field reflected from plate MP
300	MP	MPP	0	Field reflected from plate MP then reflected from plate MPP
600	MP	ME	0	Field diffracted from edge ME of plate MP
650	MP	ME	0	Field diffracted from the corners of edge ME of plate MP
700	MR	MP	ME	Field reflected from plate MR then diffracted from edge ME of plate MP
750	MR	MP	ME	Field reflected from plate MR then diffracted by the corners of edge ME of plate MP
800	MP	ME	MR	Field diffracted from edge ME of plate MP then reflected from plate MR
850	MP	ME	MR	Field diffracted from the corners of edge ME of plate MP then reflected from plate MR
110	0	0	0	Direct field when only cylinders alone are present
120	0	0	0	Geometrical optics field reflected by cylinder (for comparison only)
130	0	0	0	Field scattered by the curved surface of the cylinder
150	MC	0	0	Field reflected by end cap MC of the cylinder
500	MC	0	0	Field diffracted by the end cap rim MC of the cylinder
240	MP	0	0	Geometrical optics field reflected from plate MP then reflected from the curved surface of the cylinder. (For comparison only)
250	MP	0	0	Field reflected from plate MP and then scattered by the curved surface of the cylinder
410	MP	0	0	Geometrical optics field reflected from the curved surface of the cylinder and then reflected from plate MP. (For comparison only)
420	MP	0	0	Field scattered from the curved surface of the cylinder then reflected from plate MP
940	MP	ME	0	Field reflected from the curved surface of the cylinder then diffracted by edge ME of plate MP
950	MP	ME	0	Field diffracted from edge ME of plate MP then reflected from the curved surface of the cylinder
IANGLE	IANGLE	INDEX	INDEX	Sum of fields of a given type (INDEX) for a given angle (IANGLE)
1000	IANGLE	IANGLE	IANGLE	Total field for a given angle (IANGLE)

C. <u>Command UN:</u>

This command enables the user to specify the units of all the linear dimensions to be input after the command is called. (The one exception is the source length HS and width HAWS, see command US:)

1. READ: IUNIT

   a) IUNIT: This is an integer variable that indicates the units for the input data that follows, such that if

$$IUNIT = \begin{cases} 1 \rightarrow \text{meters} \\ 2 \rightarrow \text{feet} \\ 3 \rightarrow \text{inches} \end{cases}$$

FLOW DIAGRAM FOR UN:

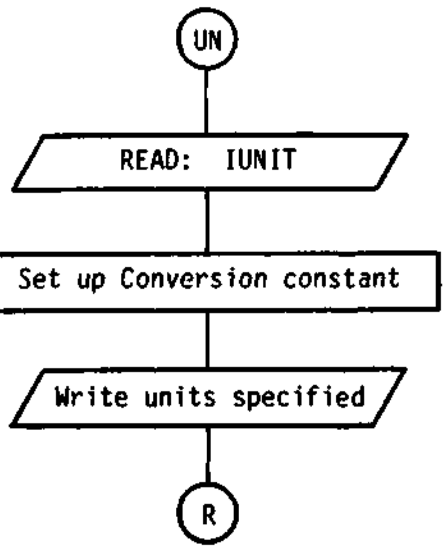

D. Command US:

This command enables the user to specify the units of the source length HS and width HAWS to be input after the command is called. These variables are in the command SG:.

1. READ: IUNST

a) IUNST: This is an integer variable that indicates the units for the input data HS and HAWS that follows, such that if

$$IUNST = \begin{cases} 0 \rightarrow \text{wavelengths} \\ 1 \rightarrow \text{meters} \\ 2 \rightarrow \text{feet} \\ 3 \rightarrow \text{inches} \end{cases}$$

Note that if the units are specified to be wavelengths for one source it must be wavelengths for all of the sources specified.

FLOW DIAGRAM FOR US:

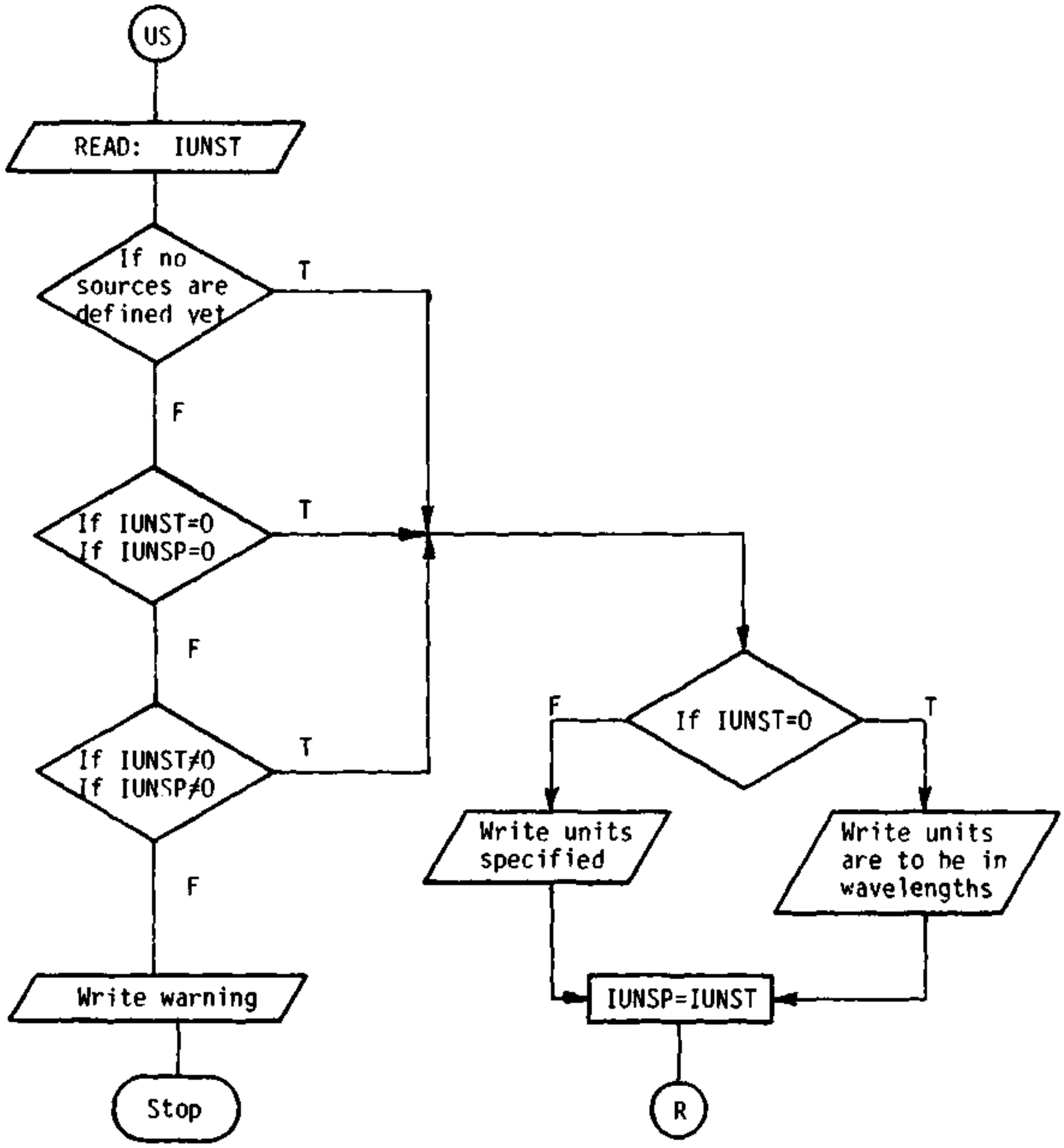

E. Command FR:

This command enables the user to define the frequency in gigahertz.

1. READ: FRQG

a) FRQG: This is a real variable which is used to define the frequency in gigahertz.

FLOW DIAGRAM FOR FR:

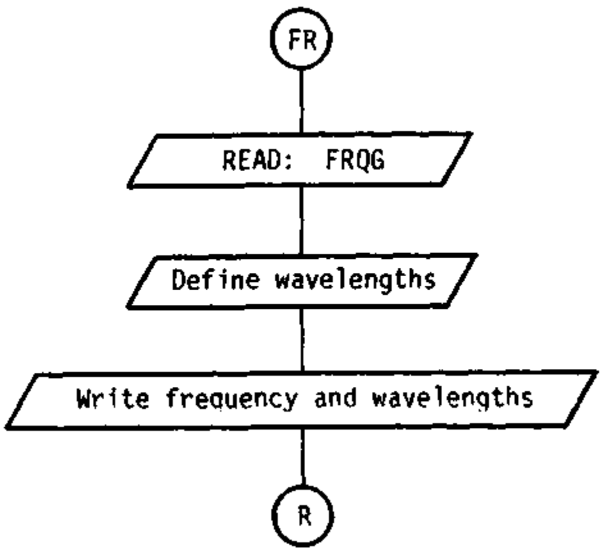

F. Command PD:

This command enables the user to define the pattern coordinate system, the pattern cut, and the angular range that is desired. The geometry is illustrated in Figure 1.

1. READ: THCZ, PHCZ, THCX, PHCX

   a) THCZ,PHCZ: These are real variables. They are input in degrees as spherical angles that define the z_p-axis of the pattern coordinate system as if it was a radial vector in the reference coordinate system.

   b) THCX,PHCX: These are real variables, They are input in degrees as spherical angles that define the x_p-axis of the pattern coordinate system as if it was a radial vector in the reference coordinate system.

Note that the new x_p-axis and z_p-axis must be defined orthogonal to each other. The new y_p-axis is found from the cross product of the x_p- and z_p-axis.

2. READ: LCNPAT, TPPD

   a) LCNPAT: This is a logical variable that defines the pattern cut desired, such that if

   $$\text{LCNPAT} = \begin{cases} \text{T} \rightarrow \text{THETA CUT(conic cut)} \\ \text{F} \rightarrow \text{PHI CUT (PHI constant)} \end{cases}$$

   b) TPPD: This is a real variable that defines the pattern angle that is to be held constant, such that if

   $$\text{LCNPAT} = \begin{cases} \text{T} \rightarrow \text{TPPD = THP constant} \\ \text{F} \rightarrow \text{TPPD = PHP constant} \end{cases}$$

3. READ: IB, IE, IS

   a) IB,IE,IS: These are integer variables used to define angles in degrees. They are, respectively, the beginning, ending, and incremental values of the pattern angle.

FLOW DIAGRAM FOR PD:

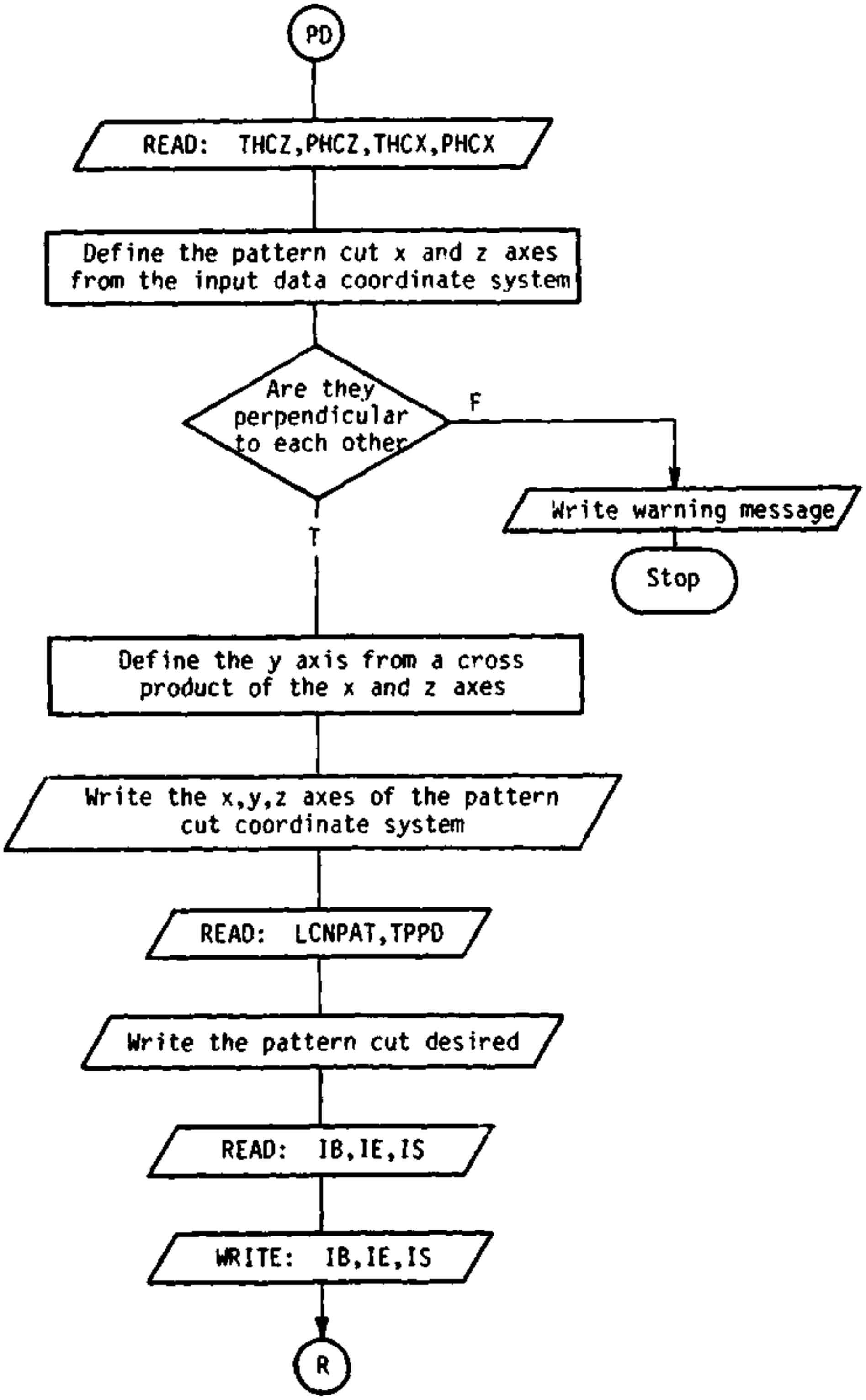

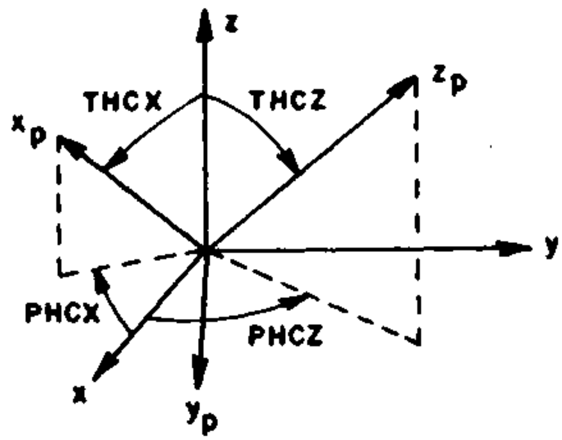

Figure 1a. Definition of pattern coordinate system.

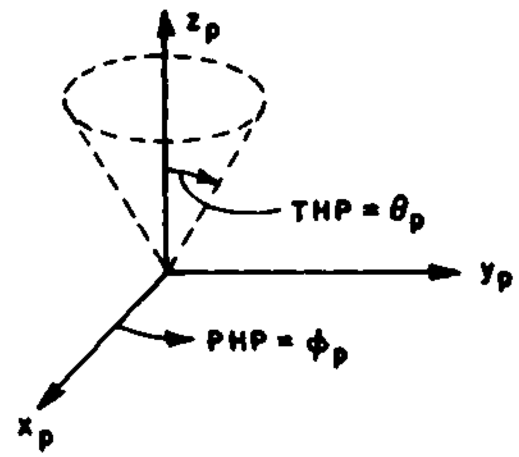

Figure 1b. Conic pattern cut, LCNPAT=.TRUE., TPPD=THP.

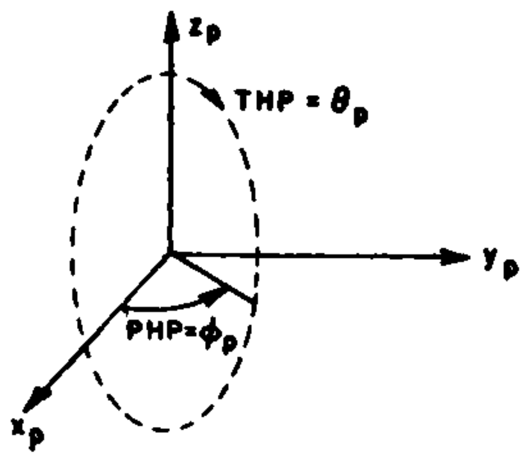

Figure 1c. Constant Phi pattern cut, LCNPAT=.FALSE., TPPD=PHP.

G. Command RG:

This command enables the user to specify a far field distance, R, to the observer. The fields are then normalized by the factor exp(-jkR)/R.

1. READ: RANGS

   a) This is a real variable which is used to specify the far field range, R.

Note that R should be in the far field of the scattering structure, that is, $R > 2D^2/\lambda$ where D is the maximum dimension of the structure. However, if $R \geq 10^{30}$, then the factor exp(-jkR)/R is suppressed.

FLOW DIAGRAM FOR RG:

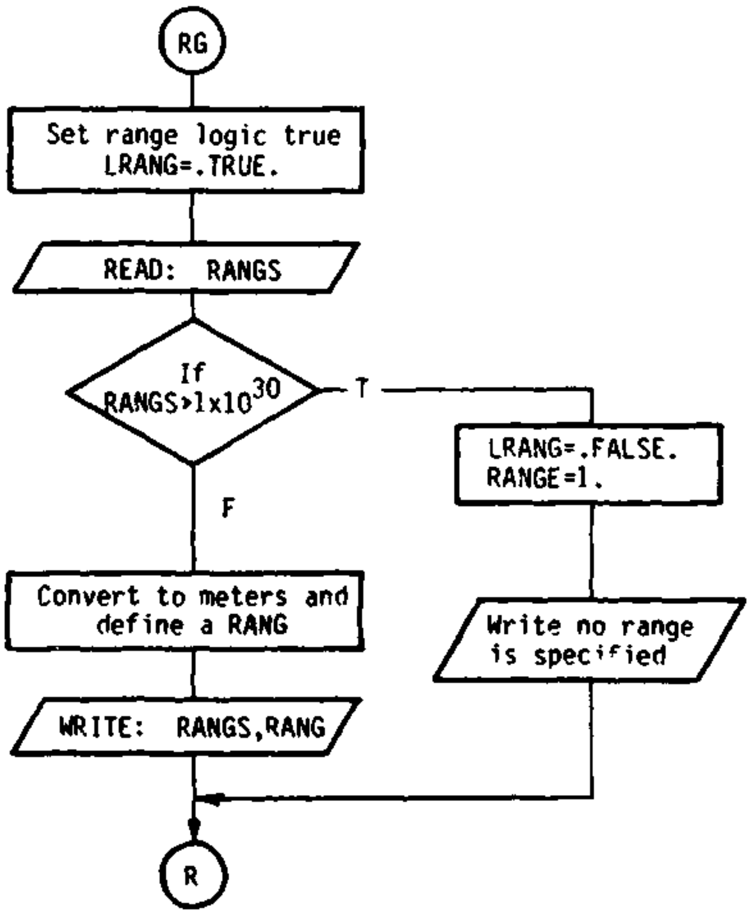

H. Command RT:

This command enables the user to translate and/or rotate the coordinate system used to define the input data in order to simplify the specification of the plate, cylinder, and source geometries. The geometry is illustrated in Figure 2.

1. READ: (TR(N), N=1,3)

   a) TR(N): This is a dimensional real variable. It is used to specify the origin of the new coordinate system to be used to input the data for the source or the scattering structures. It is input on a single line with the real numbers being the x,y,z coordinates of the new origin which corresponds to N=1,2,3, respectively.

2. READ: THZP, PHZP, THXP, PHXP

   a) THZP, PHZP: These are real variables. They are input in degrees as spherical angles that define the z-axis of the new coordinate system as if it was a radial vector in the reference coordinate system.

   b) THXP, PHXP: These are real variables. They are input in degrees as spherical angles that define the x-axis of the new coordinate system as if it was a radial vector in the reference coordinate system.

The new x-axis and z-axis must be defined orthogonal to each other. The new y-axis is found from the cross product of the x- and z-axes. All the subsequent inputs will be made relative to this new coordinate system, which is shown as x_t, y_t, z_t , unless command "RT:" is called again and redefined.

FLOW DIAGRAM FOR RT:

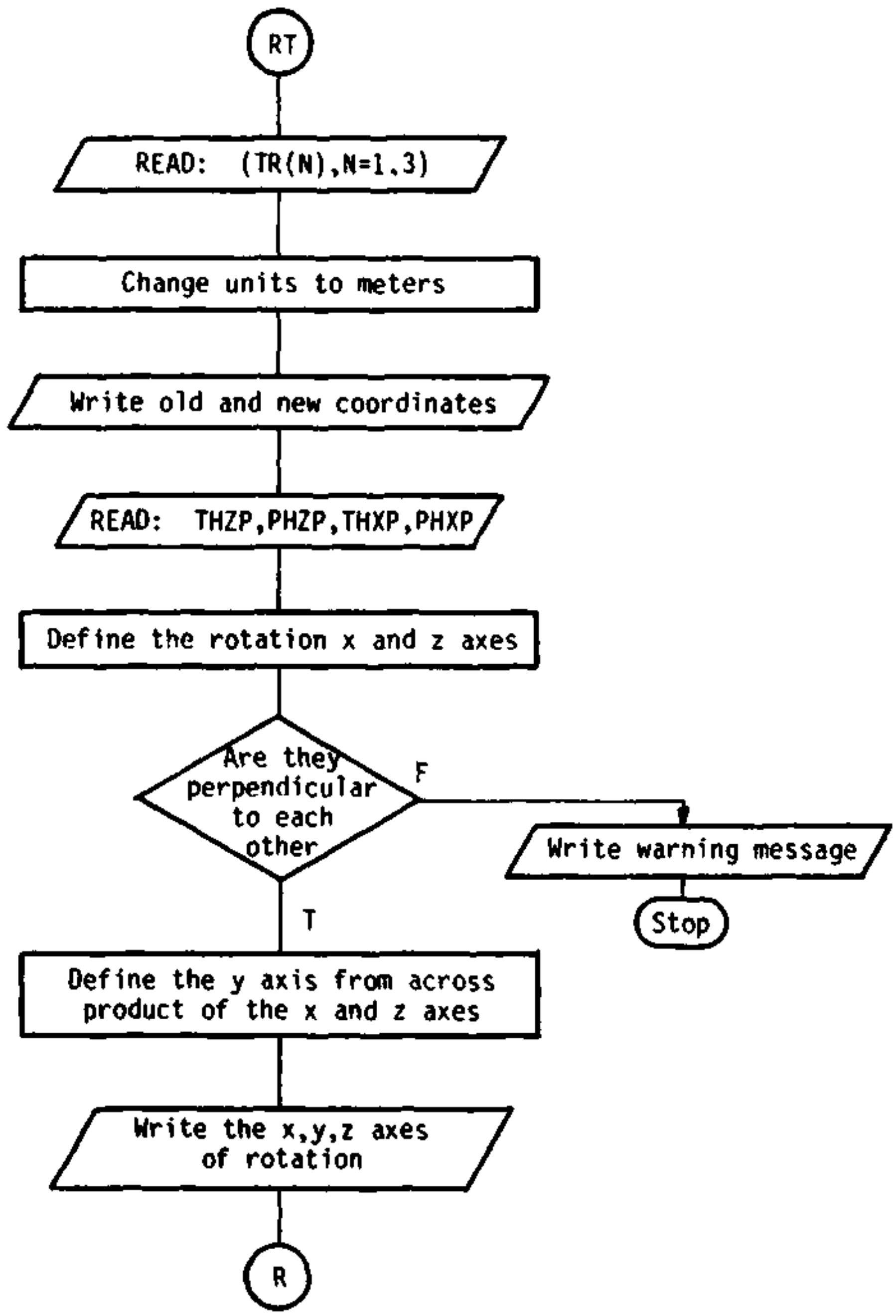

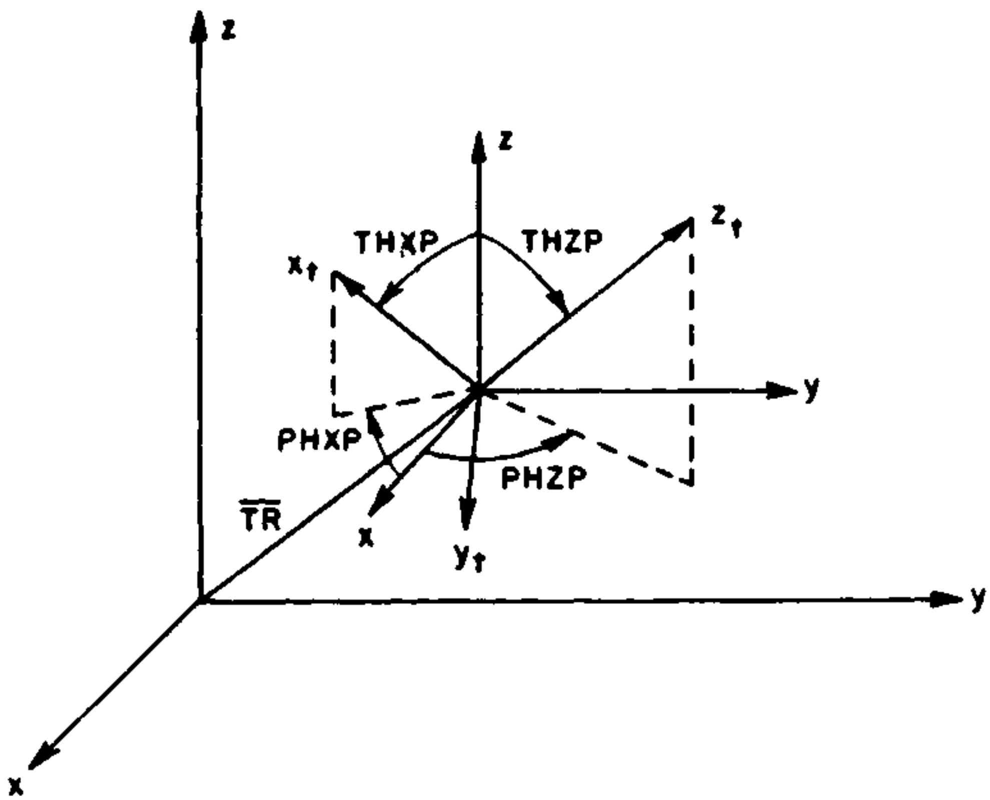

Figure 2. Definition of rotate-translate coordinate system geometry.

I. <u>Command PG:</u>

This command enables the user to define the geometry of the flat plate structures to be considered. The geometry is illustrated in Figure 3. One call to this command defines one plate. The number of plates in the structure are automatically counted by the number of calls to this command.

1. READ: MEP(MP)

   a) MEP (MP): This is a dimensioned integer variable. It is used to define the number of corners (or edges) on the MP^{th} plate.

2. READ: (XX(MP,ME,N), N=1,3)

   a) XX(MP,ME,N): This is a triply dimensioned real variable. It is used to specify the location of the ME^{th} corner of the MP^{th} plate. It is input on a single line with the real numbers being the x,y,z coordinates of the corner, in the specified coordinate system, which correspond to N=1,2,3, respectively, in the array. For example, the array will contain the following for plate #1 and corner #2 located at x=2., y=4., z=6.:
   XX(1,2,1)=2.
   XX(1,2,2)=4.
   XX(1,2,3)=6.
   This data is input as: 2.,4.,6.

This read statement will be called MEP(MP) times so that all the corners are defined. As an example, the input data for the flat plate structure given in Figure 3, is given by

```
 4             :number of corners for plate #1
 1., 1., 0     : corner #1
-1., 1., 0.    : corner #2
-1.,-1., 0.    : corner #3
 1.,-1., 0.    : corner #4 .
```

See Chapter IV for further details on how to number the corners.

Note that the program will keep increasing the number of plates in the solution by the number of calls to this command unless the NP: or NX: commands are called to reinitialize the plate geometry.

Presently: $1 \leq MP \leq 14$
$1 \leq ME \leq 6$
$1 \leq N \leq 3$

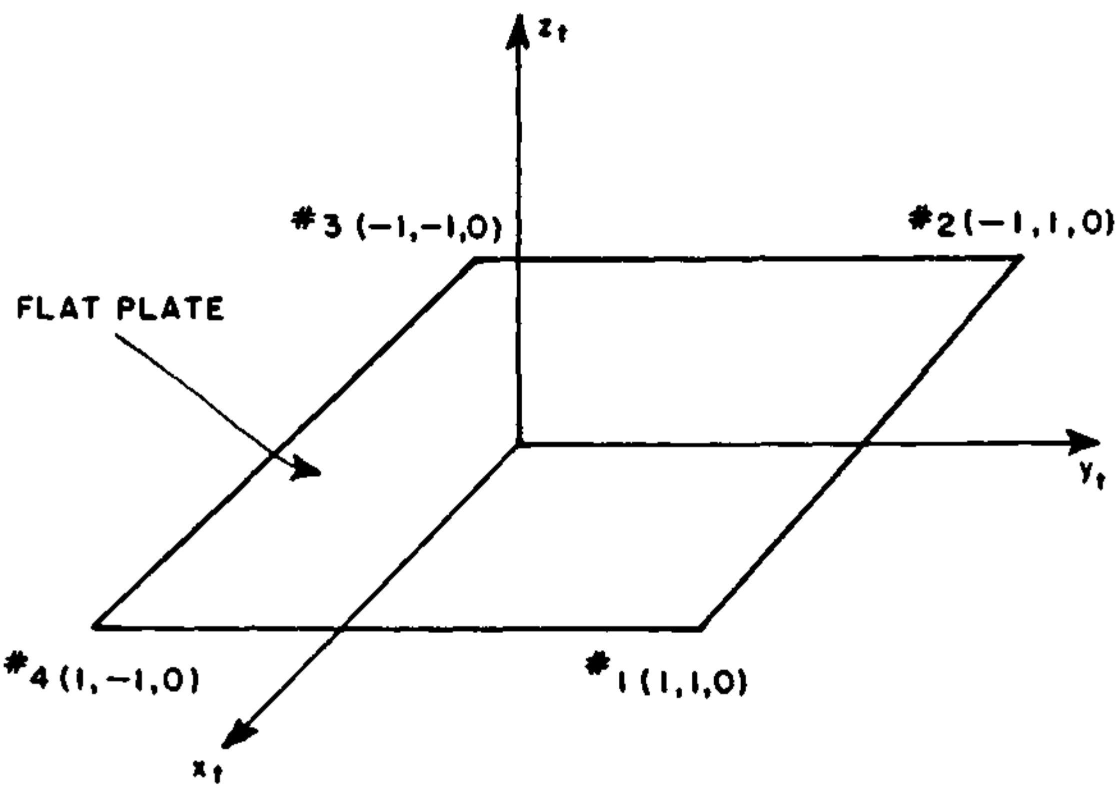

Figure 3. Definition of flat plate geometry.

FLOW DIAGRAM FOR PG:

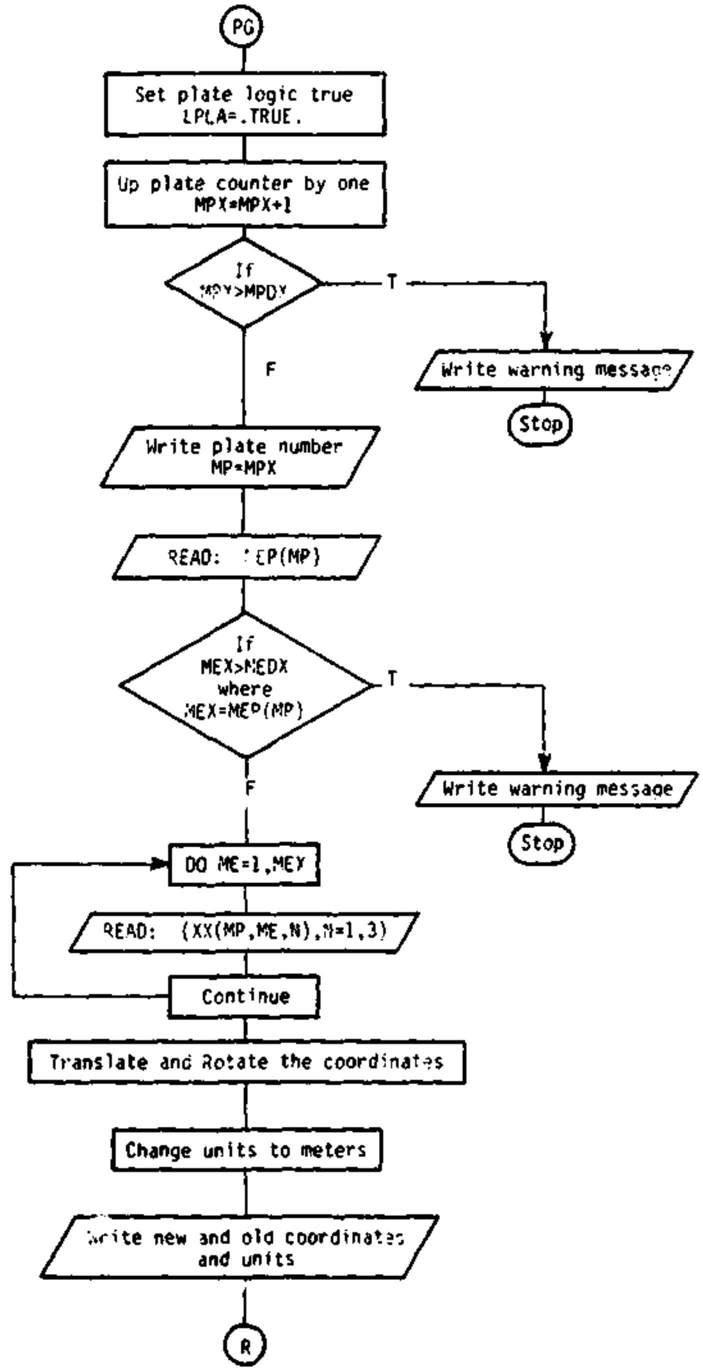

J. Command GP:

This command enables the user to specify a perfectly-conducting infinite ground plane in the x_t-y_t plane.

FLOW DIAGRAM FOR GP:

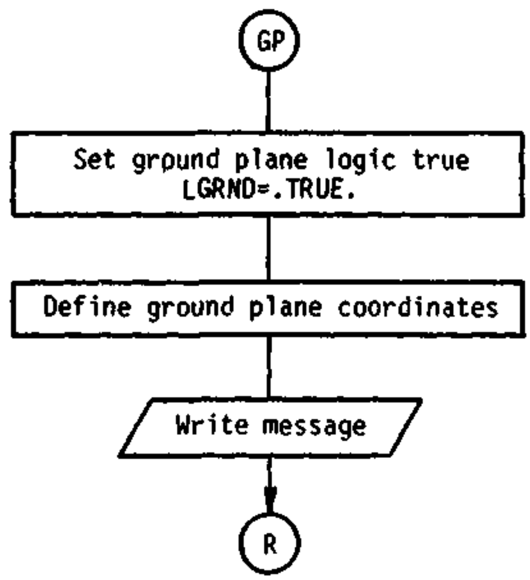

K. Command CG:

This command enables the user to define the geometry of the finite elliptic cylinder structure to be considered. Note only one may be specified. The geometry is illustrated in Figure 4.

1. READ: AA, BB

   a) AA: This is a real variable which defines the radius of the elliptic cylinder on the x_t-axis of the cylinder.

   b) BB: This is a real variable which defines the radius of the elliptic cylinder on the y_t-axis of the cylinder.

2. READ: ZCN, THTN, ZCP, THTP

   a) ZCN: This is a real variable that defines the position of the center of the most negative endcap on the z_t-axis of the cylinder.

   b) THTN: This is a real variable. It is input in degrees and defines the angle the surface of the most negative endcap makes with the negative z_t-axis in the x_t-z_t plane.

   c) ZCP: This is a real variable that defines the position of the center of the most positive endcap on the z_t-axis of the cylinder.

   d) THTP: This is a real variable. It is input in degrees and defines the angle the surface of the most positive endcap makes with the positive z_t-axis in the x_t-z_t plane.

FLOW DIAGRAM FOR CG:

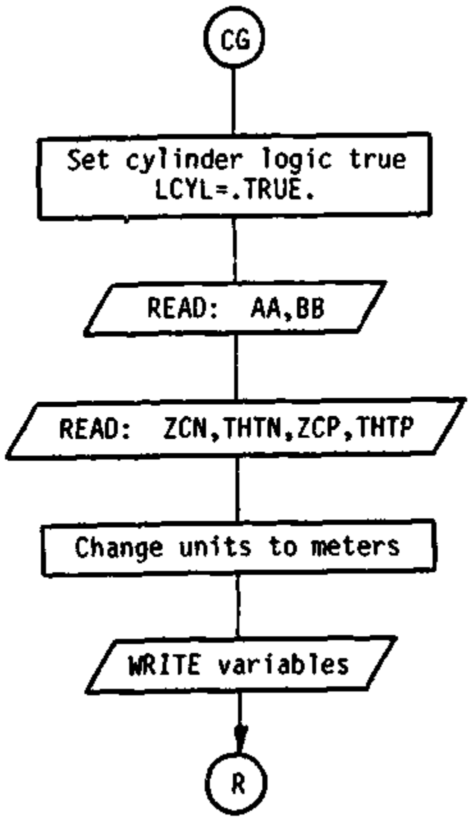

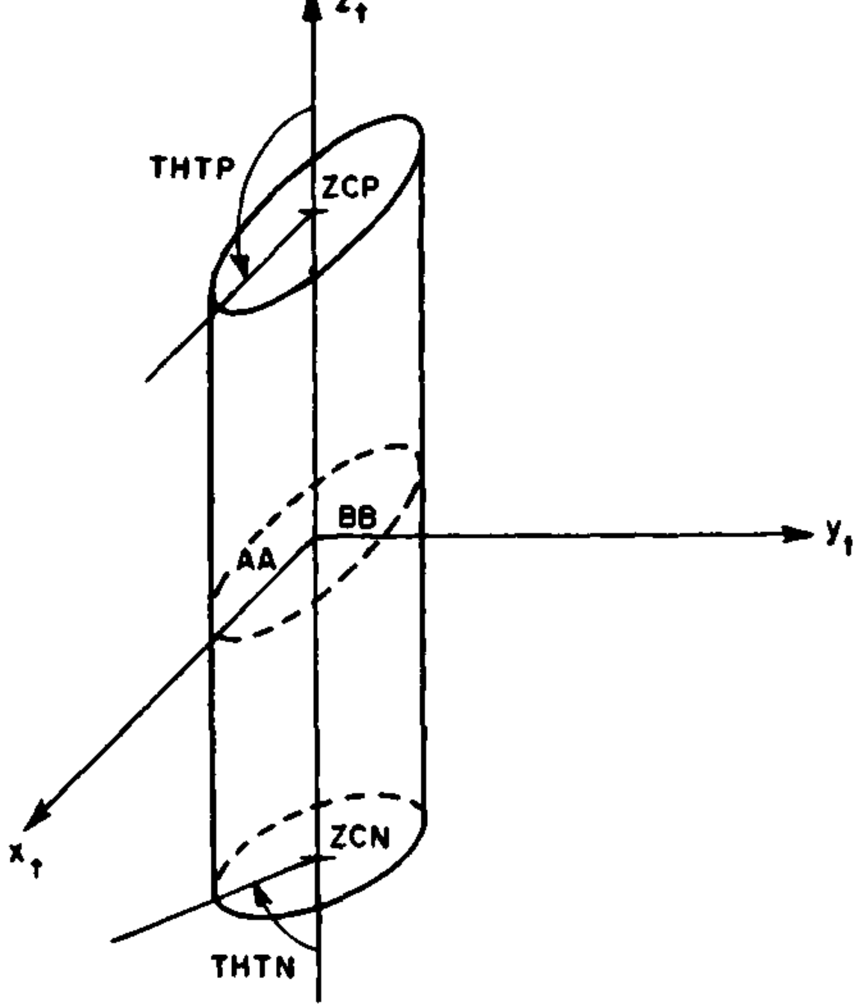

Figure 4. Definition of finite elliptic cylinder geometry.

L. Command SG:

This command enables the user to specify the location and type of source to be used. The geometry is illustrated in Figure 5. One call to this command defines one source. The number of sources in the problem are automatically counted by the number of calls to this command.

1. READ: (XSS (MS,N) N=1,3)

   a) XSS (MS,N): This is a doubly dimensioned real array which is used to define the x,y,z location of the MS^{th} elemental radiator in the specified cartesian coordinate system. Again, a single line of data contains the x,y,z (N=1,2,3) locations.

2. READ: THOZ(MS), PHOZ(MS), THOX(MS), PHOX(MS)

   a) THOZ(MS),PHOZ(MS): These are real arrays which are used to define the orientation of the MS^{th} element in the specified cartesian coordinate system. They are input in degrees, as spherical angles, that define a radial direction which is parallel to the MS^{th} element current flow for a dipole antenna or which is parallel to the length of an aperture antenna.

   b) THOX(MS),PHOX(MS): These are real arrays which are used to define the orientation of the MS^{th} element in the specified cartesian coordinate system. They are input in degrees, as spherical angles, that define a radial direction which is parallel to the MS^{th} elements aperture width or which is parallel to a slots width. For a dipole antenna, these angles can be made in a convenient direction.

The x-axis and z-axis specified by these angles must be defined orthogonal to each other. The y-axis is found by the cross product of the x- and z-axes.

3. READ: IMS(MS), HS(MS), HAWS(MS)

a) IMS(MS): This is an integer array which is used to define whether the MS^{th} source is an electric or magnetic elemental radiator.
IMS(MS) = 0 → electric
IMS(MS) = 1 → magnetic

b) HS(MS): This is a real array which is used to input the length of the MS^{th} element.

c) HAWS(MS) This is a real array which is used to input the width of the MS^{th} element in the case of an aperture antenna. If HAWS(MS)=0 then it is assumed to be a dipole antenna.

Note that the units of the variables HS(MS) and HAWS(MS) can be specified by the US: command. If wavelength is chosen as the units then all the sources must be specified in wavelengths.

4. READ: WM(MS), WP(MS)

a) WM(MS), WP(MS): These are real dimensioned arrays used to define the excitation associated with the MS^{th} element. The magnitude is given by WM and the phase in degrees by WP.

Note that the program will keep increasing the number of sources in the solution by the number of calls to this command unless the NS: or NX: commands are called to reinitialize the source geometry.

Presently, $1 \leq MS \leq 50$
$1 \leq N \leq 3$

FLOW DIAGRAM FOR SG:

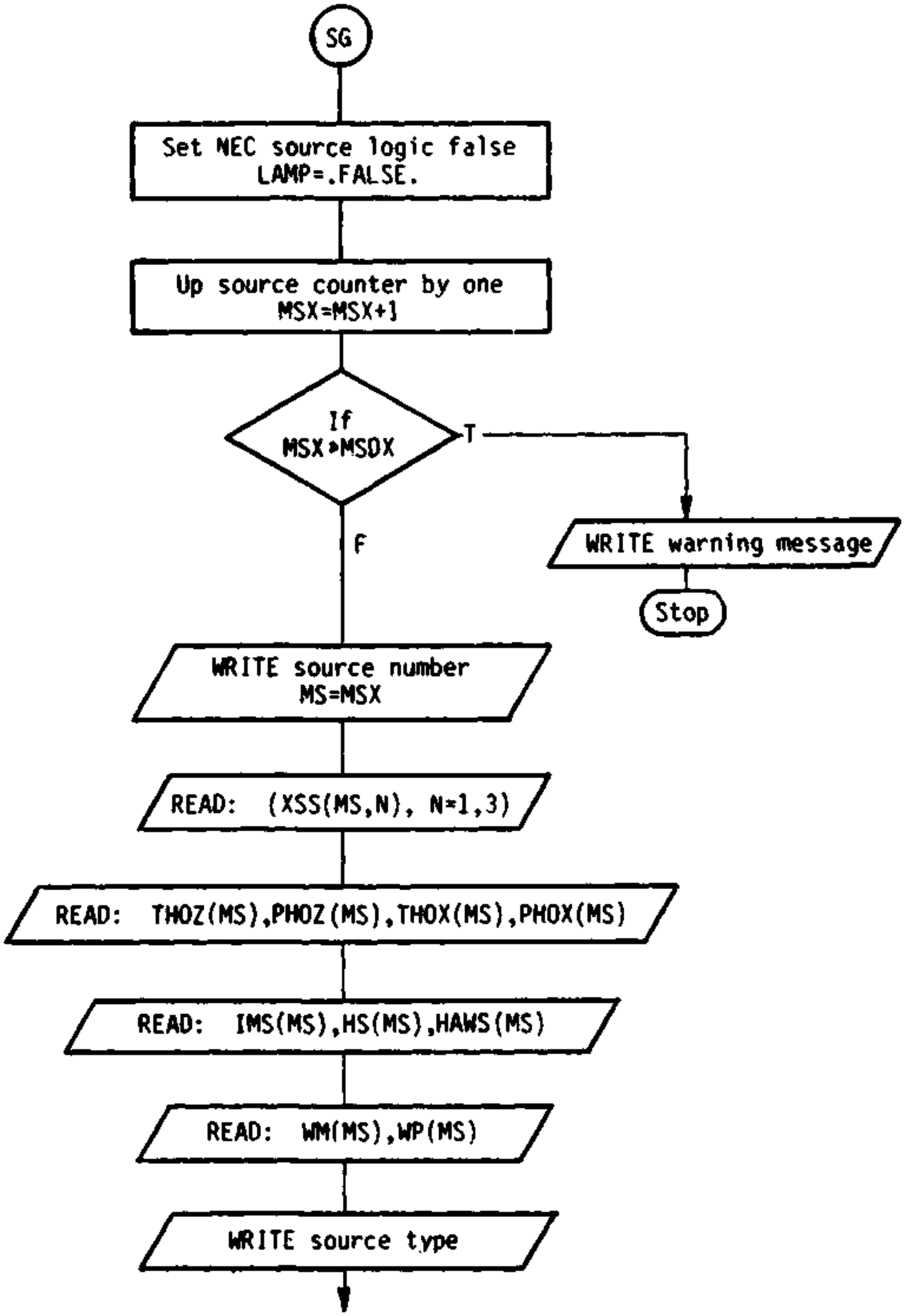

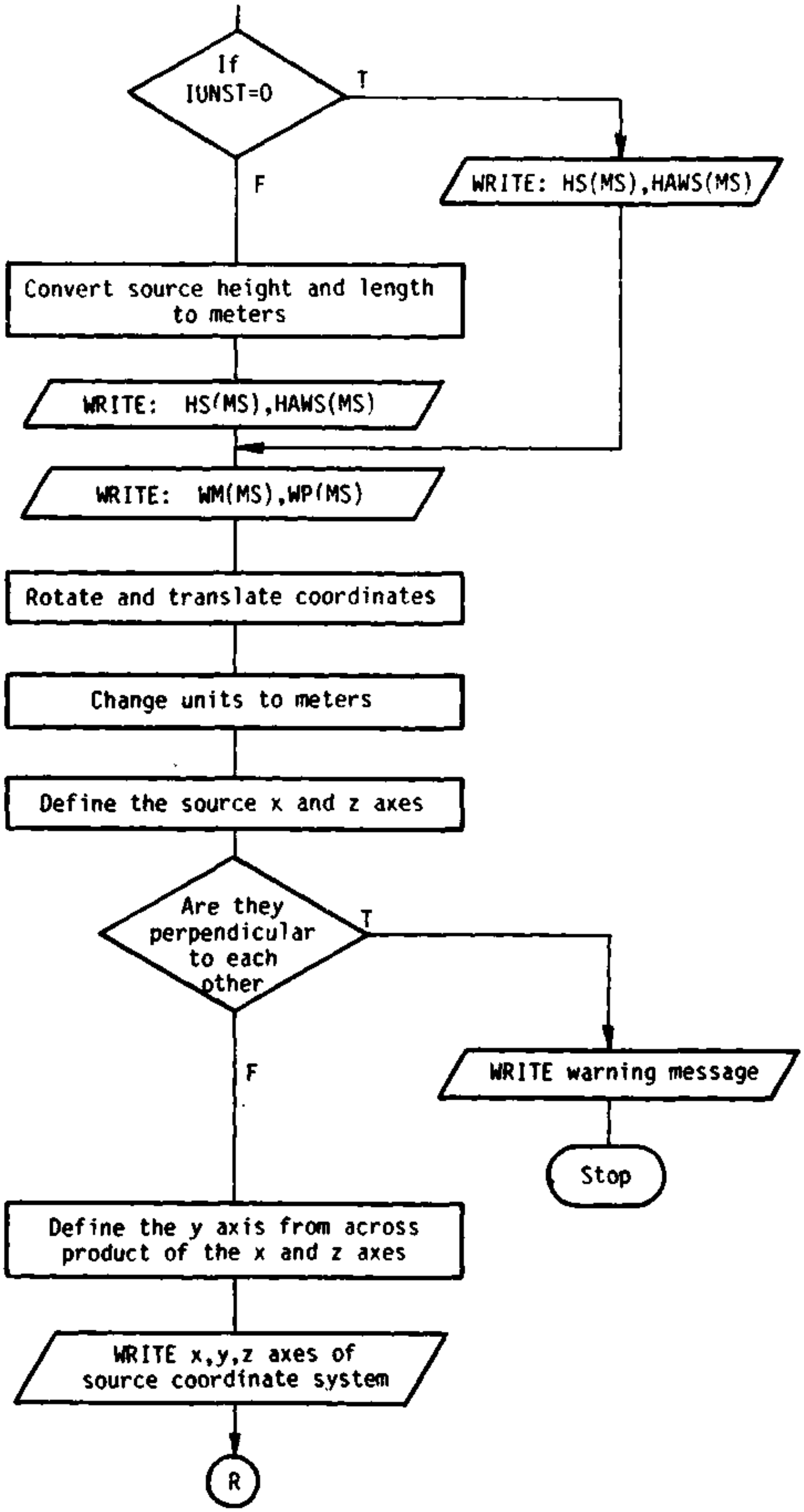

If IUNST=0
T
F
WRITE: HS(MS),HAWS(MS)
Convert source height and length to meters
WRITE: HS(MS),HAWS(MS)
WRITE: WM(MS),WP(MS)
Rotate and translate coordinates
Change units to meters
Define the source x and z axes
Are they perpendicular to each other
T
F
WRITE warning message
Stop
Define the y axis from across product of the x and z axes
WRITE x,y,z axes of source coordinate system
R

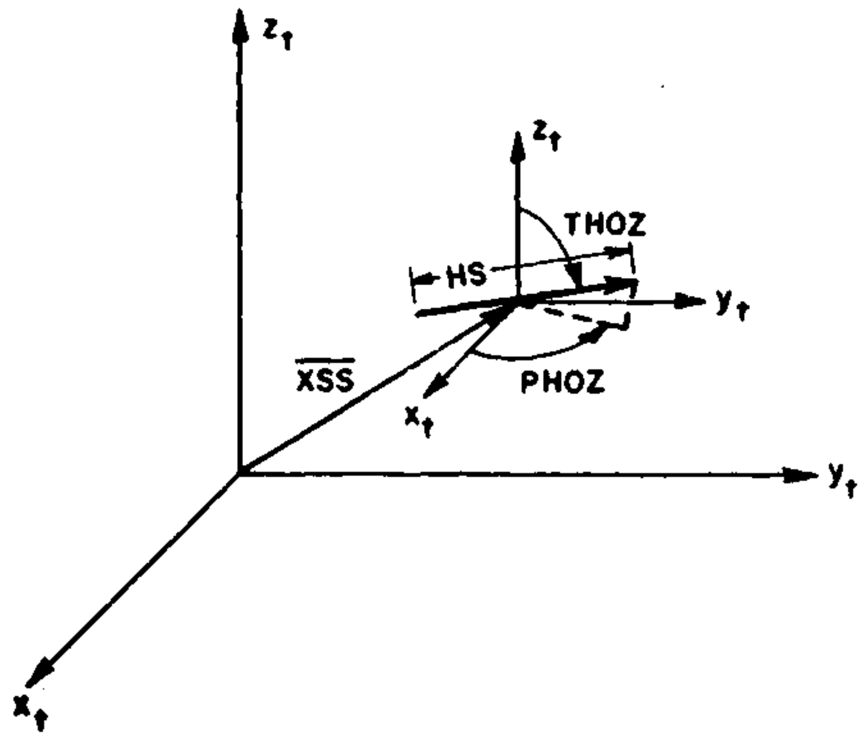

Figure 5a. Definition of source geometry for dipole antennas.

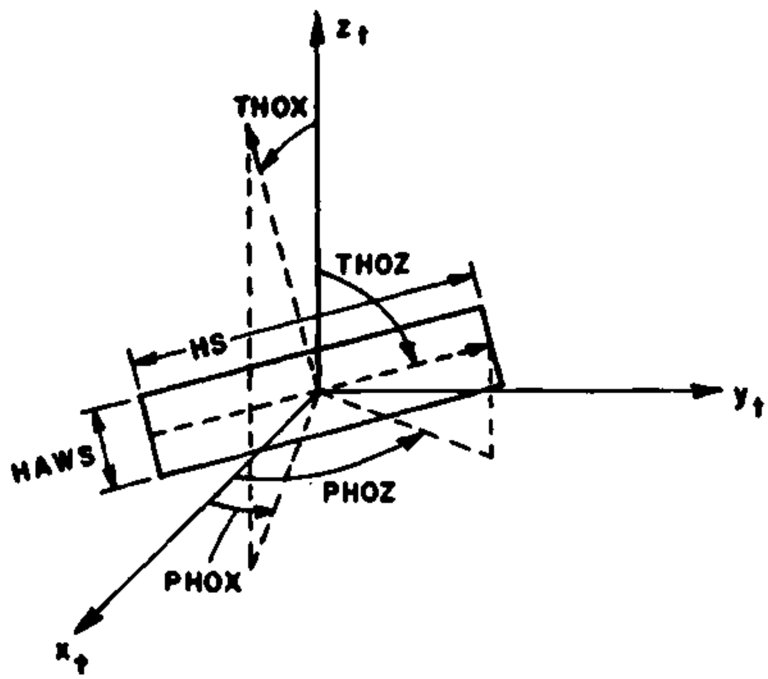

Figure 5b. Definition of source geometry for aperture antennas.

M. Command AM:

This command enables the user to interface the Numerical Electromagnetics Code (NEC)-Moment Method Code with the Basic Scattering Code in order to use the antenna modeling capabilities of NEC to specify the needed source data such as location and current weights of the elements. The geometry is illustrated in Figure 6.

1. READ: PRAD

   a) PRAD: This is a real variable which is used to define the total power radiated in watts from the NEC modeled antenna. This allows the directive gain to be computed. If P_{in} is substituted for P_{rad} the power gain will be computed.

2. READ: MSX

   a) MSX: This is an integer variable which defines the maximum number of elemental wire radiators that have been used in the NEC code to model the antenna.

3. READ: (XSS(MS,N),N=1,3), HS(MS), THOZ(MS), PHOZ(MS)

   a) XSS(MS,N): This is a doubly dimensioned real array which is used to define the x,y,z location of the MS^{th} elemental radiator in the specified cartesian coordinate system.

   b) HS(MS): This is a real array which is used to input the length of the MS^{th} element in the units specified by IUNIT from the UN: command or from the default option.

   c) THOZ(MS), PHOZ(MS): These are real arrays which are used to define the orientation of the MS^{th} element in the specified cartesian coordinate system. The THOZ, PHOZ angles are in degrees and define a radial direction which is parallel to the MS^{th} element current flow. The angle THO is the angle of the element measured up from the x-y plane. The angle PHO is the phi angle in a normal spherical coordinate system.

4. READ: WM(MS), WP(MS)

a) WM(MS), WP(MS): There are real dimensioned arrays used to define the excitation associated with the MS^{th} element. The real part is given by WM and the imaginary part by WP.

Presently, $1 \leq MS \leq 50$.
$1 \leq N \leq 3$

Note that for the NEC code input all the elements are assumed to be electric current elements.

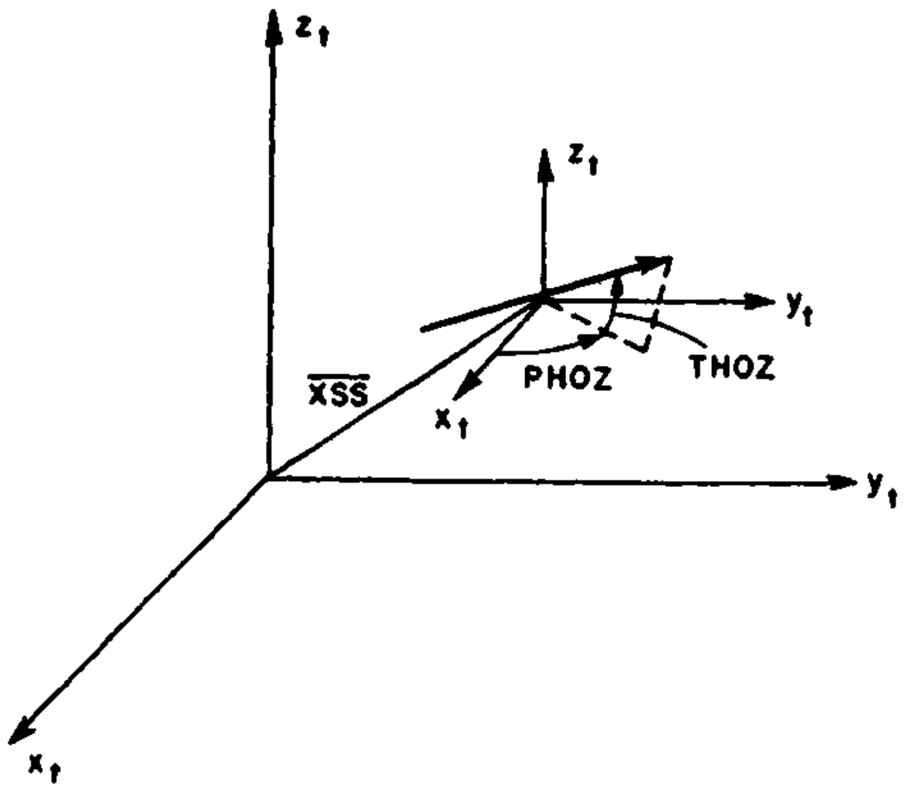

Figure 6. Definition of NEC geometry.

FLOW DIAGRAM FOR AM:

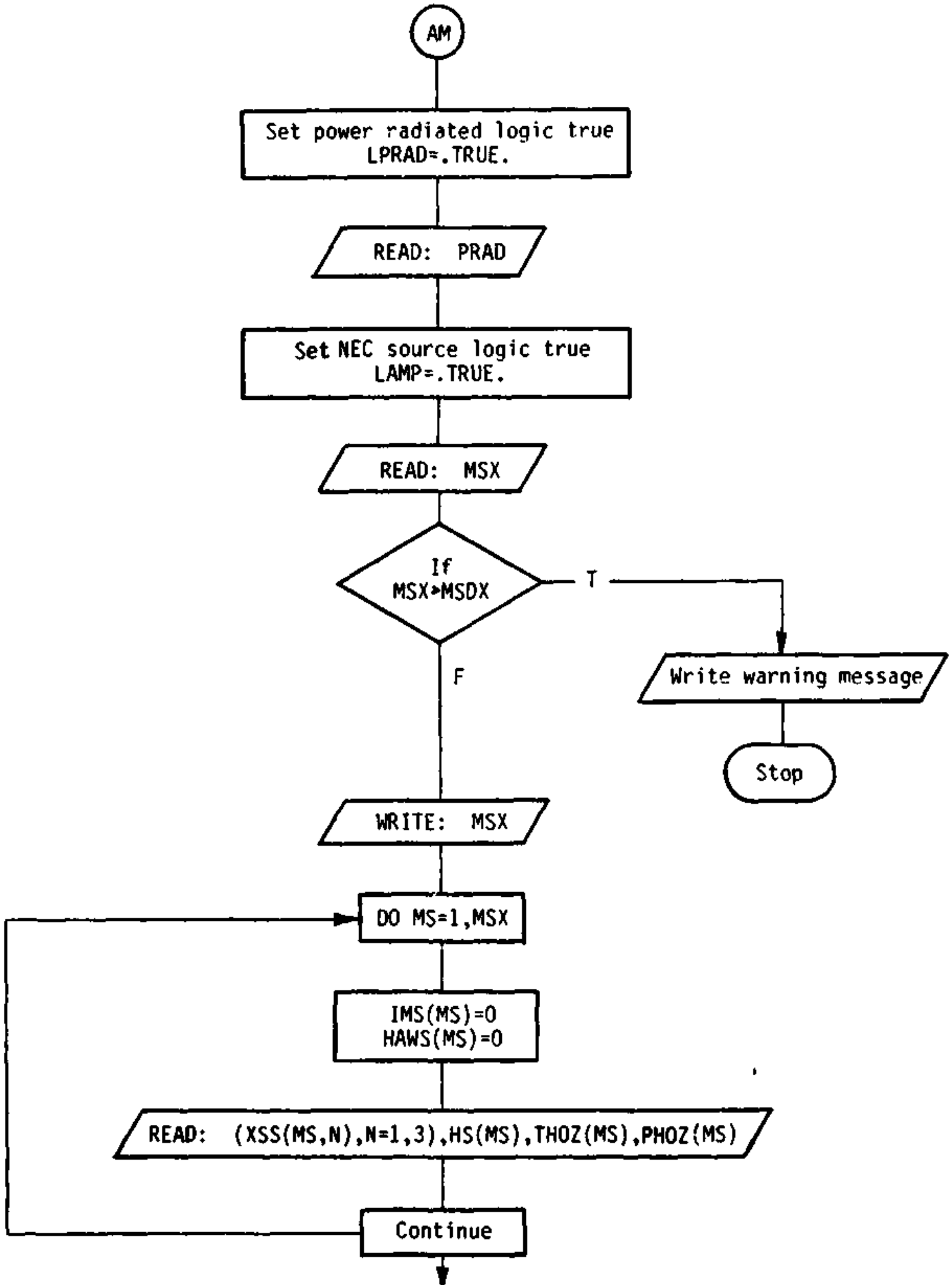

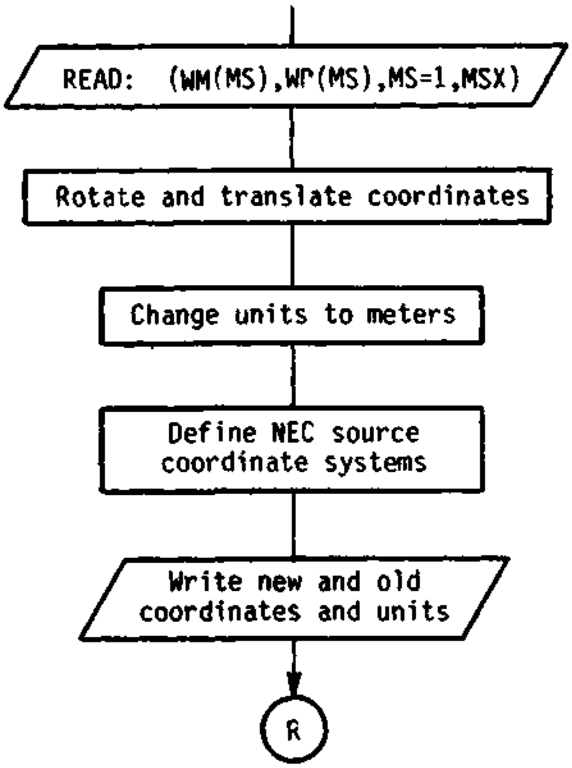
READ: (WM(MS),WP(MS),MS=1,MSX)
Rotate and translate coordinates
Change units to meters
Define NEC source coordinate systems
Write new and old coordinates and units
R

N. Command PR:

This command enables the user to specify the total power radiated by the antenna or the input power to the antenna.

1. READ: PRAD

a) PRAD: This is a real variable. It is input in watts and defines the total power radiated by the antenna (or input power to the antenna).

Note that if PRAD $\leq 10^{-30}$, it will be assumed that the power radiated (or input power) was not specified.

FLOW DIAGRAM FOR PR:

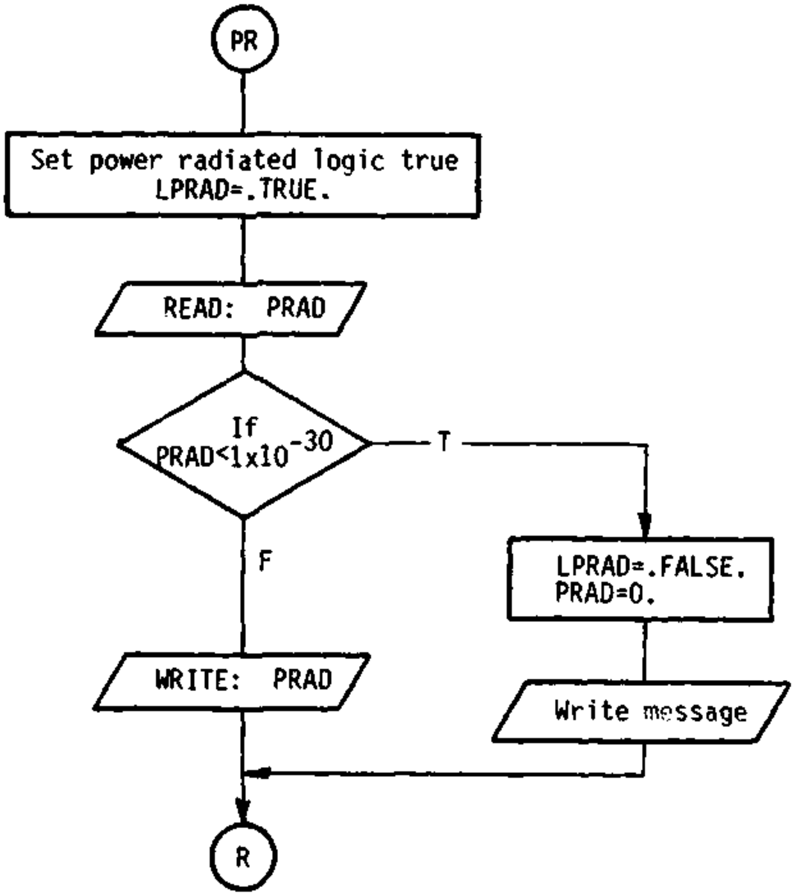

O. Command NP:

This command enables the user to initialize the plate data. All of the plates are removed from the problem unless they are re-specified following this command.

FLOW DIAGRAM FOR NP:

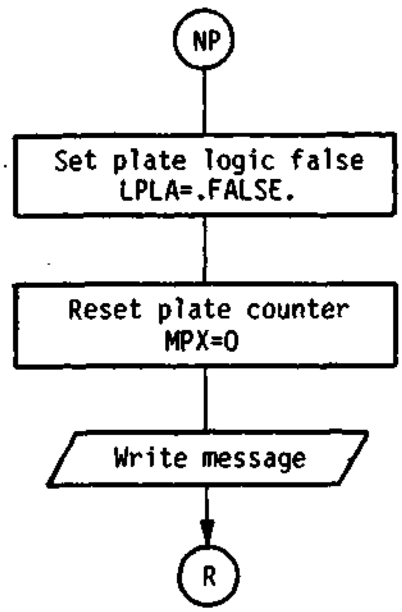

P. Command NG:

This command enables the user to initialize the infinite ground plane. The ground plane is removed from the problem unless it is respecified following this command.

FLOW DIAGRAM FOR NG:

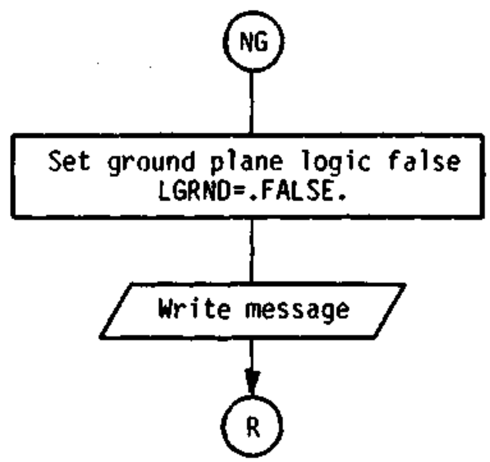

Q. Command NC:

This command enables the user to initialize the cylinder data. The cylinder is removed from the problem unless it is respecified following this command.

FLOW DIAGRAM FOR NC:

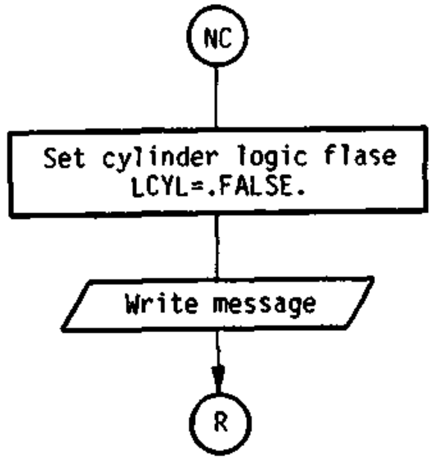

R. Command NS:

This command enables the user to initialize the source data. All of the sources are removed from the problem unless they are re-specified following this command.

FLOW DIAGRAM FOR NS:

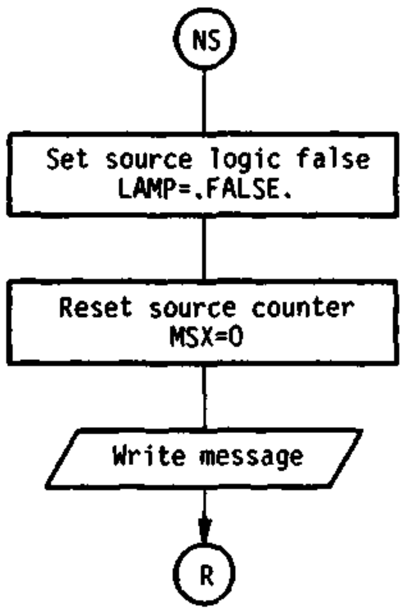

S. Command NX:

This command enables the user to reinitialize the commands to their default conditions specified in the list at the beginning of the main program.

FLOW DIAGRAM FOR NX:

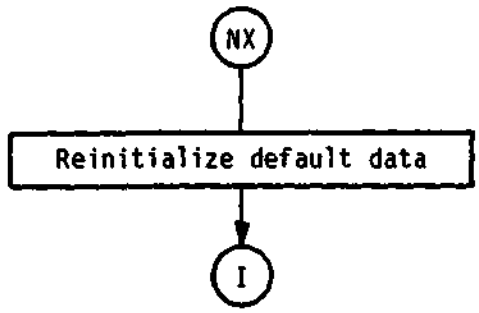

T. Command LP:

This command enables the user to specify whether a line printer listing of the results is desired.

1. READ: LWRITE

a) LWRITE: This is a logical variable defined by T or F. It is used to indicate if a line printer listing of the total fields ($E_{\theta p}$, $E_{\phi p}$) is desired.
(normally set true)

FLOW DIAGRAM FOR LP:

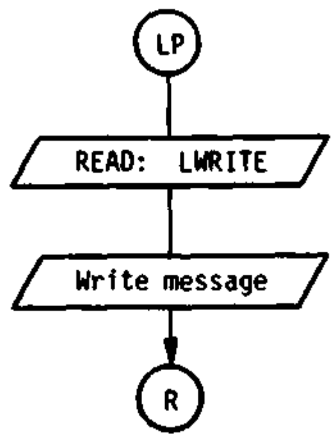

U. Command PP:

This command enables the user to specify whether a polar plot of the results are desired.

1. READ: LPLT

a) LPLT: This is a logical variable defined by T or F. It is used to indicate if a polar plot of the total fields ($E_{\theta p}, E_{\phi p}$) is desired. If LPLT is false the rest of the READ statements for this command will be skipped.

2. READ: RADIUS,IPLT

a) RADIUS: This is a real variable that is used to specify the radius of the polar plot.

b) IPLT: This is an integer variable that indicates the type of polar plot desired, such that if

$$\mathrm{IPLT} = \begin{cases} 1 \rightarrow \text{field plot} \\ 2 \rightarrow \text{power plot} \\ 3 \rightarrow \text{dB plot.} \end{cases}$$

The fields will be normalized by their maximum field values.

FLOW DIAGRAM FOR PP:

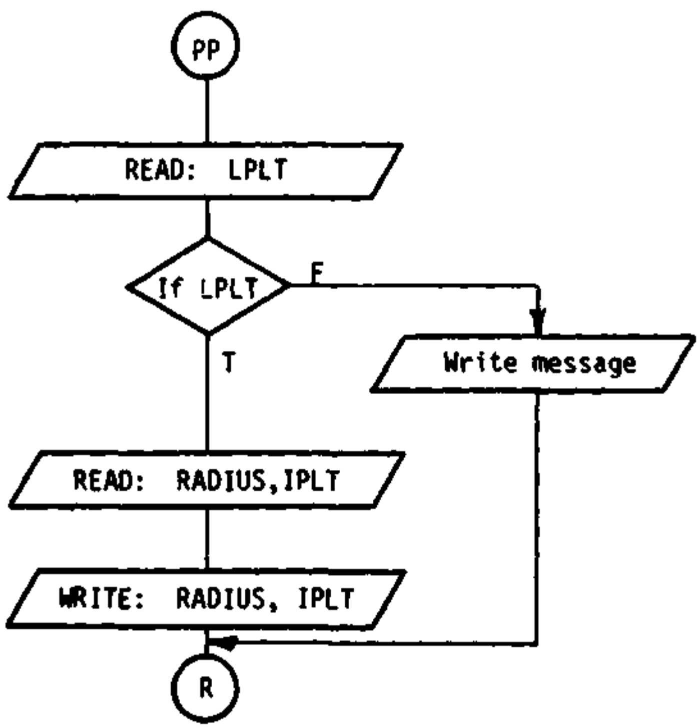

V. <u>Command XQ:</u>

This command is used to execute the scattering code so that the total fields may be computed. After execution the code returns for another possible command word.

FLOW DIAGRAM FOR XQ:

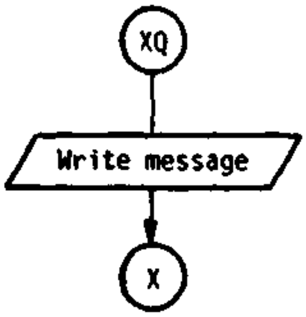

W. Command EN:

This command enables the user to terminate the execution of the scattering code.

FLOW DIAGRAM FOR EN:

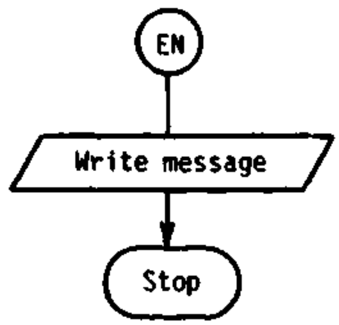

This concludes the definition of all the input parameters to the program. The program would, then, run the desired data and output the results on unit #6. However as with any sophisticated program, the definition of the input data is not sufficient for one to fully understand the operation of the code. In order to overcome this difficulty the next chapter discusses how the input data are interpreted and used in the program.

CHAPTER IV
INTERPRETATION OF INPUT DATA

This computer code is written to require a mimumum amount of user information such that the burden associated with a complex geometry will be organized internal to the computer code. For example, the operator need not instruct the code that two plates are attached to form a convex or concave structure. The code flags this situation by recognizing that two plates have a common set of corners (i.e., a common edge). So if the operator wishes to attach two plates together he needs only define the two plates as though they were isolated. However, the two plates will have two identical corners. All the geometry information associated with plates with common edges is then generated by the code. The present code also will allow a plate to intersect another plate as shown in Figure 7. It is necessary that the corners defining the attachment be positioned a small amount (approximately 10^{-5} wavelengths) through the plate surface to which it is being connected.

In defining the plate corners it is necessary to be aware of a subtlety associated with simulating convex or concave structures in which two or more plates are used in the computation. This problem results in that each plate has two sides. If the plates are used to simulate a closed or semi-closed structure, then possibly only one side of the plate will be illuminated by the antenna. Consequently, the operator must define the data in such a way that the code can infer which side of the plate is illuminated by the antenna. This is accomplished by defining the plate according to the right-hand rule. As one's fingers of the right hand follow the edges of the plate around in the order of their definition, his thumb should point toward the illuminated region above the plate. To illustrate this constraint associated with data format, let us consider the definition of a rectangular box. In this case, all the plates of

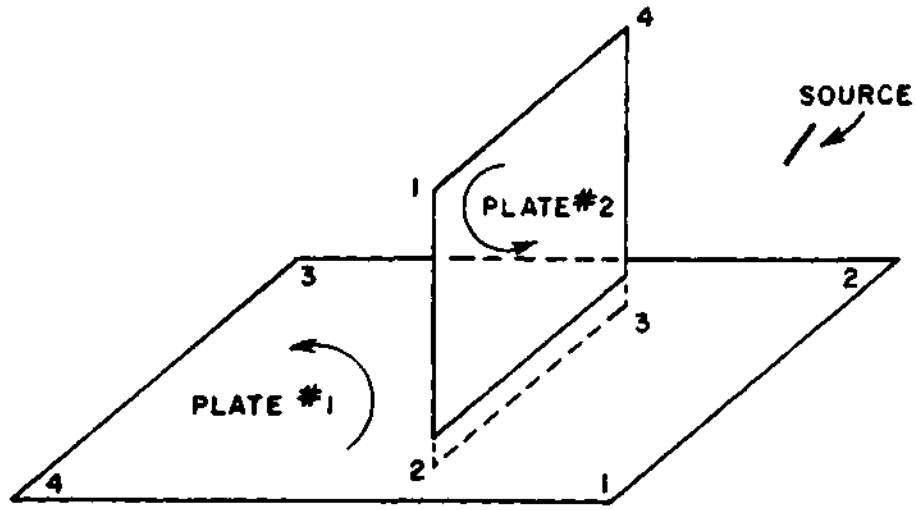

Figure 7. Data format used to define a flat plate intersecting another flat plate.

the box must be specified such that they satisfy the right-hand rule with the thumb pointing outward as illustrated in Figure 8. If this rule were not satisfied for a given plate, then the code would assume that the antenna is within the box as far as the scattering from that plate is concerned.

Another situation which must be kept in mind is associated with antenna elements mounted on a plate. The code automatically determines that the antenna element is mounted on the plate. It assumes that the element will radiate on the side of the plate into which the normal points. This is accomplished in the code by automatically positioning the source a small distance (10^{-5} wavelengths above the plate in the direction of the normal as illustrated in Figure 9. It is important, therefore, to follow the simple rules above for defining the plate normals when dealing with plate mounted antennas.

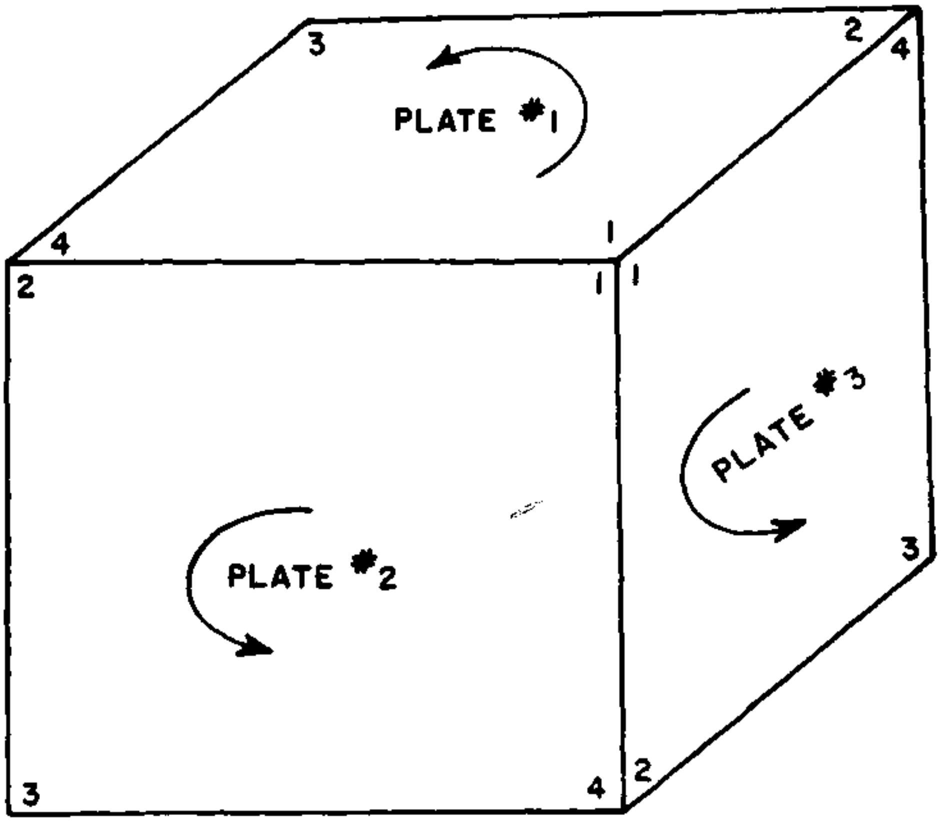

Figure 8. Data format used to define a box structure.

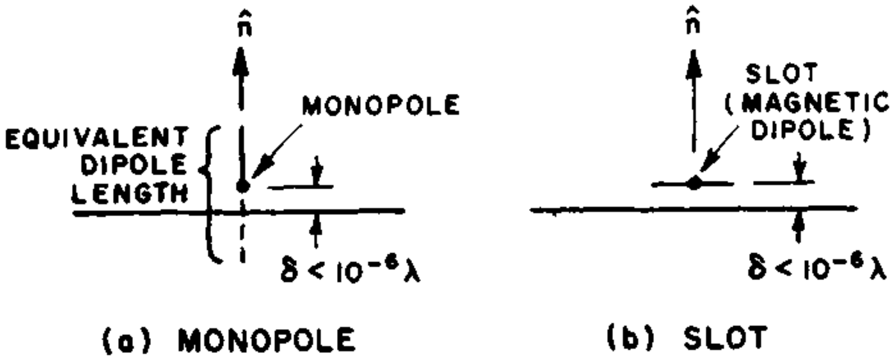

Figure 9. Illustration of geometry for plate-mounted antennas.

There is, also, another point associated with antennas mounted on perfectly-conducting flat structures. If a plate-mounted monopole is considered in the computation, one should input the equivalent dipole length and not the monopole length (i.e., the monopole plus image length should be used as shown in Figure 9a). The code automatically handles the half dipole modes associated with the monopole. The plate-mounted slot is, also, automatically taken care of by the code as shown in Figure 9b if a magnetic dipole is used.

The same situation arises when the antenna is mounted on the elliptic cylinder's end caps. It should also be remembered that the antenna can not be mounted on the curved part of the cylinder. In general, the antenna should be kept a wavelength away, however, this can often be relaxed to approximately a quarter-wavelength.

In the present code, the attachment of a plate corner to the curved surface of the cylinder is automatically detected, however, a diffracted field from the plate-cylinder junction is not considered in this version. If the plate-cylinder junction forms a straight, orthogonal edge, as shown in the aircraft models of Figure 27, image theory alone will give the correct results. The diffracted fields, therefore, are not needed. If the plate-cylinder junction forms a curved edge or one in which the plate and cylinder surface are not orthogonal a diffracted field from that edge will be required in the solution. This will be added when time and effort permit.

Chapter VI has a set of sample problems to illustrate how the operator can realize the versatility of the code and still satisfy the few constraints associated with the input data format.

CHAPTER V

INTERPRETATION OF OUTPUT

The basic output from the computer code is a line printer listing of the results. The results are referenced to the pattern coordinate system that was described in Chapter III and is illustrated in Figure 1. Thus the total electric field is given by

$$\overline{E}(\theta_p,\phi_p) = \hat{\theta}_p E_{\theta p} + \hat{\phi}_p E_{\phi p}.$$

The fields are assumed to be peak values given in volts/unit when the factor e^{-jkR}/R is suppressed in the far field. If an R value is specified using the "RG:" command then the results will be in volts/meter. The results are displayed in three sections. The first output associated with the $E_{\theta p}$ field, the second is output associated with the $E_{\phi p}$ field, and the third is output associated with the total field. The first section is displayed as follows: θ_p, ϕ_p, $E_{\theta p}$, $\underline{/E_{\theta p}}$ (phase of $E_{\theta p}$), $|E_{\theta p}|$ (magnitude of $E_{\theta p}$), $G_{d\theta}$ (directive gain $E_{\theta p}$), $|E_{\theta p}|/|E_{\theta p}|_{max}$ (normalized magnitude of $E_{\theta p}$), $G_{d\ norm}$ (normalized value of the directive gain). The second section is similarly done for the $E_{\phi p}$ field. The third section is displayed as follows: θ_p, ϕ_p, $G_{d\ major}$ (directive gain of E_{major}), $G_{d\ minor}$ (directive gain of E_{minor}), γ (tilt angle of polarization ellipse, axial ratio, G_d (total directive gain), $G_{d\ norm}$ (normalized total directive gain). The above quantities are defined as follows:

$$G_d = \frac{2\pi R^2}{\eta_o P_{rad}} \overline{E} \cdot \overline{E}^* ,$$

$$G_{d\theta} = \frac{2\pi R^2}{\eta_o P_{rad}} |E_{\theta p}|^2$$

$$G_{d\phi} = \frac{2\pi R^2}{\eta_o P_{rad}} |E_{\phi p}|^2 ,$$

$$G_{d\ major} = \frac{2\pi R^2}{\eta_o P_{rad}} |E_{major}|^2 ,$$

$$G_{d\ minor} = \frac{2\pi R^2}{\eta_o P_{rad}} |E_{minor}|^2 ,$$

$$E_{major} = [(|E_{\theta p}|\cos\gamma + |E_{\phi p}|\cos\psi\sin\gamma)^2 + |E_{\phi p}|^2 \sin^2\psi \sin^2\gamma]^{1/2} ,$$

$$E_{minor} = [(|E_{\theta p}|\sin\gamma - |E_{\phi p}|\cos\psi\cos\gamma)^2 + |E_{\phi p}|^2 \sin^2\psi \cos^2\gamma]^{1/2} ,$$

$$\psi = \underline{/E_{\phi p}} - \underline{/E_{\theta p}} , \qquad [7,10]$$

$$\gamma = \frac{1}{2} \tan^{-1}\left(\frac{2|E_{\theta p}||E_{\phi p}| \cos\psi}{|E_{\theta p}|^2 - |E_{\phi p}|^2} \right)$$

$$\text{axial ratio} = \left| \frac{E_{minor}}{E_{major}} \right|$$

η_o = free space impedance.

The value P_{rad} is the power radiated. It is input into the basic scattering code through the AM: command for the NEC moment method data or through the PR: command. If a value for P_{rad} is not given to the code, the output will be given in terms of the radiation intensity rather than the directive gain. The radiation intensity, U, can be defined in terms of the directive gain as

$$G = \frac{4\pi U}{P_{rad}} \quad .$$

A very convenient means of displaying the results of the program is through a polar plot representation. However, because of the difficulty of delivering standard plot routines from one computer system to another, our plot package is not included as an integral part of this computer code. A simple polar plot routine is given in Appendix I which can be used if desired.

The next chapter displays the results in either polar or rectangular dB plots to compare against measured results whenever possible. The results are normalized to either 0 dB or the measured patterns maximum.

CHAPTER VI
APPLICATION OF CODE TO SEVERAL EXAMPLES

The following nine examples are used to illustrate the various features of the computer code. Each example is designed to show how a set of commands can be put together to solve a single problem or a group of problems. In most cases, the input data sets can be constructed in more than one way to accomplish the same results. The particular form of these examples have been chosen so that all the commands are used. As an aid to the user, an echo of the input data is given on the line printer in the form that the computer code has interpreted the data. This is useful for checking that the correct problem has been properly constructed. Also, messages are given when the code misinterprets the data or when an error has been made in the input set. This makes it easier to debug the input data sets. Example 1A illustrates this type of print out. The other examples do not show this output in order to save space in this report.

The computer code has a default list at the beginning of the main program. This list can be set up at the convenience of the user. If the defaults are set up correctly for the particular applications of the user, the same data will not have to be input in the data sets every time. For example, the default list is set up initially to have the code give a line printer output of the results. Since most user's will want this output all the time the LP: command need never be specified as shown in the examples that follow. However, the LP: command can be used to suppress this output if desired. The pen plotter command, PP:, on the other hand, has been set false initially. This is because most computer facilities have different procedures for plotter output. Once the user determines the best way to use this command for his needs and the appropriate plot routines are included in the code, the PP: command can be called to instate the plots or the default list can be changed accordingly.

In the examples that follow, all the results have been shown graphically in some form. This is the most concise way to show the results and to illustrate the validity of the codes operation by comparing against measurements. A few of the examples, however, contain the line printer output of the results so that the output numbers can be checked to verify that the computer being used is giving correct results. Different computers have different accuracies so that the numbers may not check in the last few decimal places. Example 9 can be conveniently used to check the operation of the code on a new computer. It contains three examples that have line printer output.

Example 1A. Consider the pattern of an electric dipole in the presence of a finite ground plane as shown in Figure 10a. The input data for the H-plane pattern is given by

```
CE:   PLATE TEST, EXAMPLE 1A.
UN:   UNITS IN INCHES
3
FR:   FREQUENCY IN GHZ.
8.Ø
PD:   PATTERN CUT
Ø.,Ø.,9Ø.,Ø.
1,9Ø.
Ø,36Ø,1
PG:   PLATE GEOMETRY
4
Ø.,3.5,3.5
Ø.,-3.5,3.5
Ø.,-3.5,-3.5
Ø.,3.5,-3.5
SG:   SOURCE GEOMETRY
5.12,Ø.,Ø.
Ø.,Ø.,9Ø.,Ø.
Ø,Ø.5,Ø.
1.,Ø.
XQ:   EXECUTE CODE
EN:   END CODE
```

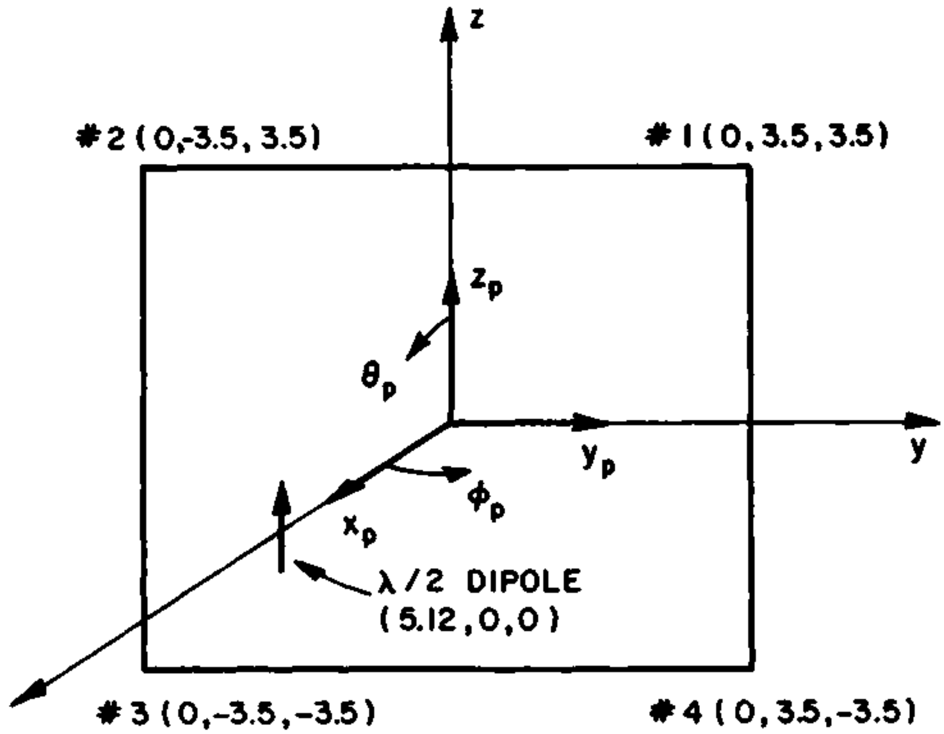

Figure 10a. Dipole in presence of a square ground plane.

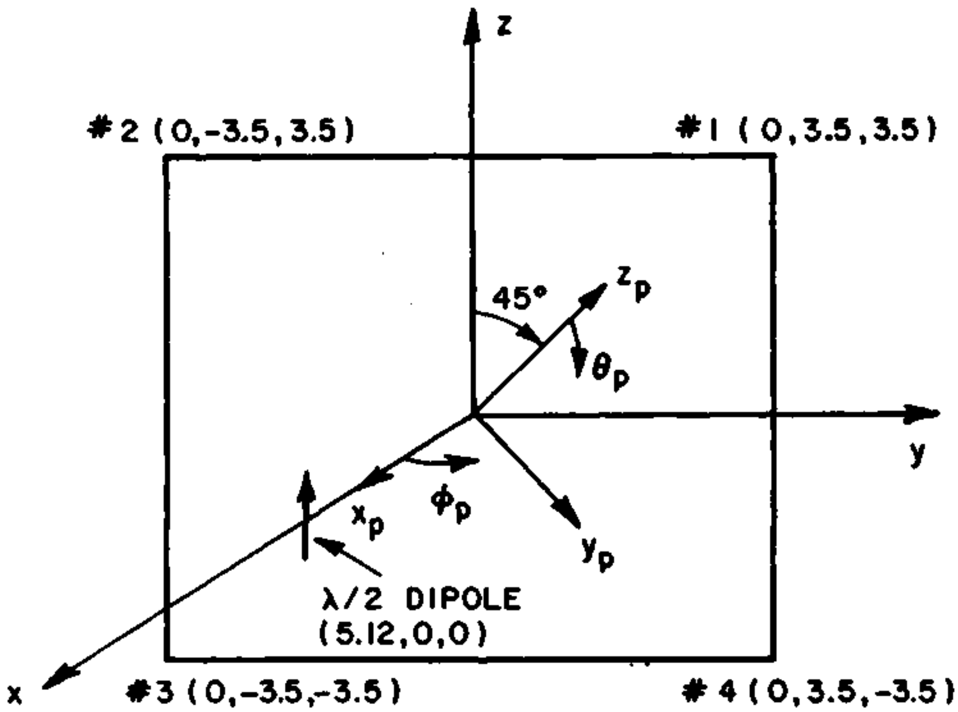

Figure 10b. Dipole in presence of a square ground plane with a pattern cut corresponding to Example 1c.

The computer code prints out on the line printer the information in Figure 11 pertaining to the input data. This information can help the user decipher how the computer code interpreted the input data. It also provides messages to the user if the input data is found to be incorrect by the code.

The calculated results for the electric field are printed out on the line printer as shown in Figure 12. The output shown in Figure 12 is for 10° increments from 0° to 180°. This is from the input data in Example 9. Note that the normalized data columns may be slightly different for the 10° increment case than for the 1° increment case, since the maximum value may be found to be a different number.

The $E_{\theta p}$ pattern is compared with the measured results in Figure 13a. The $E_{\phi p}$ pattern is not plotted because it is of negligible value.

```
CE:   PLATE TEST, EXAMPLE 1A.
```

```
UN:   UNITS IN INCHES

   ALL THE LINEAR DIMENSIONS BELOW ARE ASSUMED TO BE IN INCHES
```

```
FR:   FREQUENCY IN GHZ.

   FREQUENCY=   8.000 GIGAHERTZ

   WAVELENGTH=    .037474 METERS
```

```
PD:   PATTERN CUT

   THE PATTERN AXES ARE AS FOLLOWS:

   XPD(1)=   1.00000  XPD(2)=   0.00000  XPD(3)=    .00000

   YPD(1)=   0.00000  YPD(2)=   1.00000  YPD(3)=   0.00000

   ZPD(1)=   0.00000  ZPD(2)=   0.00000  ZPD(3)=   1.00000

   PHI IS BEING VARIED WITH THETA=   90.00000

   THE RANGE OF PATTERN ANGLE INDICES FOR THIS RUN ARE:   0,360,  1
```

Figure 11. Line printer output for the code's interpretation of the input data set of Example 1A. The figure is continued on the next page.

```
PG:   PLATE GEOMETRY

   THIS IS PLATE NO.   1 IN THIS SIMULATION.

PLATE#  CORNER#   INPUT LOCATION IN INCHES    ACTUAL LOCATION IN METERS
------  -------  -------------------------   --------------------------

   1       1       0.000,  3.500,  3.500     0.000,    .089,    .089
   1       2       0.000, -3.500,  3.500     0.000,   -.089,    .089
   1       3       0.000, -3.500, -3.500     0.000,   -.089,   -.089
   1       4       0.000,  3.500, -3.500     0.000,    .089,   -.089
```

```
SG:   SOURCE GEOMETRY

   THIS IS SOURCE NO.   1 IN THIS COMPUTATION.

   THIS IS AN ELECTRIC SOURCE.
   SOURCE LENGTH=    .50000 AND WIDTH=   0.00000 WAVELENGTHS
   THE SOURCE WEIGHT WAS MAGNITUDE=   1.00000 AND PHASE=   0.00000

 SOURCE#    INPUT LOCATION IN INCHES     ACTUAL LOCATION IN METERS
 -------   -------------------------   -------------------------

    1       5.120,   0.000,   0.000       .130,   0.000,   0.000

   THE FOLLOWING SOURCE ALIGNMENT IS USED:
 VXSS(1,1, 1)=  1.00000  VXSS(1,2, 1)=  0.00000  VXSS(1,3, 1)=   .00000
 VXSS(2,1, 1)=  0.00000  VXSS(2,2, 1)=  1.00000  VXSS(2,3, 1)=  0.00000
 VXSS(3,1, 1)=  0.00000  VXSS(3,2, 1)=  0.00000  VXSS(3,3, 1)=  1.00000
```

```
XQ:   EXECUTE CODE
```

```
EN:   END CODE
```

E-THETA PATTERN

THE FIELDS ARE REFERENCED TO THE PATTERN COORDINATE SYSTEM

THETA	PHI	E-THETA				PHASE	UNNORMALIZED MAGNITUDE		UNNORMALIZED DB INTEN.	NORMALIZED MAGNITUDE	NORMALIZED DB
90.00000	0.00000	.12376E	1	-.12724E	2	-84.44437	.12784E	2	-6.64028	.11351	-18.89917
90.00000	10.00000	-.51460E	2	.88321E	1	170.26131	.52213E	2	5.58193	.46361	-6.67696
90.00000	20.00000	-.11261E	3	.19488E	1	179.00853	.11262E	3	12.25889	1.00000	-.00000
90.00000	30.00000	-.78109E	1	.19556E	2	111.77550	.21061E	2	-2.30399	.18701	-14.56208
90.00000	40.00000	.75193E	2	-.33694E	2	-24.13689	.82397E	2	9.54460	.73162	-2.71429
90.00000	50.00000	-.56752E	2	.25964E	2	155.41561	.62409E	2	7.13134	.55414	-5.12755
90.00000	60.00000	.46746E	2	-.40074E	1	-4.90002	.46918E	2	4.65316	.41659	-7.60574
90.00000	70.00000	-.63154E	2	.13912E	2	167.57705	.64668E	2	7.44917	.57420	-4.81872
90.00000	80.00000	.35070E	2	-.58629E	2	-59.11327	.68317E	2	7.91701	.60660	-4.34199
90.00000	90.00000	.14806E	1	.49803E	2	88.28796	.49825E	2	5.17536	.44241	-7.08354
90.00000	100.00000	-.37052E	2	-.58629E	2	-122.29206	.69356E	2	8.04803	.61582	-4.21087
90.00000	110.00000	.47546E	2	.13912E	2	16.30925	.49540E	2	5.12544	.43987	-7.13345
90.00000	120.00000	-.72733E	2	-.40074E	1	-176.84619	.72844E	2	8.47422	.64679	-3.78448
90.00000	130.00000	.62367E	2	.25964E	2	22.60283	.67556E	2	7.01963	.59984	-4.43926
90.00000	140.00000	-.25491E	2	-.33694E	2	-127.10975	.42250E	2	3.74292	.37515	-8.51597
90.00000	150.00000	-.37427E	1	.19556E	2	100.83462	.19910E	2	-2.79198	.17679	-15.05088
90.00000	160.00000	.71048E	1	.19488E	1	15.33842	.73672E	1	-11.42759	.06541	-23.68648
90.00000	170.00000	.79130E	1	.88321E	1	48.14149	.11858E	2	-7.29311	.10529	-19.55208
90.00000	180.00000	.23466E	2	-.12724E	2	-28.46747	.26694E	2	-.24534	.23702	-12.50423

Figure 12a. Line printer output for the $E_{\theta p}$ fields of Example 1A and Example 9.

E-PHI PATTERN

THE FIELDS ARE REFERENCED TO THE PATTERN COORDINATE SYSTEM

THETA	PHI	E-PHI		PHASE	UNNORMALIZED MAGNITUDE	UNNORMALIZED DB INTEN.	NORMALIZED MAGNITUDE	NORMALIZED DB
90.00000	0.00000	-.85227E-12	-.17738E-11	0.00000	.10000E -9	-220.77361	.00202	-53.88047
90.00000	10.00000	-.51251E -8	.28640E -7	100.14552	.29095E -7	-179.49721	.58857	-4.60406
90.00000	20.00000	-.49160E -7	.25512E -8	177.02926	.49226E -7	-174.92966	.99580	-.03652
90.00000	30.00000	.11629E -7	-.41580E -7	-74.37535	.43176E -7	-176.06880	.87341	-1.17566
90.00000	40.00000	.22661E -7	.15428E -7	34.24736	.27414E -7	-180.01413	.55456	-5.12099
90.00000	50.00000	-.13908E -7	.12032E -7	139.13588	.18390E -7	-183.48202	.37201	-8.58887
90.00000	60.00000	.19378E -9	-.12225E -8	-80.99254	.12377E -8	-206.92105	.02504	-32.02790
90.00000	70.00000	.64132E -9	-.39100E -9	-31.37004	.75111E -9	-211.25954	.01519	-36.36640
90.00000	80.00000	.30234E -9	-.82856E-10	-15.32556	.31349E -9	-218.84921	.00634	-43.95607
90.00000	90.00000	.11125E-10	-.10214E -9	-90.00000	.10274E -9	-228.53844	.00208	-53.64530
90.00000	100.00000	-.30234E -9	.82856E-10	164.67444	.31349E -9	-218.84921	.00634	-43.95607
90.00000	110.00000	-.64132E -9	.39100E -9	148.62996	.75111E -9	-211.25954	.01519	-36.36640
90.00000	120.00000	-.19378E -9	.12225E -8	99.00746	.12377E -8	-206.92105	.02504	-32.02790
90.00000	130.00000	.13928E -7	-.12047E -7	-40.85977	.18415E -7	-183.47010	.37252	-8.57696
90.00000	140.00000	-.22549E -7	-.15521E -7	-145.45982	.27374E -7	-180.02690	.55375	-5.13376
90.00000	150.00000	-.11669E -7	.41403E -7	105.73944	.43016E -7	-176.10095	.87018	-1.20780
90.00000	160.00000	.49362E -7	-.26603E -8	-3.08493	.49434E -7	-174.89314	1.00000	.00000
90.00000	170.00000	.50898E -8	-.28707E -7	-79.94580	.29155E -7	-179.47942	.58977	-4.59628
90.00000	180.00000	.76510E-12	.15983E-11	0.00000	.10000E -9	-220.77361	.00202	-53.88047

Figure 12b. Line printer output for the $E_{\phi p}$ fields of Example 1A and Example 9.

TOTAL RADIATION INTENSITY IN DB.

THE FIELDS ARE REFERENCED TO THE PATTERN COORDINATE SYSTEM

THETA	PHI	MAJOR	MINOR	TILT ANG	AXIAL RATIO	TOTAL INTEN.	NORM INTEN.
90.00000	0.00000	-6.64028	-128.77361	.00000	.00000	-6.64028	-18.89917
90.00000	10.00000	5.58193	-128.77361	.00000	.00000	5.58193	-6.67696
90.00000	20.00000	12.25889	-128.77361	.00000	.00000	12.25889	-.00000
90.00000	30.00000	-2.30399	-128.77361	-.00000	.00000	-2.30399	-14.56288
90.00000	40.00000	9.54460	-128.77361	.00000	.00000	9.54460	-2.71429
90.00000	50.00000	7.13134	-128.77361	.00000	.00000	7.13134	-5.12755
90.00000	60.00000	4.65316	-128.77361	.00000	.00000	4.65316	-7.60574
90.00000	70.00000	7.44017	-128.77361	-.00000	.00000	7.44017	-4.81872
90.00000	80.00000	7.91701	-128.77361	.00000	.00000	7.91701	-4.34189
90.00000	90.00000	5.17536	-128.77361	-.00000	.00000	5.17536	-7.08354
90.00000	100.00000	8.04803	-128.77361	.00000	.00000	8.04803	-4.21087
90.00000	110.00000	5.12544	-128.77361	-.00000	.00000	5.12544	-7.13345
90.00000	120.00000	8.47422	-128.77361	.00000	.00000	8.47422	-3.78468
90.00000	130.00000	7.81963	-128.77361	.00000	.00000	7.81963	-4.43926
90.00000	140.00000	3.74292	-128.77361	.00000	.00000	3.74292	-8.51597
90.00000	150.00000	-2.79198	-128.77361	.00000	.00000	-2.79198	-15.05088
90.00000	160.00000	-11.42759	-128.77361	.00000	.00000	-11.42759	-23.68648
90.00000	170.00000	-7.29311	-128.77361	-.00000	.00000	-7.29311	-19.55200
90.00000	180.00000	-.24534	-128.77361	.00000	.00000	-.24534	-12.50423

Figure 12c. Line printer output for the total radiation intensity of Example 1A and Example 9.

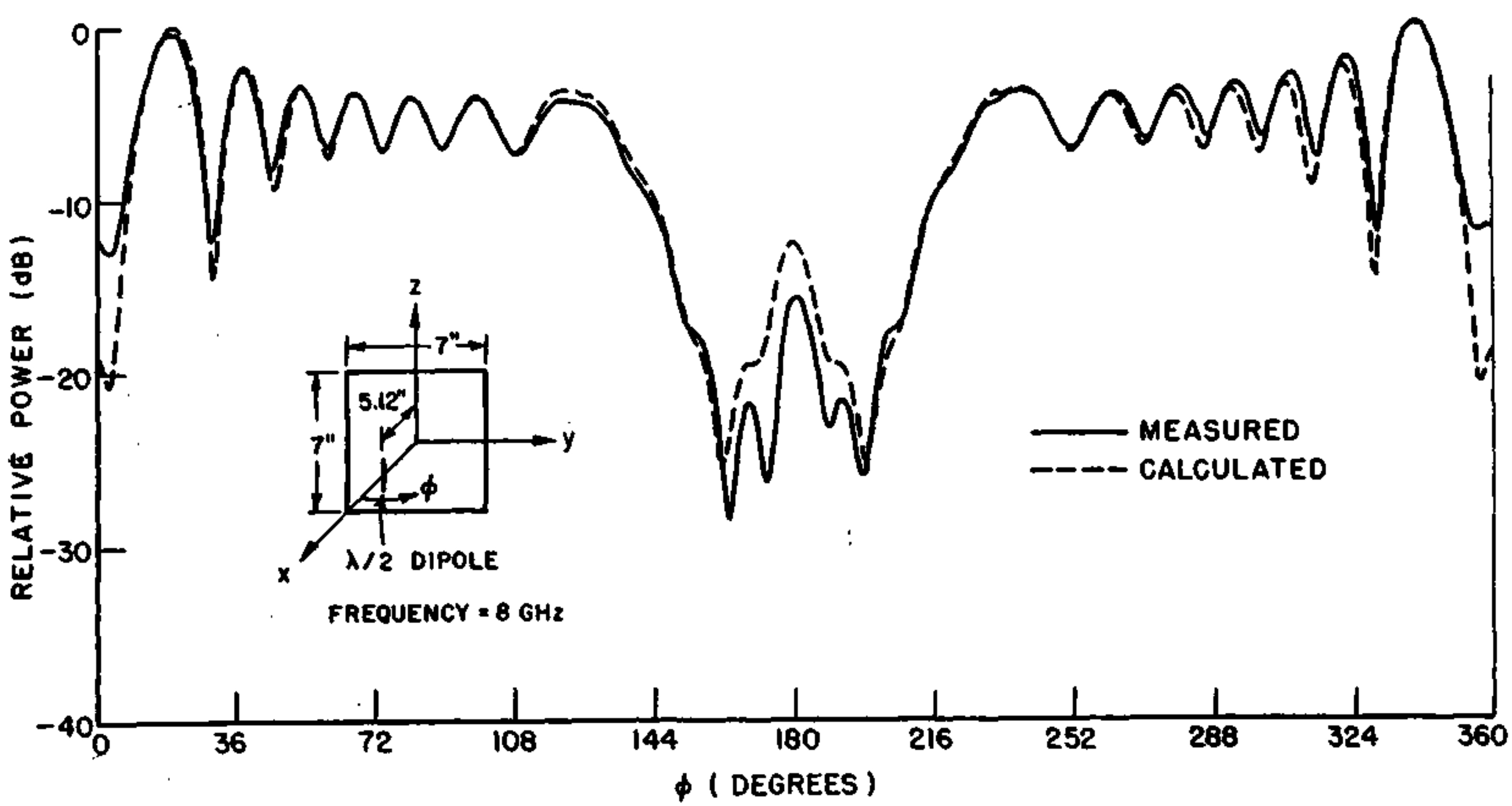

Figure 13a. Comparison of measured and calculated H-plane pattern ($E_{\theta p}$) for a half-wave dipole located above a square plate.

Example 1B. Consider the E-plane pattern of the electric dipole in the presence of the finite ground plane in Figure 10a. This problem is the same as Example 1A except that the pattern cut information is changed so that the phi angle is fixed and the theta angle is varied. The input data is given by

```
CE:    PLATE TEST, EXAMPLE 1B.
US:    UNITS IN INCHES
3
FR:    FREQUENCY IN GHZ.
6.0
PD:    PATTERN CUT
0.,0.,90.,0.
F,0.
0,360,1
PG:    PLATE GEOMETRY
4
0.,3.5,3.5
0.,-3.5,3.5
0.,-3.5,-3.5
0.,3.5,-3.5
SG:    SOURCE GEOMETRY
5.12,1.,0.
0.,0.,90.,0.
0,0.5,0.
1.,0.
XQ:    EXECUTE CODE
EN:    END CODE
```

The $E_{\theta p}$ pattern is compared with the measured results in Figure 13b. The $E_{\phi p}$ pattern is not plotted because it is of negligible value.

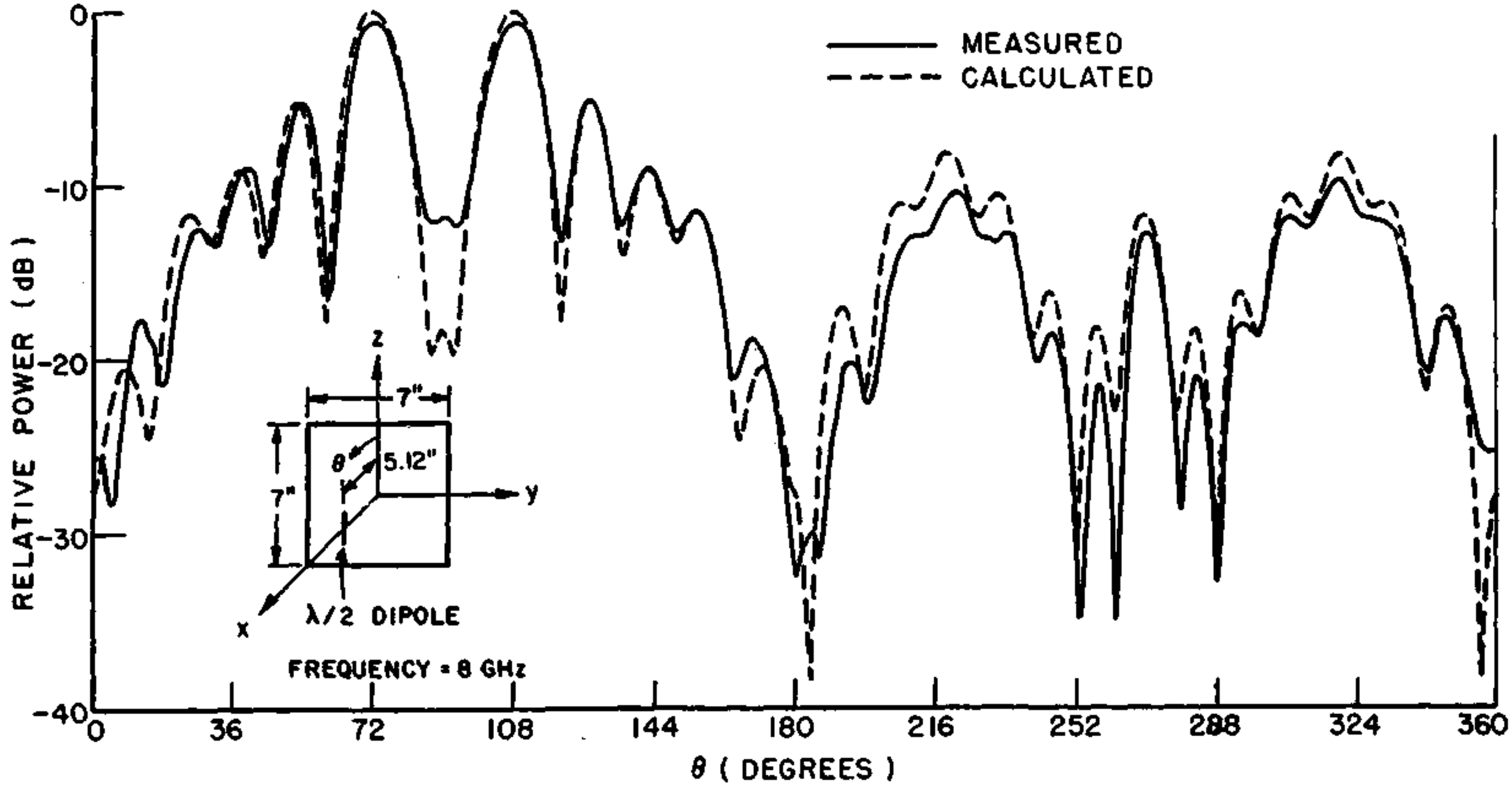

Figure 13b. Comparison of measured and calculated E-plane pattern ($E_{\theta p}$) for a half-wave dipole located above a square plate.

Example 1C. Consider the pattern of the electric dipole taken across the corner of the finite ground plane in Figure 10b. This problem is the same as in Example 1A except that the pattern cut coordinate system is changed. The input data is given by

```
CE:   FLAT TEST, EXAMPLE 1C.
CE:   UNITS IN INCHES
3
FR:   FREQUENCY IN GHZ.
6.6
PD:   PATTERN CUT
45.,90.,90.,0.
1,90.
0,360,1
PG:   PLATE GEOMETRY
4
0.,3.5,3.5
0.,-3.5,3.5
0.,-3.5,-3.5
0.,3.5,-3.5
SG:   SOURCE GEOMETRY
5.12,0.,0.
0.,0.,90.,0.
0.,.5,0.
1.,0.
XQ:   EXECUTE CODE
EN:   END CODE
```

The $E_{\theta p}$ pattern is compared with its measured result in Figure 13c and the $E_{\phi p}$ pattern compared with its measured result in Figure 13d.

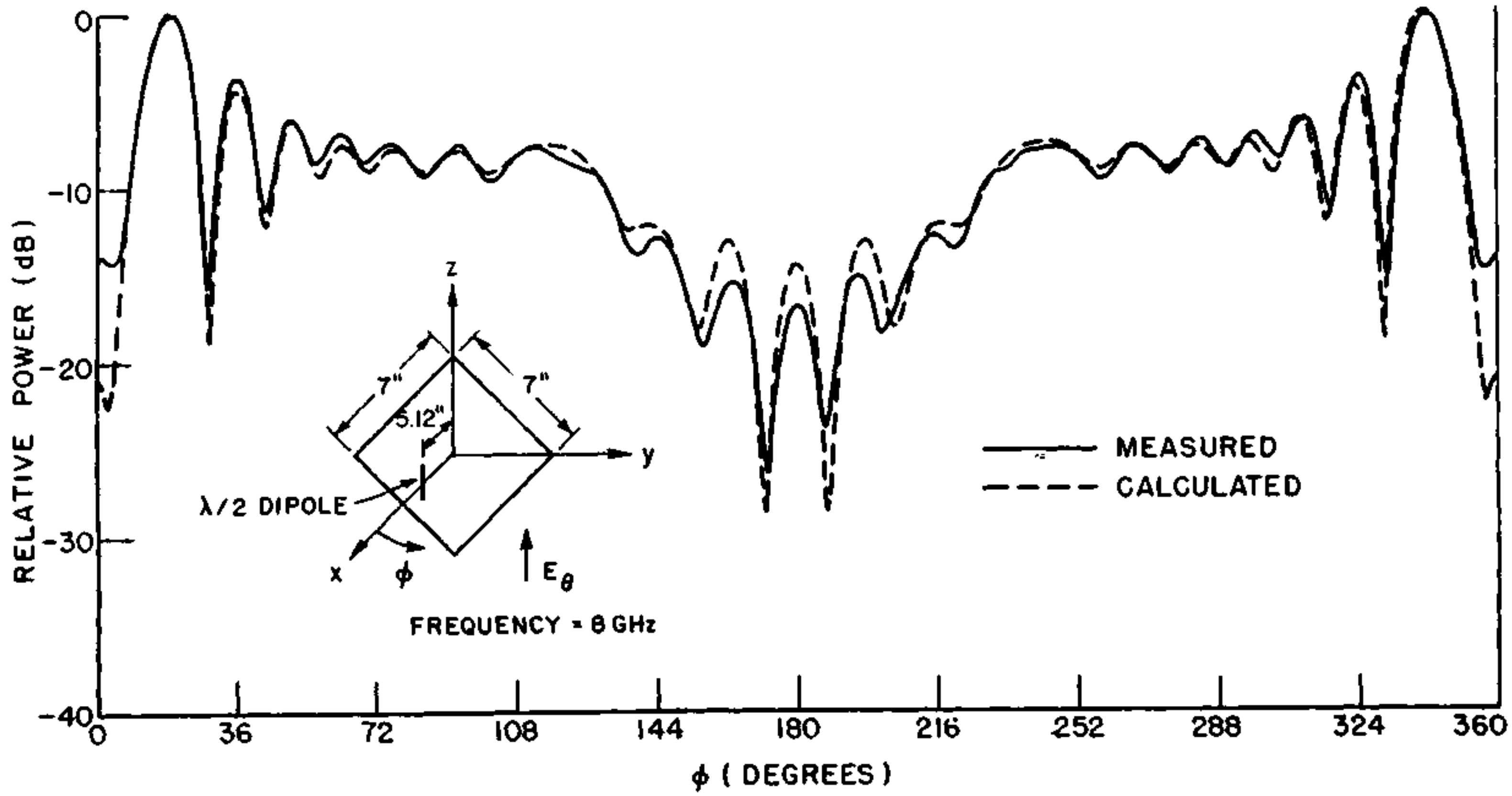

Figure 13c. Comparison of measured and calculated $E_{\theta\theta}$ pattern taken over the corner of a square plate with a half-wave dipole mounted above it.

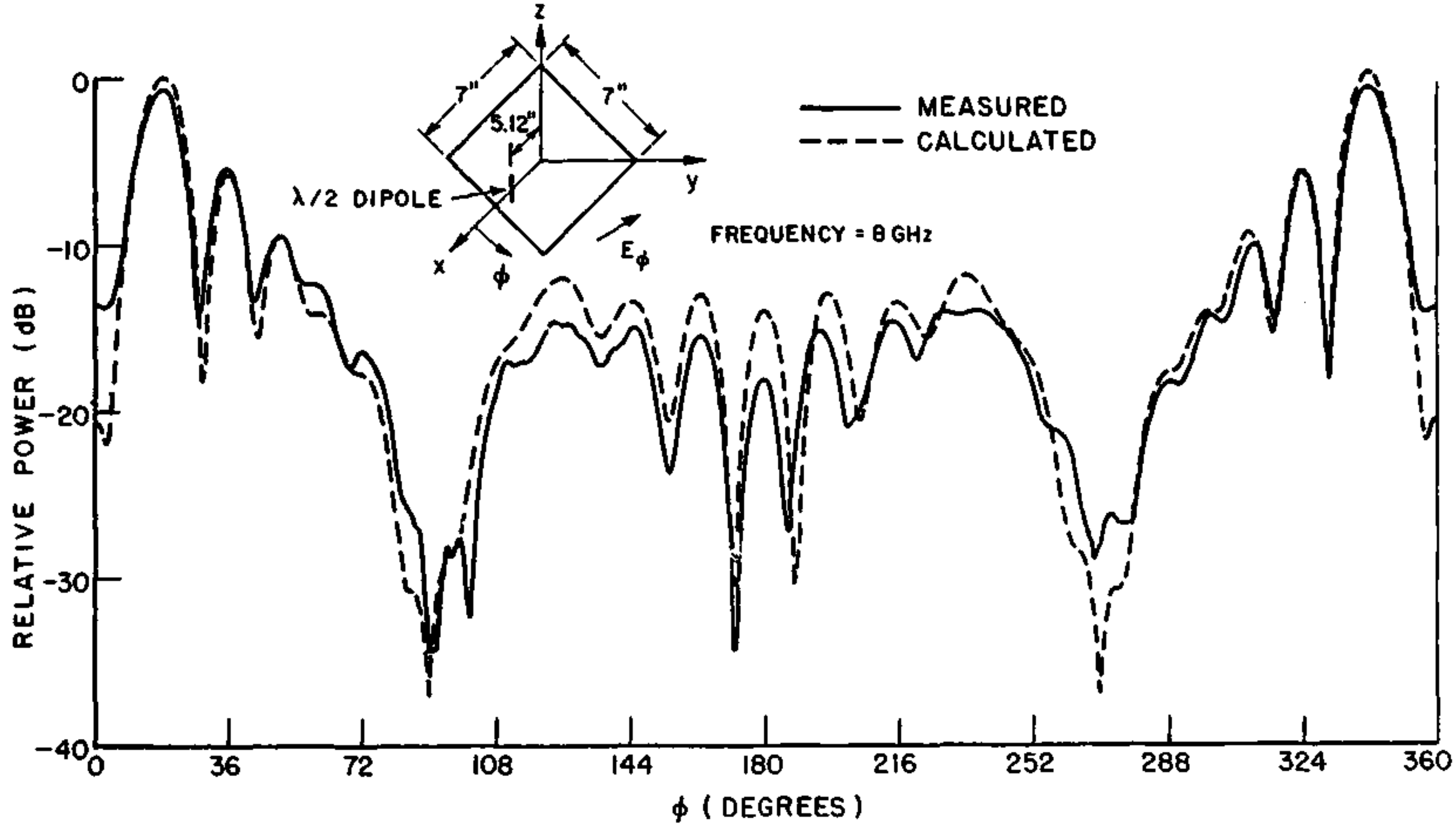

Figure 13d. Comparison of measured and calculated $E_{\phi p}$ pattern taken over the corner of a square plate with a half-wave dipole mounted above it.

Example 2. Consider the pattern of a $\lambda/2$ slot antenna mounted in the center of a square ground plane as shown in Figure 14. The pattern cut is taken across the corner of the plate. This example illustrates how the TO: command can be used to show the strength of a particular diffraction mechanism by removing the mechanism from the computation for comparison. In this case the corner diffracted fields are removed in the second execution by setting LCORNR=.FALSE. Of course, other fields can be modified in other problems by using the JMN's and JMX's numbers. The input data for this example is given by

```
CE:    PLATE TEST, EXAMPLE 2.
UN:
3
FR:
1Ø.
PD:    PATTERN CUT OVER CORNER
Ø.,Ø.,9Ø.,Ø.
F,45.
Ø,36Ø,1
PG:
4
6.,6.,Ø.
-6.,6.,Ø.
-6.,-6.,Ø.
6.,-6.,Ø.
SG:
Ø.,Ø.,Ø.
9Ø.,9Ø.,9Ø.,Ø.
1,Ø.5,Ø.
1.,Ø.
XQ:
TO:    REMOVE CORNER DIFFRACTION
F,F,F
T,F,F
1,7,1,3,1,4
XQ:
EN:
```

The results with and without the corner diffracted fields included are compared in Figure 15a and b for the $E_{\theta p}$ and $E_{\phi p}$ fields, respectively.

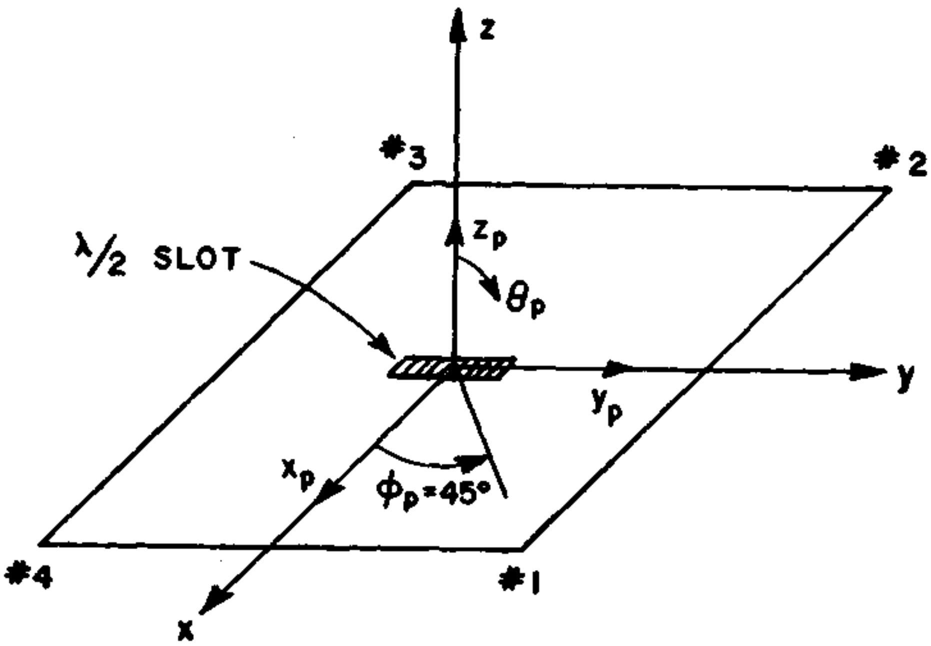

Figure 14. A λ/2 slot mounted on top of a square ground plane.

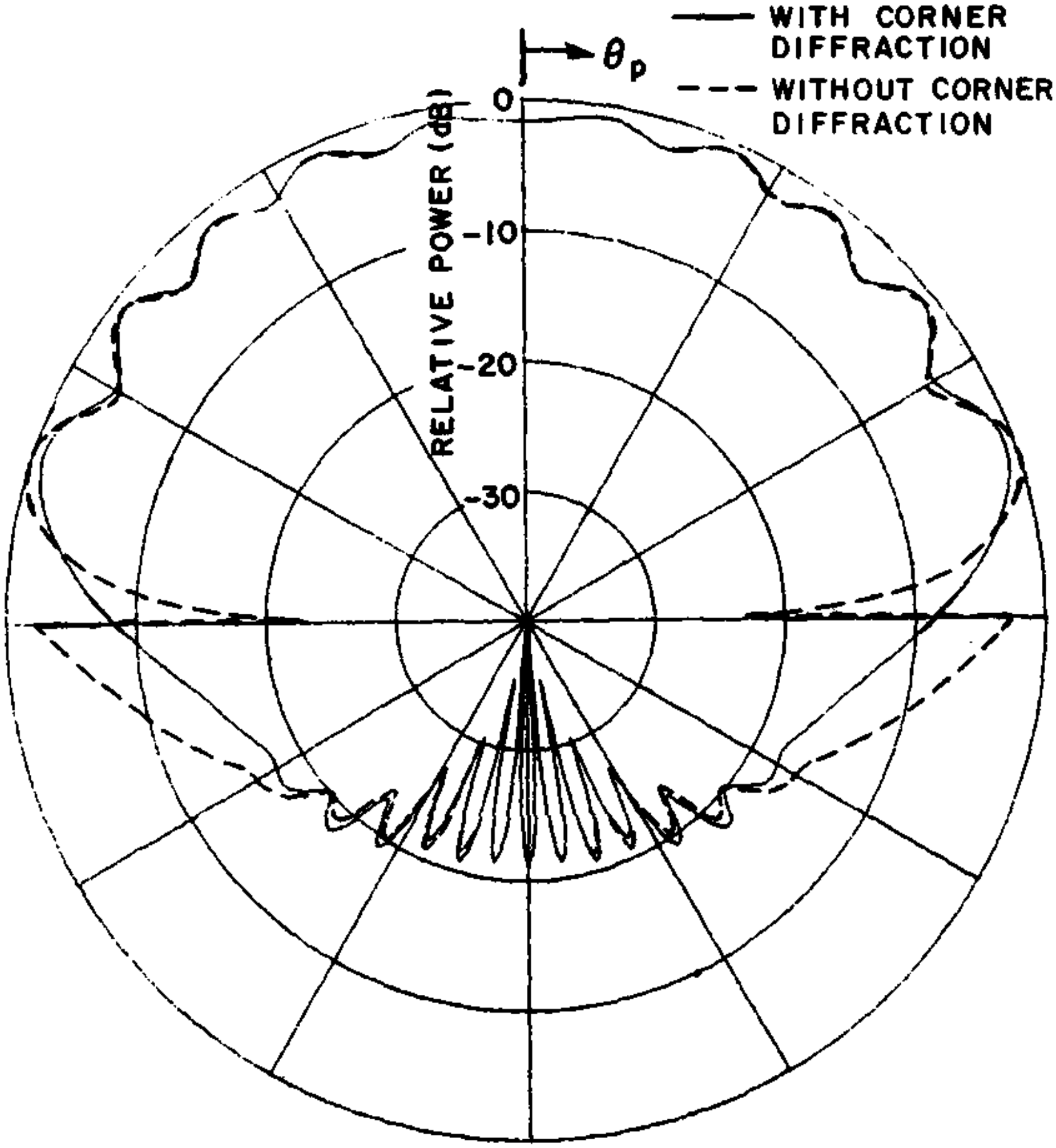

Figure 15a. Comparison of E_{θ_p} pattern with and without corner diffracted fields for a half-wave slot antenna mounted on a square plate.

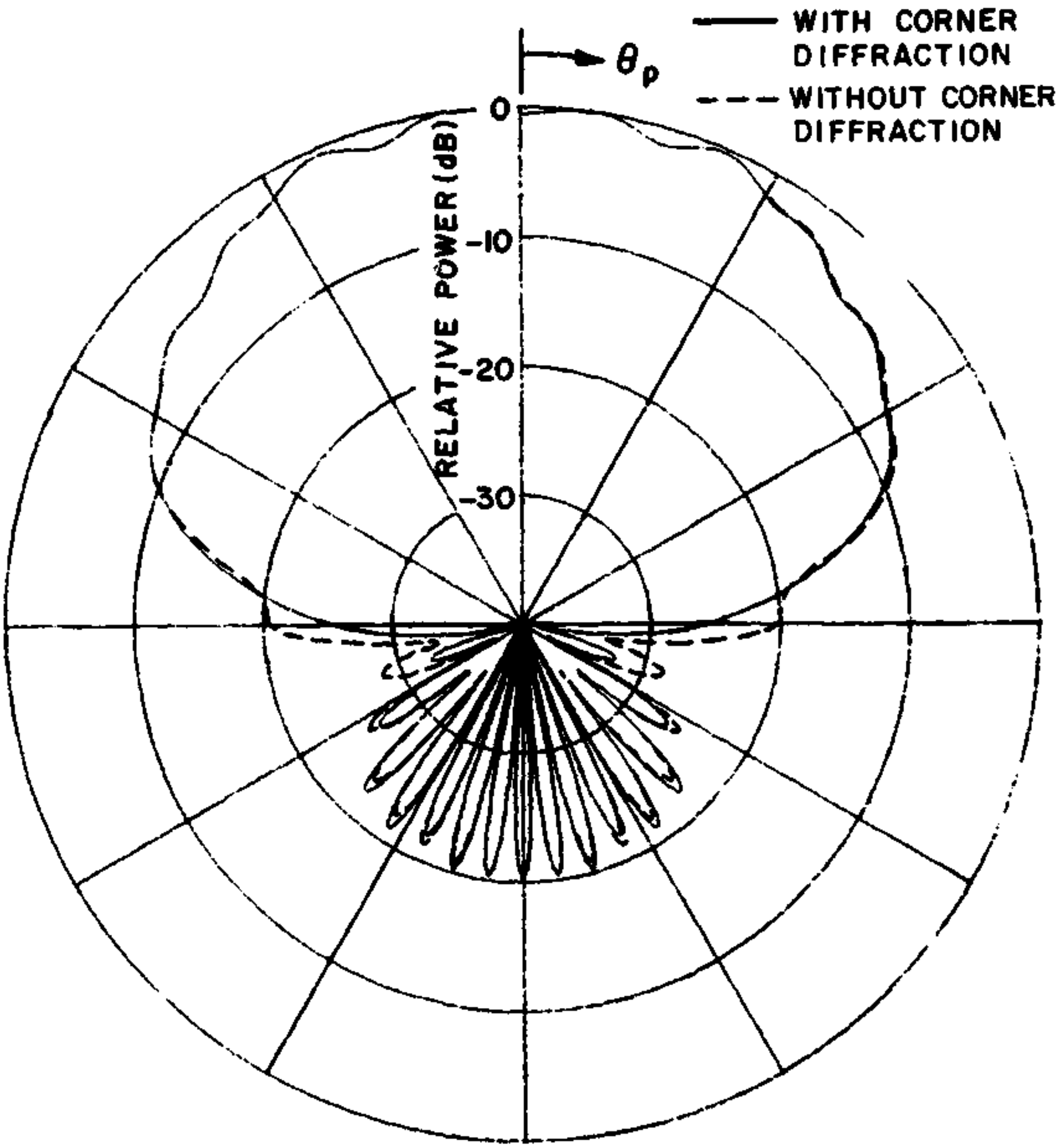

Figure 15b. Comparison of $E_{\phi p}$ pattern with and without corner diffracted fields for a half-wave slot antenna mounted on a square plate.

Example 3. Consider the pattern of an electric dipole in the presence of an eight-sided box as shown in Figure 16. The input data is given by

```
CE:   EIGHT SIDED BOX TEST, EXAMPLE 3.
FR:
9.94
PD:
Ø.,Ø.,9Ø.,Ø.
T,9Ø.
Ø,36Ø,1
SG:
.212,Ø.,Ø.
9Ø.,9Ø.,9Ø.,Ø.
Ø,Ø.5,Ø.Ø
1.,Ø.
PG:  FRONT
4
.122,.1Ø23,-.1
.122,.1Ø23,.1
.122,-.1Ø23,.1
.122,-.1Ø23,-.1
PG:  RIGHT FRONT
4
Ø.,.17Ø7,-.1
Ø.,.17Ø7,.1
.122,.1Ø23,.1
.122,.1Ø23,-.1
PG:  RIGHT BACK
4
-.122,.1Ø23,-.1
-.122,.1Ø23,.1
Ø.,.17Ø7,.1
Ø.,.17Ø7,-.1
PG:  BACK
4
-.122,-.1Ø23,-.1
-.122,-.1Ø23,.1
-.122,.1Ø23,.1
-.122,.1Ø23,-.1
PG:  LEFT BACK
4
Ø.,-.17Ø7,-.1
Ø.,-.17Ø7,.1
-.122,-.1Ø23,.1
-.122,-.1Ø23,-.1
```

```
PG: [illegible]
4
.122,-.1023,-.1
.122,-.1023,.1
0.,-.1707,.1
0.,-.1707,-.1
PG: TOP
0
0.,.1707,.1
-.122,.1023,.1
-.122,-.1023,.1
0.,-.1707,.1
.122,-.1023,.1
.122,.1023,.1
PG: BOTTOM
0
0.,.1707,-.1
.122,.1023,-.1
.122,-.1023,-.1
0.,-.1707,-.1
-.122,-.1023,-.1
-.122,.1023,-.1
XQ:
[illegible]:
```

The $E_{\theta p}$ pattern is compared with measured results[11] in Figure 17. The $E_{\phi p}$ pattern is not plotted because it is of negligible value.

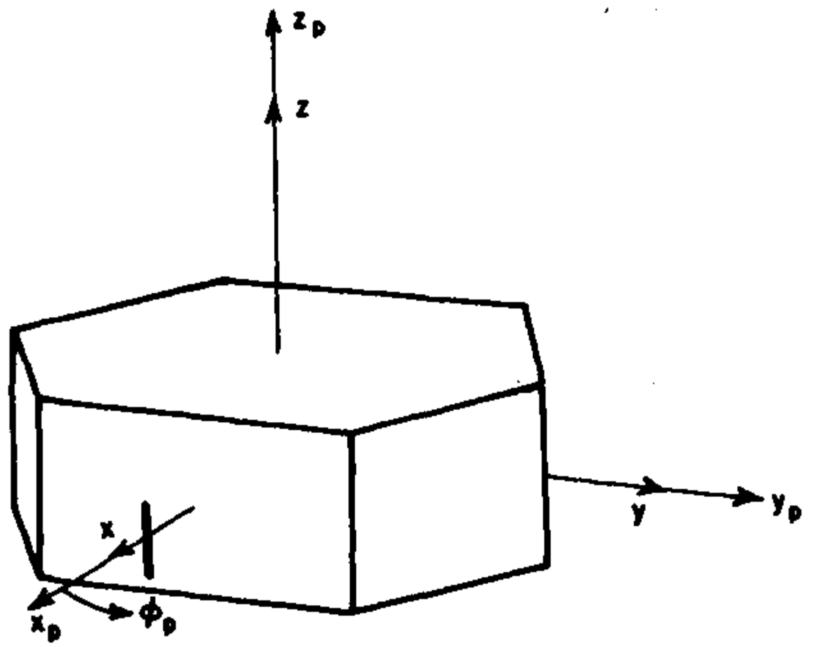

Figure 16. Electric dipole in the presence of an eight sided box.

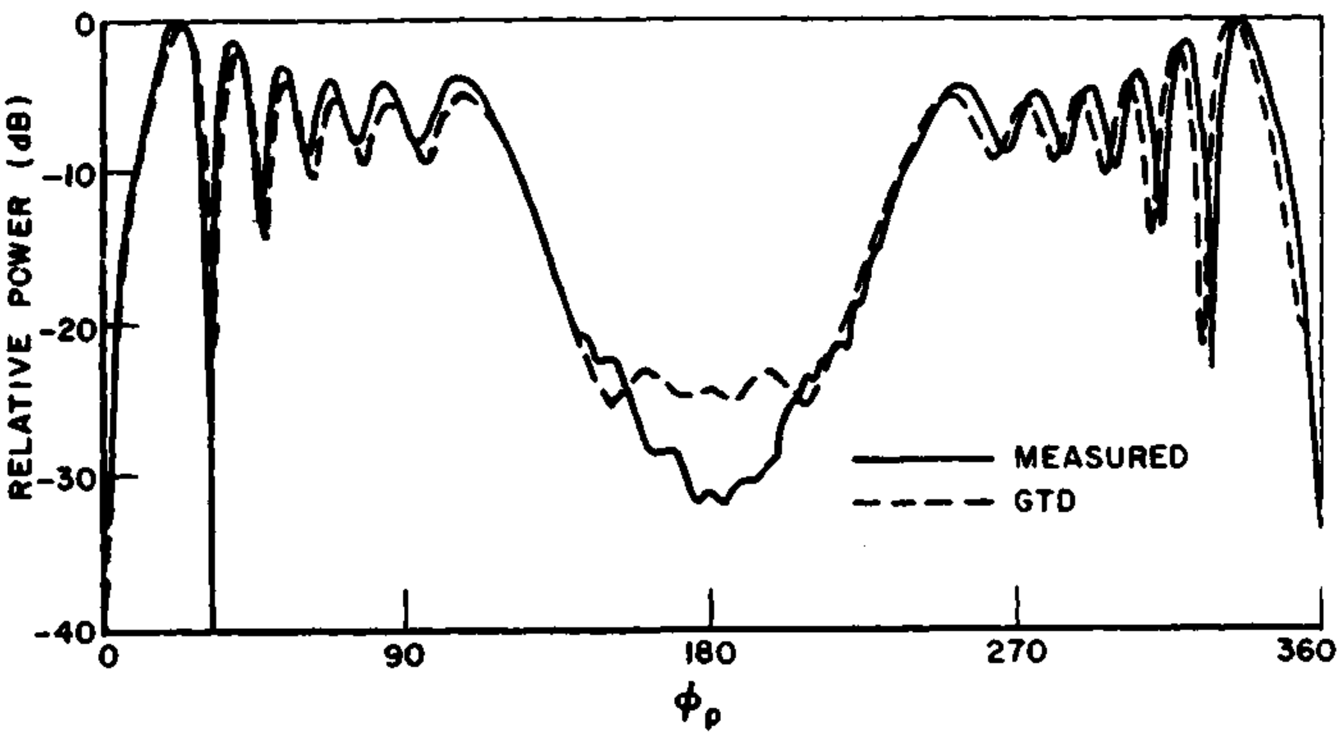

Figure 17. Comparison of measured (Bach) and calculated radiation pattern for E_{θ_p} for an electric dipole in the presence of an eight sided box.

Example 4. Consider an electric dipole in the presence of a finite circular cylinder as shown in Figure 18. This example illustrates how once the cylinder geometry is set up different cases can be run by just varying the data which needs to be changed for that particular case. The input data is given by

```
CE:    CYLINDER TEST, EXAMPLE 4A.
FR:
9.94
PD:
Ø.,Ø.,9Ø.,Ø.
T,9Ø.
Ø,36Ø,1
SG:
Ø.,Ø.19,Ø.
9Ø.,Ø.,18Ø.,Ø.
Ø,Ø.5,Ø.
1.,Ø.
CG:
Ø.1,Ø.1
-Ø.11,9Ø.,Ø.11,9Ø.
XQ:
CE:    CYLINDER TEST, EXAMPLE 4B.
PD:    CHANGE PATTERN CUT
Ø.,Ø.,9Ø.,Ø.
P,9Ø.
Ø,36Ø,1
XQ:
CE:    CYLINDER TEST, EXAMPLE 4C.
NS:    CALL FOR NEW SOURCE
SG:
Ø.Ø7Ø,Ø.,Ø.2
9Ø.,Ø.,18Ø.,Ø.
Ø,Ø.5,Ø.
1.,Ø.
XQ:
EN:
```

The line printer output of the results for Example 4A are shown in Figure 19. The input data is really that of Example 9 where only half the pattern is computed in 10^0 increments.

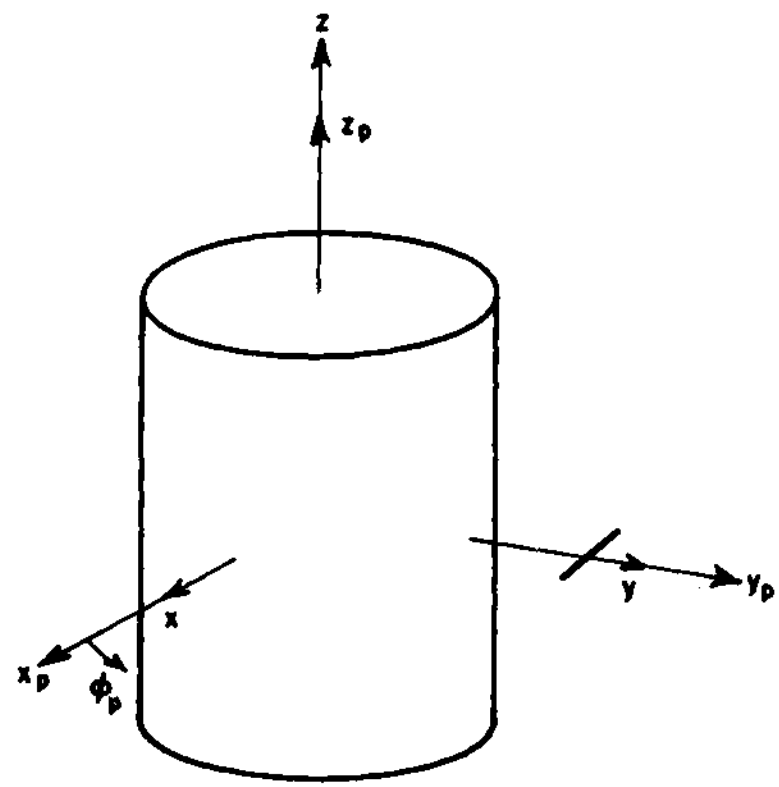

Figure 18a. An electric dipole in the presence of a finite circular cylinder (pattern taken in x-y plane).

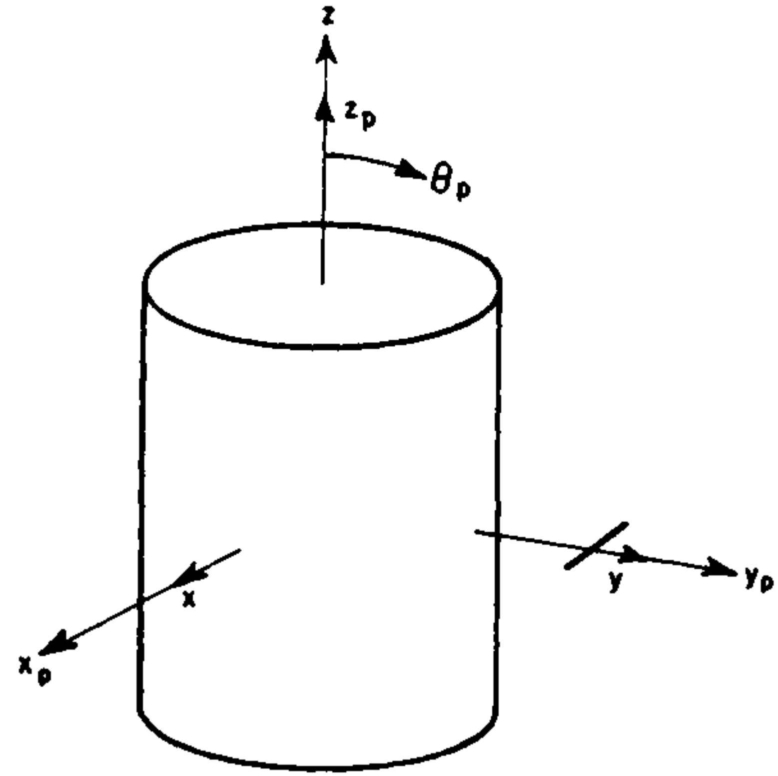

Figure 18b. An electric dipole in the presence of a finite circular cylinder (pattern taken in y-z plane).

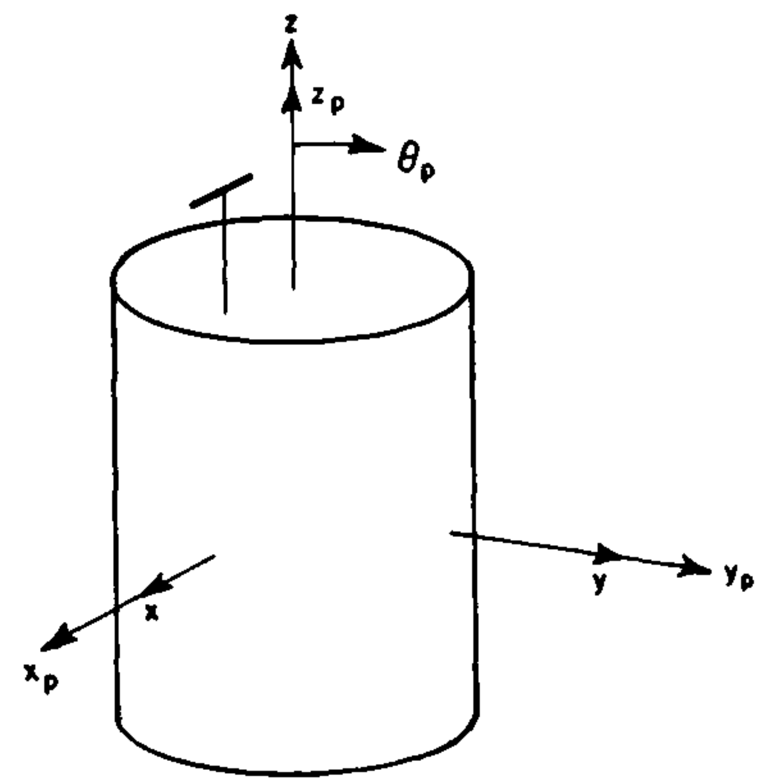

Figure 18c. An electric dipole in the presence of a finite circular cylinder (pattern in the y-z plane).

E-THETA PATTERN

THE FIELDS ARE REFERENCED TO THE PATTERN COORDINATE SYSTEM

THETA	PHI	E-THETA		PHASE	UNNORMALIZED MAGNITUDE	UNNORMALIZED DB INTEN.	NORMALIZED MAGNITUDE	NORMALIZED DB
90.00000	90.00000	.55804E -7	-.18217E -6	-72.96877	.19053E -6	-163.17452	.11189	-19.02436
90.00000	100.00000	-.65566E -7	.39394E -7	149.00128	.76490E -7	-171.10150	.04492	-26.95134
90.00000	110.00000	.10927E -6	.11868E -6	47.36456	.16133E -6	-164.61950	.09474	-20.46934
90.00000	120.00000	-.27695E -7	-.16625E -6	-99.45760	.16855E -6	-164.23929	.09898	-20.08912
90.00000	130.00000	.15375E -6	.74234E -7	25.77237	.17073E -6	-164.12723	.10026	-19.97707
90.00000	140.00000	-.27142E -7	.12922E -6	101.86264	.13204E -6	-166.35973	.07754	-22.20957
90.00000	150.00000	-.21023E -6	.67938E -7	162.70764	.22856E -6	-161.59369	.13422	-17.44353
90.00000	160.00000	-.11468E -6	.23510E -6	115.98700	.26154E -6	-160.42290	.15359	-16.27274
90.00000	170.00000	-.84570E -9	-.31349E -7	-91.54526	.31361E -7	-178.84587	.01842	-34.69571
90.00000	180.00000	-.21769E -6	.14652E -6	146.05503	.26241E -6	-160.39406	.15410	-16.24389
90.00000	190.00000	.40348E -6	.56650E -7	7.99215	.40744E -6	-156.57232	.23927	-12.42215
90.00000	200.00000	-.18656E -6	.11776E -6	147.74042	.22062E -6	-161.90076	.12956	-17.75059
90.00000	210.00000	.20126E -6	.87974E -7	23.61038	.21965E -6	-161.93895	.12899	-17.78879
90.00000	220.00000	-.15030E -8	.20433E -6	90.42143	.20433E -6	-162.56676	.12000	-18.41660
90.00000	230.00000	-.10883E -6	.31141E -9	179.83606	.10883E -6	-168.03848	.06391	-23.88932
90.00000	240.00000	.12171E -7	-.41643E -7	-73.45481	.43442E -7	-176.01545	.02551	-31.86529
90.00000	250.00000	.12241E -7	.11760E -7	43.84778	.16977E -7	-184.17664	.00997	-40.02649
90.00000	260.00000	-.63202E -8	.19912E -8	162.51264	.66265E -8	-192.34794	.00389	-48.19779
90.00000	270.00000	.94996E -6	-.14132E -5	-56.09226	.17028E -5	-144.15016	1.00000	.00000

Figure 19a. Line printer output for the $E_{\theta p}$ fields of Example 4 and Example 9.

AD-A097 416 OHIO STATE UNIV COLUMBUS ELECTROSCIENCE LAB F/G 20/14
NUMERICAL ELECTROMAGNETIC CODE (NEC)-BASIC SCATTERING CODE. PAR--ETC(U)
SEP 79 R J MARHEFKA, W D BURNSIDE N00123-76-C-1371
UNCLASSIFIED ESL-784508-18 NL

2 of 2

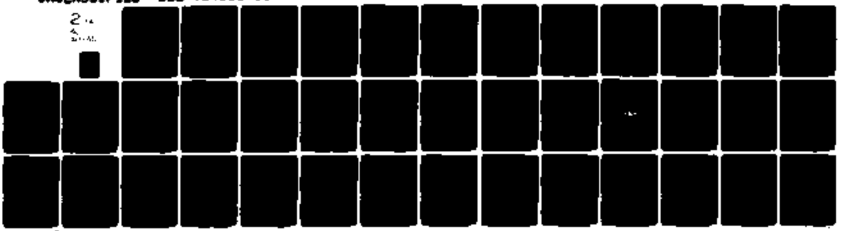

END
DATE FILMED
5-81
DTIC

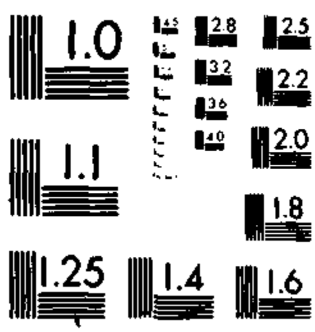

MICROCOPY RESOLUTION TEST CHART

NATIONAL BUREAU OF STANDARDS-1963-A

E-PHI PATTERN

THE FIELDS ARE REFERENCED TO THE PATTERN COORDINATE SYSTEM

THETA	PHI	E-PHI		PHASE	UNNORMALIZED MAGNITUDE	UNNORMALIZED DB INTEN.	NORMALIZED MAGNITUDE	NORMALIZED DB
90.00000	90.00000	-.26408E 2	-.29647E 1	-173.59450	.26574E 2	-.29452	.32965	-9.63891
90.00000	100.00000	-.23090E 2	.25290E 2	132.39635	.34245E 2	1.91945	.42482	-7.43594
90.00000	110.00000	.57810E 2	.35173E 2	31.31741	.67669E 2	7.83420	.83944	-1.52019
90.00000	120.00000	-.93086E 1	-.80073E 2	-96.63097	.80612E 2	9.35439	1.00000	-.00003
90.00000	130.00000	.57003E 1	.11105E 2	62.82893	.12483E 2	-6.94723	.15485	-16.20162
90.00000	140.00000	-.10556E 2	.63220E 2	99.47949	.64096E 2	7.36296	.79511	-1.99143
90.00000	150.00000	.50260E 1	-.11836E 1	-13.25185	.51635E 1	-14.51469	.06405	-23.96[illegible]
90.00000	160.00000	-.41483E 2	.54368E 1	172.53331	.41839E 2	3.65790	.51900	-5.69659
90.00000	170.00000	.16446E 2	.20007E 2	50.57901	.25899E 2	-.50932	.32128	-9.86241
90.00000	180.00000	-.15508E 2	-.14950E 2	-136.04912	.21541E 2	-2.10847	.26721	-11.46285
90.00000	190.00000	.79756E 1	.53724E 1	33.96472	.96163E 1	-9.11347	.11929	-18.46750
90.00000	200.00000	-.24842E 2	-.16540E 2	-146.34511	.29845E 2	.72369	.37022	-8.63070
90.00000	210.00000	-.10325E 2	-.11693E 2	-131.44973	.15591E 2	-4.91597	.19341	-14.27026
90.00000	220.00000	-.17029E 2	-.33175E 2	-117.15794	.37309E 2	2.66258	.46282	-6.69181
90.00000	230.00000	.38918E 2	-.13541E 2	-19.18426	.41206E 2	3.52557	.51116	-5.82892
90.00000	240.00000	-.59383E 1	.27139E 2	102.34279	.27780E 2	.10105	.34461	-9.25334
90.00000	250.00000	-.10386E 2	-.97543E 1	-136.79722	.14249E 2	-5.69820	.17675	-15.05259
90.00000	260.00000	.13912E 2	-.36031E 1	-14.51972	.14371E 2	-5.62364	.17828	-14.97803
90.00000	270.00000	-.15015E 2	.79980E 1	151.95678	.17012E 2	-4.15847	.21104	-13.51286

Figure 19b. Line printer output for the $E_{\phi p}$ fields of Example 4A and Example 9.

TOTAL RADIATION INTENSITY IN DB.

THE FIELDS ARE REFERENCED TO THE PATTERN COORDINATE SYSTEM

THETA	PHI	MAJOR	MINOR	TILT ANG	AXIAL RATIO	TOTAL INTEN.	NORM INTEN.
90.00000	90.00000	-.28452	-105.28050	-90.00000	.00001	-.28452	-9.63891
90.00000	100.00000	1.91845	-102.27020	90.00000	.00001	1.91845	-7.43594
90.00000	110.00000	7.83420	-98.01051	90.00000	.00001	7.83420	-1.52019
90.00000	120.00000	9.35439	-98.01051	90.00000	.00000	9.35439	.00000
90.00000	130.00000	-6.84723	-111.30110	90.00000	.00001	-6.84723	-16.20162
90.00000	140.00000	7.36296	-98.01051	90.00000	.00001	7.36296	-1.99143
90.00000	150.00000	-14.51468	-120.33200	-90.00000	.00001	-14.51468	-23.86907
90.00000	160.00000	3.65780	-101.02081	90.00000	.00001	3.65780	-5.69659
90.00000	170.00000	-.50802	-105.28050	-90.00000	.00001	-.50802	-9.06241
90.00000	180.00000	-2.10847	-108.29080	90.00000	.00000	-2.10847	-11.46286
90.00000	190.00000	-9.11347	-116.07231	90.00000	.00000	-9.11347	-18.46786
90.00000	200.00000	.72369	-105.28050	90.00000	.00001	.72369	-8.63070
90.00000	210.00000	-4.91587	-111.30110	-90.00000	.00000	-4.91587	-14.27026
90.00000	220.00000	2.66258	-102.27020	-90.00000	.00001	2.66258	-6.69181
90.00000	230.00000	3.52557	-104.03111	-90.00000	.00000	3.52557	-5.82882
90.00000	240.00000	.10105	-105.28050	-90.00000	.00001	.10105	-9.25334
90.00000	250.00000	-5.69820	-110.05171	-90.00000	.00001	-5.69820	-15.05259
90.00000	260.00000	-5.62364	-111.30110	-90.00000	.00001	-5.62364	-14.97803
90.00000	270.00000	-4.15847	-110.05171	-89.99999	.00001	-4.15847	-13.51286

Figure 10c. Line printer output for the total radiation intensity of Example 4A and Example 9.

The calculated results are compared with measured results[11] in the following figures.

The $E_{\phi p}$ pattern for Example 4A is shown in Figure 20a.

The $E_{\phi p}$ pattern for Example 4B is shown in Figure 20b.

The $E_{\phi p}$ pattern for Example 4C is shown in Figure 20c.

The $E_{\theta p}$ pattern for all three cases are not shown because they are of negligible value.

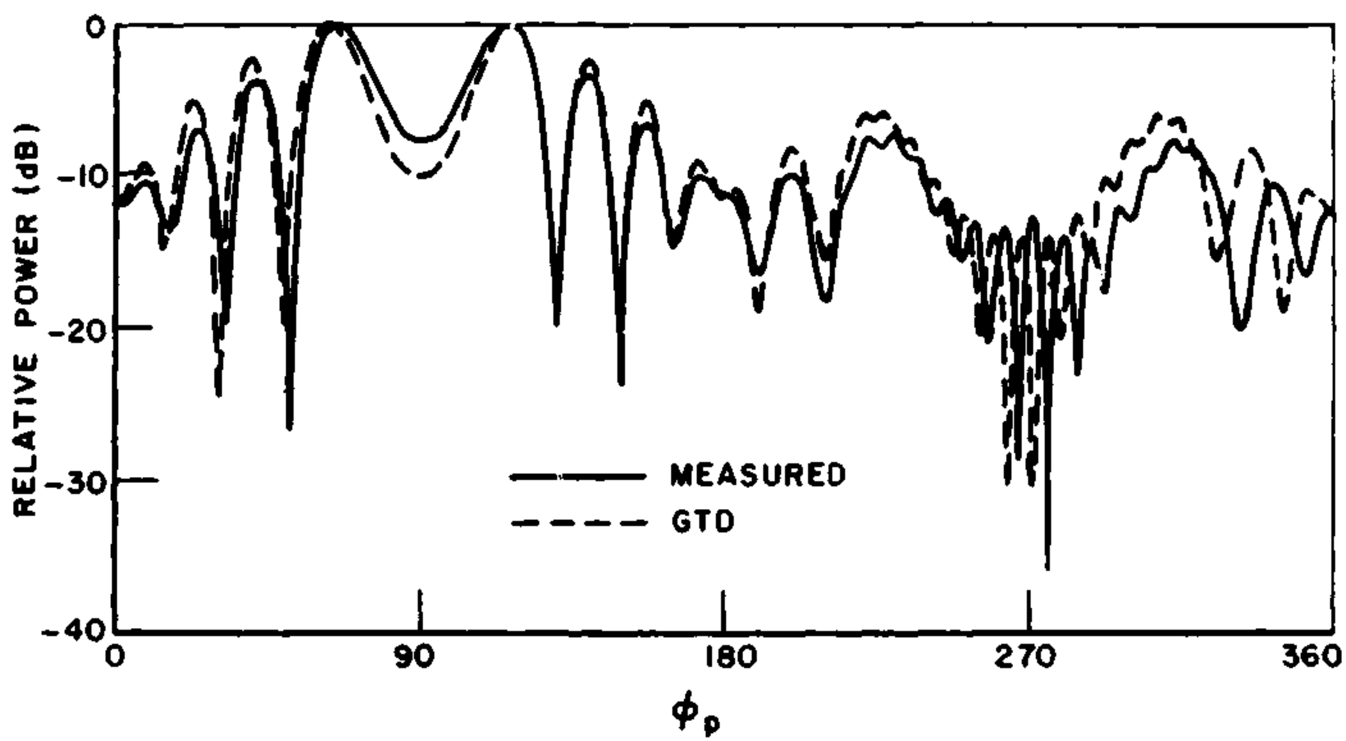

Figure 20a. Comparison of the measured (Bach) and calculated radiation pattern for $E_{\phi p}$ of an electric dipole on the y-axis parallel to the x-axis in the presence of a finite circular cylinder (pattern taken in x-y plane).

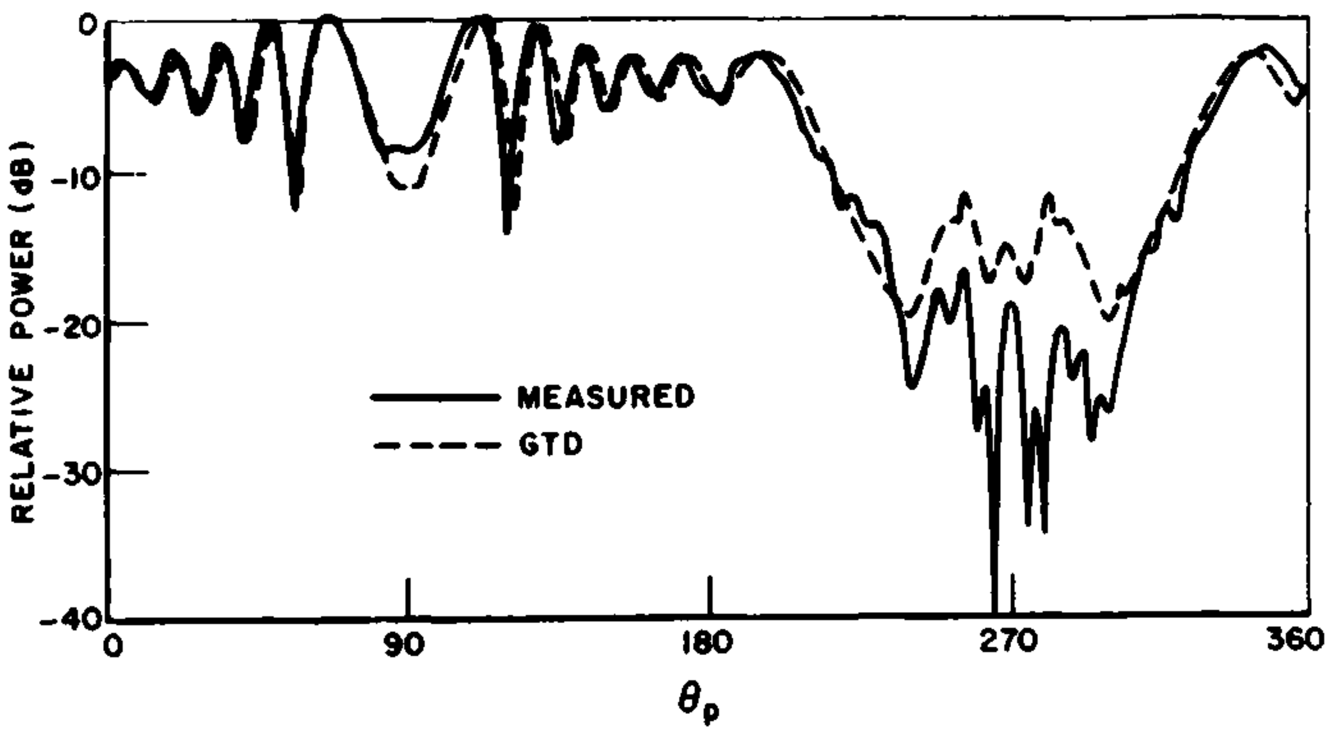

Figure 20b. Comparison of the measured (Bach) and calculated radiation pattern for $E_{\phi p}$ for an electric dipole on the y-axis parallel to the x-axis in the presence of a finite circular cylinder (pattern taken in y-z plane).

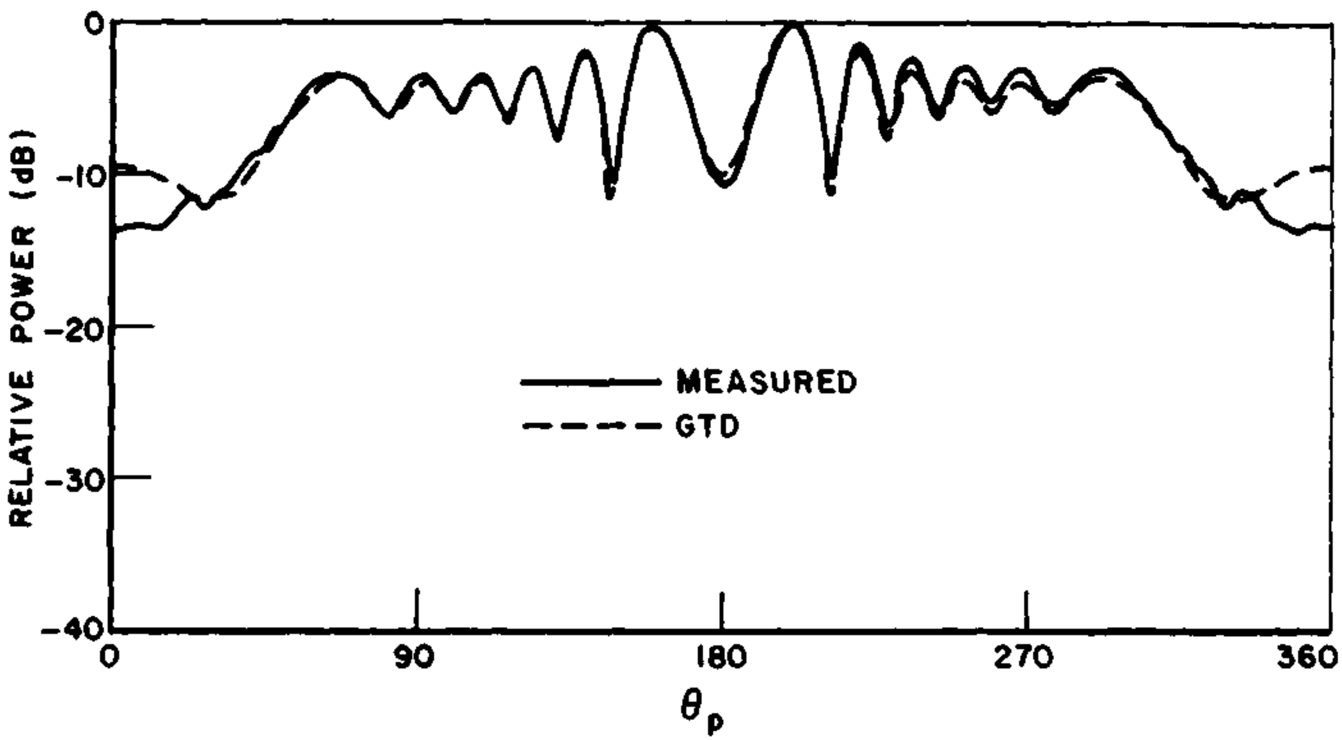

Figure 20c. Comparison of the measured (Bach) and calculated radiation pattern for $E_{\phi p}$ of an electric dipole in the x-z plane parallel to the x-axis in the presence of a finite circular cylinder (pattern taken in the y-z plane).

Example 5. Consider the pattern of a magnetic dipole in the presence of an elliptic cylinder as shown in Figure 21. This example illustrates how the LOUT parameter in the TO: command can be used to print out the individual fields reflected and diffracted by the body under consideration. Note, also, that since the units and frequency are not specified in the input set the input is therefore assumed to be given in wavelengths. The input data is given by

```
CE:   ELLIPTIC CYLINDER TEST, EXAMPLE 5.
PD:
0.,0.,90.,0.
1,90.
0,360,1
CG:
2.,1.
-500.,90.,500.,90.
SG:
2.828,2.828,0.
0.,0.,90.,0.
1,0.5,0.
1.,0.
XQ:
TO:   PRINT INDIVIDUAL FIELDS AROUND SHADOW BOUNDARY
F,F,1
T,T,F
1,7,1,3,1,4
PD:   REDUCE ANGULAR RANGE
0.,0.,90.,0.
1,90.
264,269,1
XQ:
EN:
```

The reflected and diffracted fields in the region close to one of the shadow boundaries of the elliptic cylinder, as printed by the line printer, are shown in Figure 22. The different types of fields can be interpreted by looking up the integer indices in Table 3. The first two columns of real numbers are the magnitude and phase of the E_θ field and the second two columns of real numbers are the magnitude and phase of the E_ϕ field. The polarization is referred to the reference coordinate system for this type of print out.

The $E_{\phi p}$ pattern is plotted in Figure 23 compared with a moment method solution. The $E_{\theta p}$ pattern is not plotted because it is of negligible value.

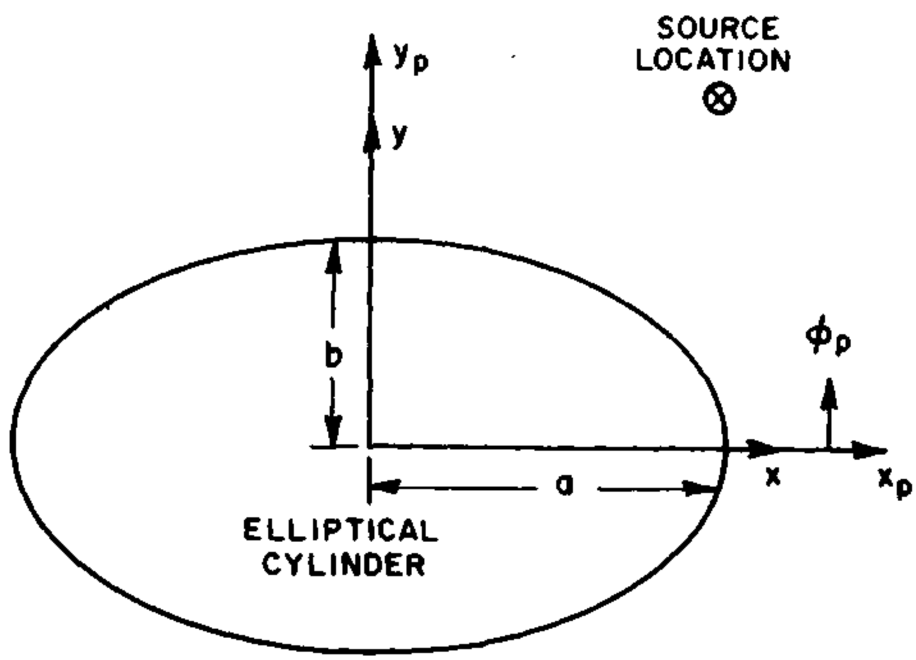

Figure 21. Elliptic cylinder configuration excited by a magnetic source parallel to the z-axis.

110	0	0	0	.000000	[illegible]	.159155	5.947200
120	0	0	0	.000000	-175.952357	.011198	4.147642
130	0	0	0	.000000	-3.485297	.057472	-157.356818
204	204	1	1	.000000	-3.485296	.105450	-3.214102
110	0	0	0	.000000	-2.953030	.159155	-2.953030
120	0	0	0	.000000	176.413737	.008648	-3.586250
130	0	0	0	.000000	-8.498972	.058288	-159.324669
205	205	1	1	.000000	-8.498972	.108303	-15.410169
110	0	0	0	.000000	-11.341138	.159155	-11.341138
120	0	0	0	.000000	168.576577	.005148	-11.423406
130	0	0	0	.000000	-13.433551	.058463	-162.395426
206	206	1	1	.000000	-13.433551	.111640	-26.022875
130	0	0	0	.000000	-34.349089	.116161	-33.964759
207	207	1	1	[illegible]	[illegible]	.116161	-33.964759
130	0	0	0	.000000	154.467240	.116297	-43.091049
208	208	1	1	.000000	154.467240	.116297	-43.091049
130	0	0	0	.000000	142.634008	.116351	-49.997145
209	209	1	1	.000000	142.634008	.116351	-49.997145
204	204	2	2	0.000000	0.000000	0.000000	0.000000
205	205	2	2	0.000000	0.000000	0.000000	0.000000
206	206	2	2	0.000000	0.000000	0.000000	0.000000
207	207	2	2	0.000000	0.000000	0.000000	0.000000
208	208	2	2	0.000000	0.000000	0.000000	0.000000
209	209	2	2	0.000000	0.000000	0.000000	0.000000
204	204	3	3	.000000	178.426564	.000000	-91.502986
205	205	3	3	.000000	-177.747439	.000000	-87.678213
206	206	3	3	.000000	-173.785438	.000000	-83.719983
207	207	3	3	.000000	-169.689851	.000000	-79.624141
208	208	3	3	.000000	-165.463221	.000000	-75.395964
209	209	3	3	.000000	-161.108193	.000000	-71.047296
1000	204	204	204	.000000	178.426564	.105450	-3.214102
1000	205	205	205	.000000	-177.747438	.108303	-15.410170
1000	206	206	206	.000000	-173.785437	.111640	-26.022875
1000	207	207	207	.000000	-169.689797	.116161	-33.964759
1000	208	208	208	.000000	-165.463221	.116297	-43.091049
1000	209	209	209	.000000	-161.108193	.116351	-49.997145

Figure 22. Line printer output of the individual fields diffracted by the elliptic cylinder of Example 5 with LOUT=.TRUE. The definition of the integer index number are given in Table 3. The real numbers represents the magnitude and phase of the $E_{\theta p}$ and $E_{\phi p}$ fields, respectively.

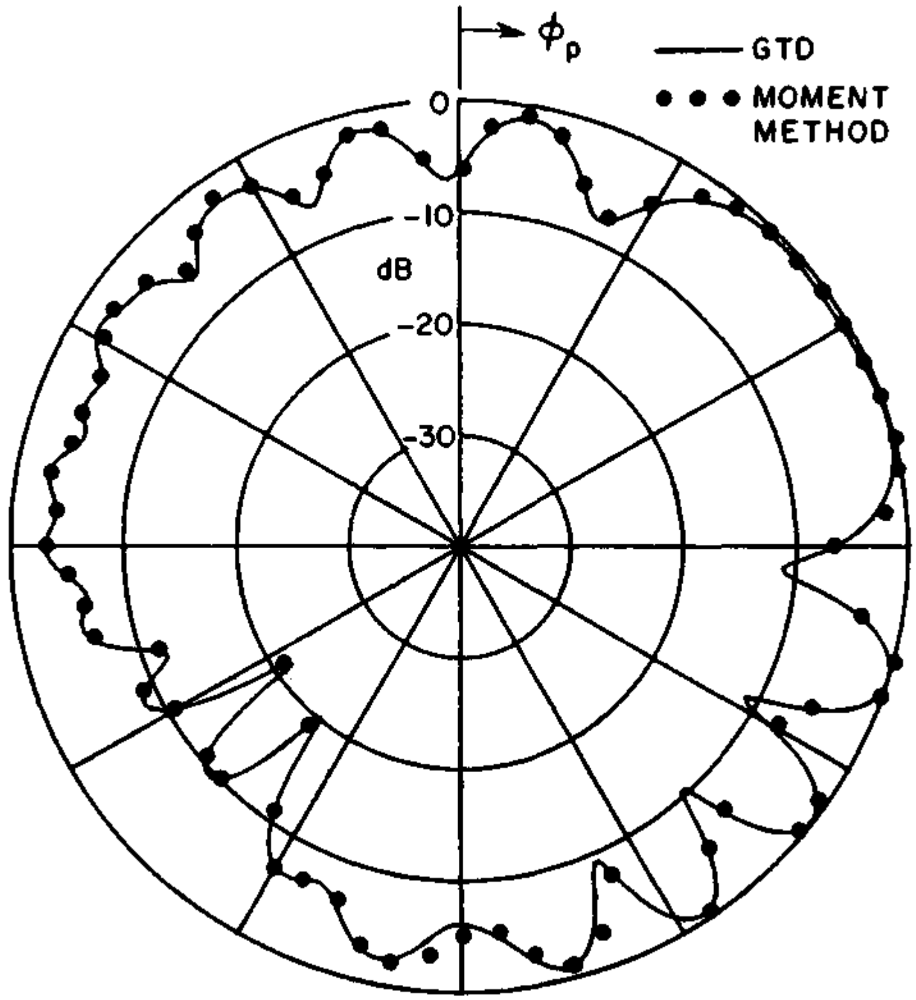

Figure 23. Comparison of GTD and moment method results for $E_{\phi p}$ pattern.

Example 6. Consider an electric dipole in the presence of a plate and a finite circular cylinder as shown in Figure 24. This example illustrates how the input data can be manipulated to analyze the effects of scattering bodies separately and in combination with one another. The following input is shown as if all four cases are run consecutively in one run. Of course, the input could easily be constructed for individual runs for each case.

```
CE:    PLATE AND CYLINDER TEST, EXAMPLE 6.
PD:
0.,0.,90.,0.
T,90.
0,.060,1
UN:
3
FR:
4.
SG:
0.,5.625,0.
90.,0.,0.,0.
0,0.588,0.0
1.,0.
PG:
4
5.,0.,5.
5.,0.,-5.
-5.,0.,-5.
-5.,0.,5.
RT:
0.,12.3125,-0.125
0.,0.,90.,0.
CG:
1.25,1.25
-8.5,90.,8.5,90.
XQ:    SOURCE, PLATE AND CYLINDER TEST
NP:    REMOVE PLATE
XQ:    SOURCE AND CYLINDER TEST
RC:    REMOVE CYLINDER
XQ:    SOURCE TEST
RT:    REINITILIZE ORIGIN
0.,0.,0.
0.,0.,90.,0.
PG:    REDEFINE PLATE
4
5.,0.,5.
5.,0.,-5.
-5.,0.,-5.
-5.,0.,5.
XQ:    SOURCE AND PLATE TEST
EN:
```

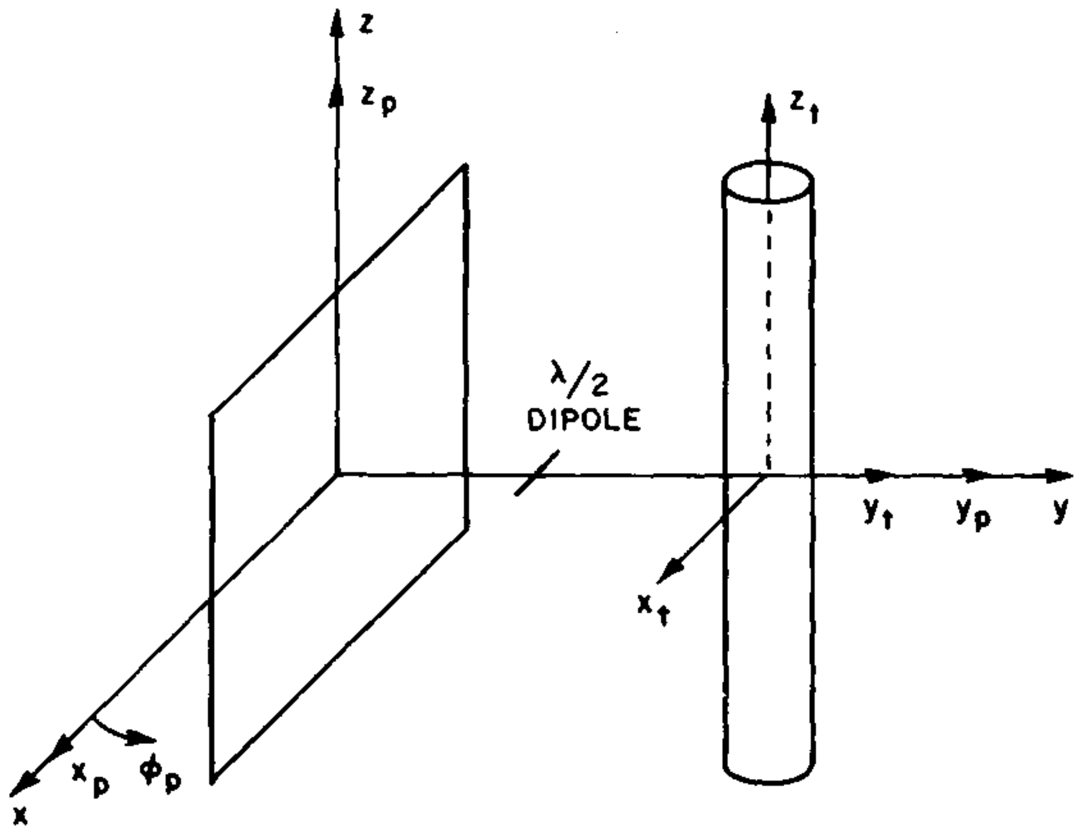

Figure 24. A λ/2 dipole in the presence of a square plate.

The line printer output of the results for the source, plate and cylinder in combination are shown in Figure 25. The input data is really that of Example 9 where only half the pattern is computed in 10^0 increments.

The calculated $E_{\phi p}$ patterns are compared with measured results in the following figures.

The $E_{\phi p}$ pattern for the source alone is shown in Figure 26a.

The $E_{\phi p}$ pattern for the source and plate is shown in Figure 26b.

The $E_{\phi p}$ pattern for the source and cylinder is shown in Figure 26c.

The $E_{\phi p}$ pattern for the source, plate and cylinder is shown in Figure 26d.

The $E_{\theta p}$ pattern for all four cases are not shown because they are of negligible value.

E-THETA PATTERN

THE FIELDS ARE REFERENCED TO THE PATTERN COORDINATE SYSTEM

THETA	PHI	E-THETA		PHASE	UNNORMALIZED MAGNITUDE	UNNORMALIZED DB INTEN.	NORMALIZED MAGNITUDE	NORMALIZED DB
90.00000	90.00000	.12332E -4	.20220E -3	86.50981	.20258E -3	-102.64187	.00004	-87.39558
90.00000	100.00000	-.29878E 1	-.12289E 1	-157.64280	.32307E 1	-18.58769	.68066	-3.34140
90.00000	110.00000	-.44696E 1	-.90296E 0	-168.57870	.45599E 1	-15.59453	.96070	-.34825
90.00000	120.00000	-.47443E 1	.14227E 0	178.28210	.47464E 1	-15.24628	1.00000	.00000
90.00000	130.00000	-.36715E 1	.11060E 1	163.23508	.38345E 1	-17.09940	.80788	-1.85311
90.00000	140.00000	-.21086E -3	.65497E -3	107.84541	.68808E -3	-92.02086	.00014	-76.77457
90.00000	150.00000	-.23122E -3	.29718E -3	127.88529	.37653E -3	-97.25753	.00008	-82.01125
90.00000	160.00000	-.49443E 0	-.46268E 0	-136.90042	.67715E 0	-32.15990	.14267	-16.91362
90.00000	170.00000	-.38084E 0	-.59970E 0	-122.41740	.71041E 0	-31.74341	.14967	-16.49713
90.00000	180.00000	-.22071E 0	-.62986E 0	-109.31108	.66741E 0	-32.28580	.14061	-17.03951
90.00000	190.00000	-.68767E -1	-.59788E 0	-96.56126	.60182E 0	-33.18431	.12679	-17.93802
90.00000	200.00000	.49397E -1	-.52712E 0	-84.64640	.52943E 0	-34.29750	.11154	-19.05122
90.00000	210.00000	.12627E 0	-.43669E 0	-73.87253	.45457E 0	-35.62151	.09577	-20.37522
90.00000	220.00000	.16331E 0	-.34201E 0	-64.47472	.37900E 0	-37.20085	.07985	-21.95457
90.00000	230.00000	.16688E 0	-.25312E 0	-56.60411	.30318E 0	-39.13963	.06388	-23.89335
90.00000	240.00000	.14499E 0	-.17511E 0	-50.37627	.22734E 0	-41.64002	.04790	-26.39374
90.00000	250.00000	.10551E 0	-.10877E 0	-45.87215	.15151E 0	-45.16354	.03193	-29.91725
90.00000	260.00000	.55271E -1	-.51808E -1	-43.14782	.75756E -1	-51.18524	.01596	-35.93896
90.00000	270.00000	.26202E -7	-.67988E -7	-68.92361	.72863E -7	-171.52351	.00000	-156.27722

Figure 25a. Line printer output for the $E_{\theta p}$ fields of Example 6 and Example 9.

E-PHI PATTERN

THE FIELDS ARE REFERENCED TO THE PATTERN COORDINATE SYSTEM

THETA	PHI	E-PHI				PHASE	UNNORMALIZED MAGNITUDE		UNNORMALIZED DB INTEN.	NORMALIZED MAGNITUDE	NORMALIZED DB
90.00000	90.00000	-.22366E	2	-.63592E	2	-109.37702	.67411E	2	7.80094	.63060	-4.00499
90.00000	100.00000	.23098E	2	[illegible]	2	[illegible]	[illegible]	2	10.39316	.94990	-1.41267
90.00000	110.00000	.88075E	2	.60581E	2	34.52145	.10690E	3	11.80583	1.00000	.00000
90.00000	120.00000	-.72215E	2	.55880E	2	142.26713	.91310E	2	10.43677	.85417	-1.36937
90.00000	130.00000	-.31835E	2	.27712E	2	138.96055	.42207E	2	3.73415	.39484	-8.07168
90.00000	140.00000	-.27207E	1	-.40540E	2	-93.83950	.40631E	2	3.40348	.38009	-8.40235
90.00000	150.00000	.11744E	2	.32469E	2	70.11547	.34527E	2	1.98966	.32299	-9.81617
90.00000	160.00000	-.27677E	2	.15398E	2	150.90987	.31672E	2	1.23991	.29628	-10.56593
90.00000	170.00000	.37552E	1	.54419E	1	55.39235	.66117E	1	-12.36732	.06185	-24.17315
90.00000	180.00000	-.28647E	1	-.55801E	1	-117.17490	.62725E	1	-12.92482	.05868	-24.63066
90.00000	190.00000	.14317E	1	.41520E	1	70.97427	.43919E	1	-15.92059	.04108	-27.72642
90.00000	200.00000	-.25231E	2	-.21597E	2	-139.43678	.33212E	2	1.65221	.31068	-10.15362
90.00000	210.00000	.10414E	2	-.30598E	2	-71.20390	.32322E	2	1.41636	.30236	-10.38947
90.00000	220.00000	-.19441E	2	.53931E	1	164.52301	.20173E	2	-2.67840	.18871	-14.48424
90.00000	230.00000	-.17815E	2	-.10135E	2	-149.87987	.20596E	2	-2.49804	.19267	-14.30387
90.00000	240.00000	-.49781E	1	-.24090E	2	-101.67572	.24599E	2	-.95540	.23011	-12.76124
90.00000	250.00000	-.22431E	2	-.38452E	1	-170.27288	.22758E	2	-1.63081	.21290	-13.43664
90.00000	260.00000	-.13187E	2	.15314E	1	173.37600	.13276E	2	-6.31254	.12419	-18.11837
90.00000	270.00000	-.15279E	2	.34034E	2	114.17651	.37306E	2	2.66194	.34899	-9.14389

Figure 25b. Line printer output for the $E_{\phi p}$ fields of Example 6 and Example 9.

TOTAL RADIATION INTENSITY IN DB.

THE FIELDS ARE REFERENCED TO THE PATTERN COORDINATE SYSTEM

THETA	PHI	MAJOR	MINOR	TILT ANG	AXIAL RATIO	TOTAL INTEN.	NORM INTEN.
90.00000	90.00000	7.80044	-99.25390	-89.99983	.00000	7.80094	-4.01279
90.00000	100.00000	10.19326	-18.55530	89.72919	.01324	10.19961	-1.41538
90.00000	110.00000	11.81252	-23.72798	-87.75247	.01671	11.81373	.00000
90.00000	120.00000	10.44444	-19.06642	87.59011	.03051	10.44919	[illegible]
[illegible]	130.00000	3.76388	-24.84998	85.25919	.03709	3.76985	-8.04388
90.00000	140.00000	3.40349	-99.25990	-89.99910	.00001	3.40349	-8.41025
90.00000	150.00000	1.98966	-97.74722	89.99967	.00001	1.99966	-9.82406
90.00000	160.00000	1.24009	-32.58667	89.62517	.02035	1.24199	-10.57184
90.00000	170.00000	-12.31754	-60.14784	-93.87160	.00406	-12.31747	-24.13119
90.00000	180.00000	-12.77691	-49.61085	83.98199	.01440	-12.77593	-24.59966
90.00000	190.00000	-15.84346	-46.57903	-82.37262	.02906	-15.83980	-27.65352
90.00000	200.00000	1.65250	-36.05292	99.47332	.01302	1.65331	-10.16042
90.00000	210.00000	1.41722	-62.26195	89.19512	.00065	1.41722	-10.39651
90.00000	220.00000	-2.67774	-39.64621	-89.29364	.01419	-2.67697	-14.49060
90.00000	230.00000	-2.49803	-34.15884	[illegible]	[illegible]	[illegible]	-14.31082
90.00000	240.00000	-.95526	-43.79355	89.66890	.00721	-.95503	-12.76876
90.00000	250.00000	-1.63075	-46.81340	-89.79346	.00549	-1.63062	-13.44434
90.00000	260.00000	-6.31245	-55.69270	-99.73725	.00340	-6.31240	-18.12613
90.00000	270.00000	2.66194	-102.27020	-90.00003	.00001	2.66194	-9.15179

Figure 25c. Line printer output for the total radiation intensity of Example 6 and Example 9.

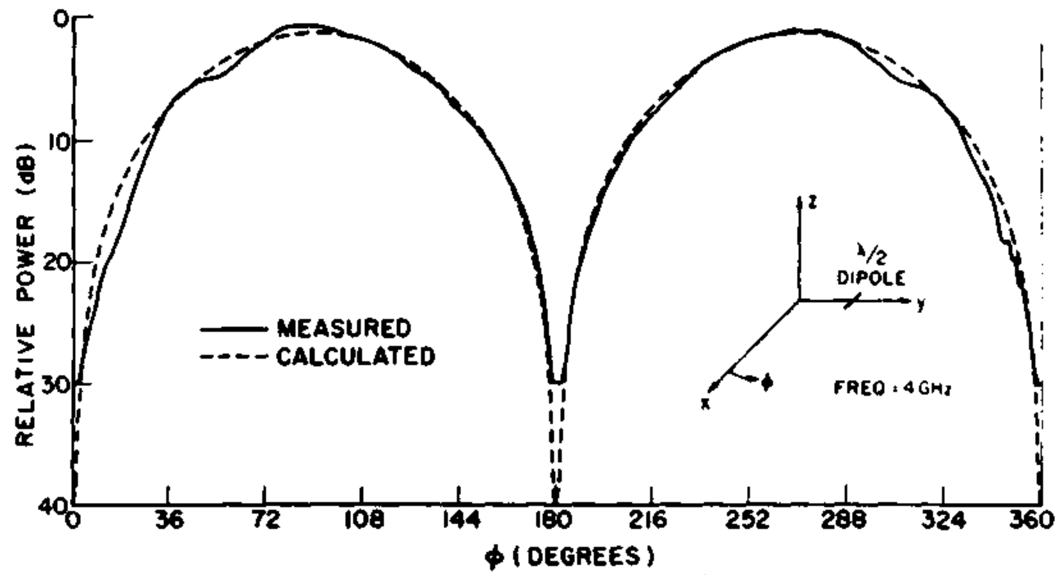

Figure 26a. Comparison of the measured and calculated E_{ϕ} radiation pattern of a ·/2 dipole.

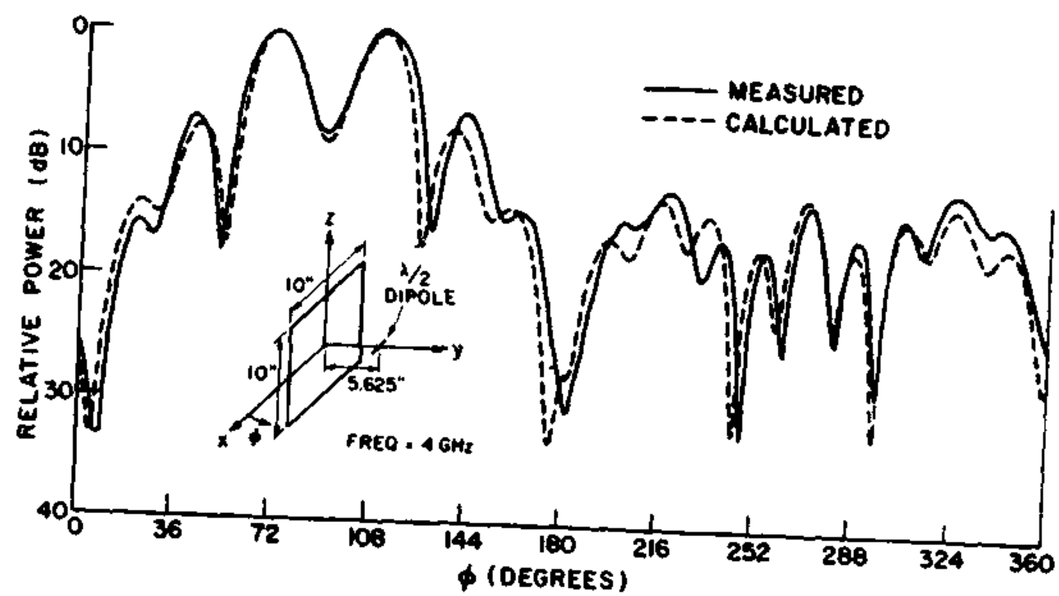

Figure 26b. Comparison of the measured and calculated E_ϕ radiation pattern of a dipole in the presence of a square plate.

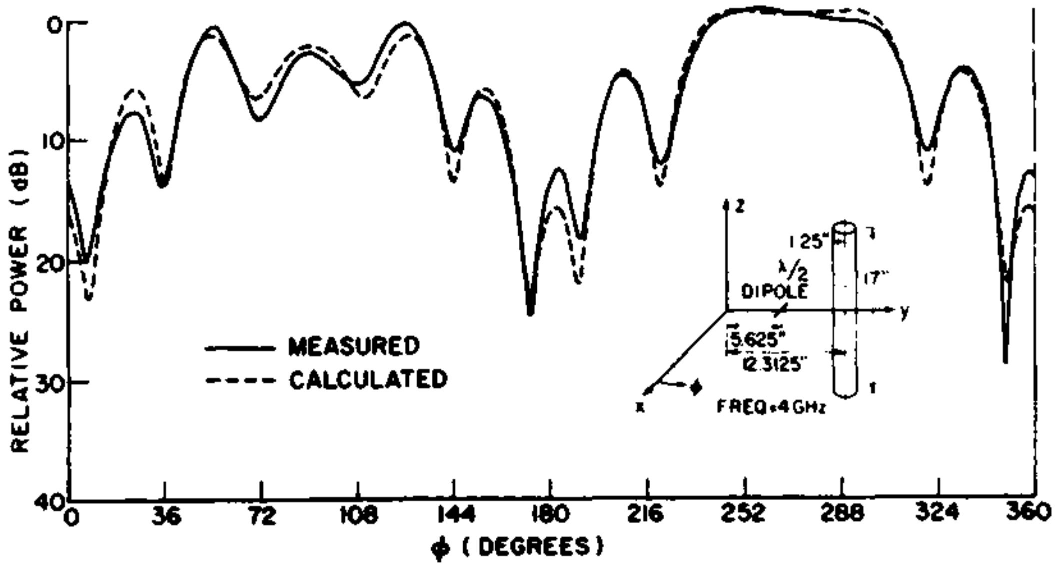

Figure 26c. Comparison of the measured and calculated E_ϕ radiation pattern of a dipole in the presence of a finite circular cylinder.

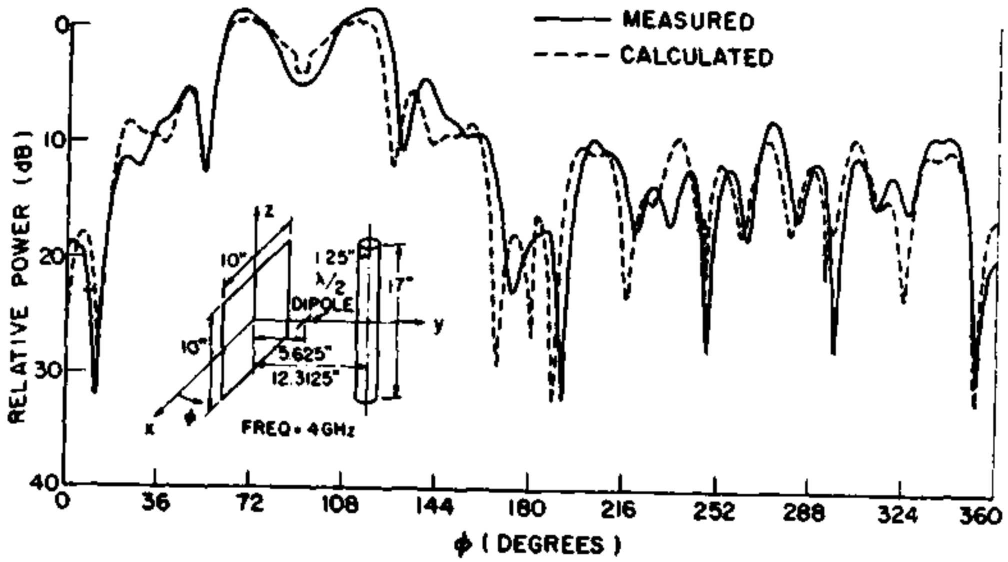

Figure 26d. Comparison of the measured and calculated (with plate-cylinder interactions) E_ϕ radiation pattern of a dipole in the presence of a square plate and a finite circular cylinder.

Example 7. Consider a slot mounted on the wing of a Boeing 737 aircraft. The computer model of the Boeing 737 is illustrated in Figure 27. The input data is given by

```
CM:    AIRCRAFT TEST, EXAMPLE 7.
CM:    BOEING 737 COMPUTER MODEL
PD:
ØØ.,9Ø.,15Ø.,9Ø.
1,9Ø.
Ø,36Ø,1
FR:
1.74Ø
UN:
3
CG:
1Ø4.1,74.7
-57Ø.5,9Ø.,26Ø.4,2Ø.
PG:    LEFT WING
5
Ø.,74.7,-212.8
Ø.,547.9,4Ø.8
Ø.,547.9,95.1
Ø.,262.8,Ø.
Ø.,74.7,Ø.
PG:    RIGHT WING
5
Ø.,-74.7,Ø.
Ø.,-263.8,Ø.
Ø.,-547.9,95.1
Ø.,-547.9,4Ø.8
Ø.,-74.7,-212.8
PG:    VERTICAL STABILIZER
4
1Ø4.1,Ø.,448.3
344.1,Ø.,516.2
344.1,Ø.,443.7
1Ø4.1,Ø.,295.5
SG:    FINITE WIDTH SLOT
Ø.,312.4,-45.3
9Ø.,9Ø.,Ø.,Ø.
1,Ø.827937,Ø.413918
1.,Ø.
XQ:
EN:
```

The $E_{\phi p}$ pattern is compared with its measured result in Figure 28. The measurement was made on a 1/20 scale model of a Boeing 737 at NASA (Hampton, Virgina). The antenna is a KA band waveguide mounted in the wing[8]. The $E_{\theta p}$ pattern is significant for this case, however, it is not shown.

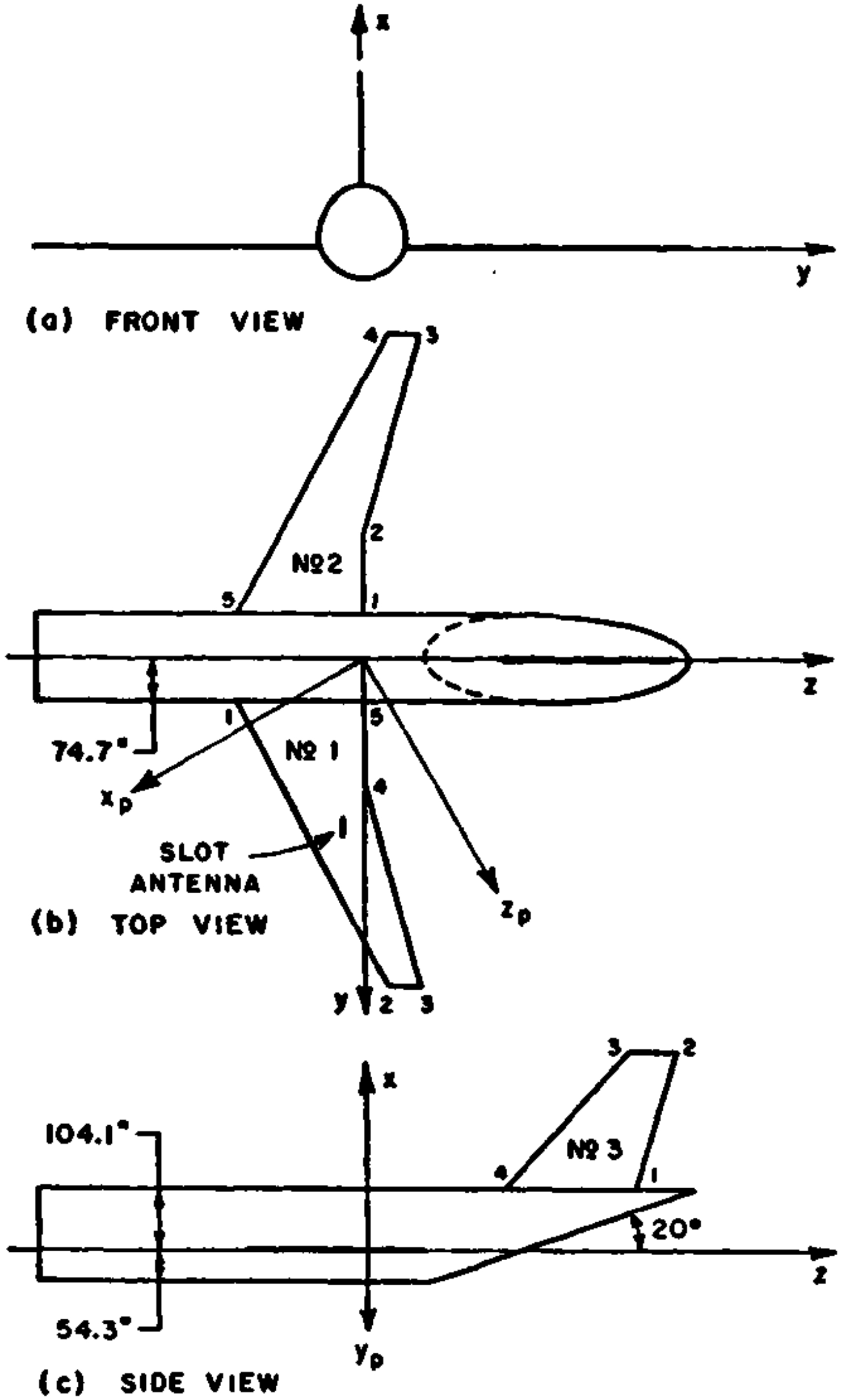

Figure 27. Illustration of geometry of Boeing 737 aircraft model used in finite elliptic cylinder model.

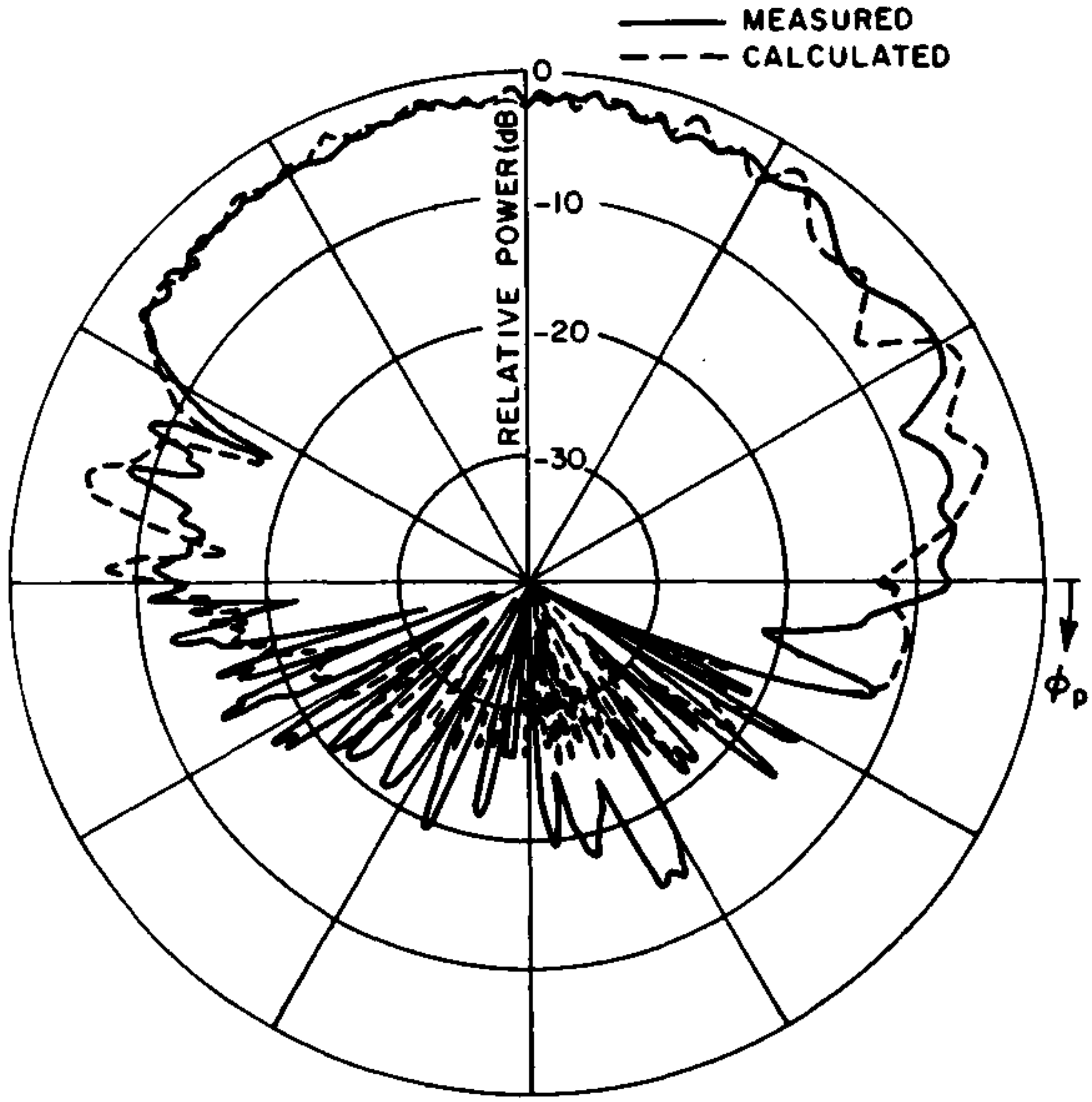

Figure 28. Comparison of measured and calculated E_{θ_p} results.

Example 8A. Consider the pattern of a set of four electric dipoles in the presence of a square plate over an infinite ground plane as shown in Figure 29. The currents are specified by the NEC-Moment Method Code as used at NOSC. The input data is given by

```
CE:    NEC INPUT TEST, EXAMPLE 8A.
PD:    PHI=0    PATTERN CUT
Ø.,Ø.,9Ø.,Ø.
F,Ø.
Ø,9Ø,1
FR:
Ø.2998
UN:
3
RO:
15Ø.
GP:    GROUND PLANE
RT:
Ø.,Ø.,28.5
Ø.,Ø.,9Ø.,Ø.
PG:
4
25.,-25.,Ø.
25.,25.,Ø.
-25.,25.,Ø.
-25.,-25.,Ø.
UN:
1
```

```
AM*    REC MOMENT METHOD INPUT
.001535
20
   -.47752    -.35560    .20637    .06096    .00000    .00000
   -.41656    -.35560    .20637    .06096    .00000    .00000
   -.35560    -.35560    .20637    .06096    .00000    .00000
   -.29464    -.35560    .20637    .06096    .00000    .00000
   -.23368    -.35560    .20637    .06096    .00000    .00000
    .23368    -.35560    .20637    .06096    .00000    .00000
    .29464    -.35560    .20637    .06096    .00000    .00000
    .35560    -.35560    .20637    .06096    .00000    .00000
    .41656    -.35560    .20637    .06096    .00000    .00000
    .47752    -.35560    .20637    .06096    .00000    .00000
   -.47752     .35560    .20637    .06096    .00000    .00000
   -.41656     .35560    .20637    .06096    .00000    .00000
   -.35560     .35560    .20637    .06096    .00000    .00000
   -.29464     .35560    .20637    .06096    .00000    .00000
   -.23368     .35560    .20637    .06096    .00000    .00000
    .23368     .35560    .20637    .06096    .00000    .00000
    .29464     .35560    .20637    .06096    .00000    .00000
    .35560     .35560    .20637    .06096    .00000    .00000
    .41656     .35560    .20637    .06096    .00000    .00000
    .47752     .35560    .20637    .06096    .00000    .00000
   .3288E-3   .1796E-2
   .6564E-3   .4092E-2
   .7673E-3   .5621E-2
   .6735E-3   .4089E-2
   .3462E-3   .1794E-2
   .3462E-3   .1794E-2
   .6735E-3   .4089E-2
   .7673E-3   .5621E-2
   .6564E-3   .4092E-2
   .3288E-3   .1796E-2
   .3288E-3   .1796E-2
   .6564E-3   .4092E-2
   .7673E-3   .5621E-2
   .6735E-3   .4089E-2
   .3462E-3   .1794E-2
   .3462E-3   .1794E-2
   .6735E-3   .4089E-2
   .7673E-3   .5621E-2
   .6564E-3   .4092E-2
   .3288E-3   .1796E-2
XO*
NG*    REMOVE GROUND PLANE
XO*
EN*
```

The line printer output for the first execution with the infinite ground plane is shown in Figure 30. The results are shown for 10^0 increments for brevity. Since a range is specified the fields are in volts/meter. Note that the range is in the far field of the maximum dimension of the plate ($R>2D^2/\lambda$). Also, since the power radiated is known from the NEC-Moment Method Code the power results are given in terms of directive gain rather than in terms of the radiation intensity.

The directive gain normalized to isotropic is plotted in Figure 31a for the $\phi=0^0$ plane. The result is compared against the infinite ground plane case and the case for the plate in free space which is given as the second execution in the input set. Similarly, the directive gains for the three different cases are plotted in Figure 31b for the $\phi=90^0$ plane.

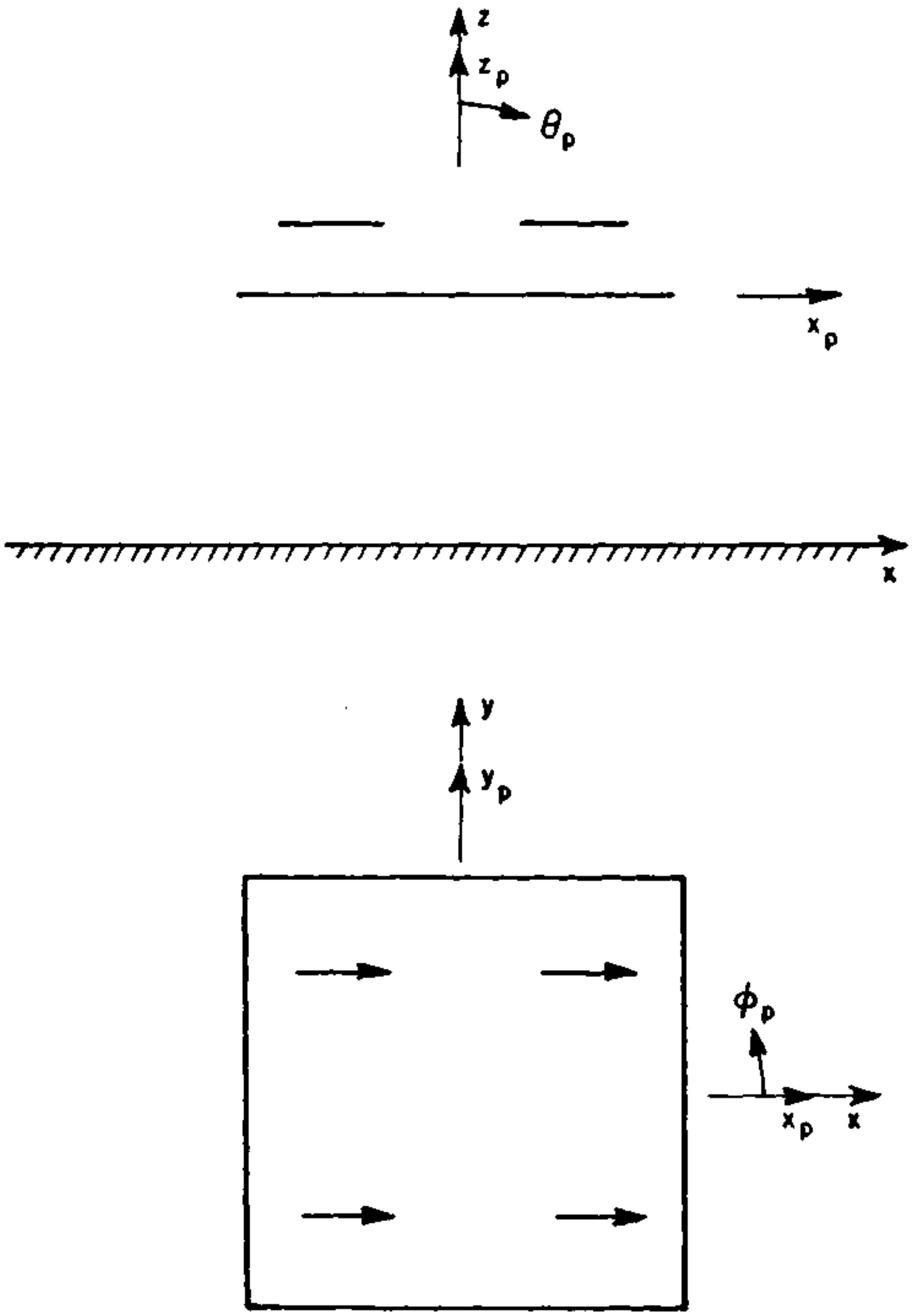

Figure 29. Geometry for the problems of dipoles over a square plate and infinite ground plane showing the side and top view.

E-THETA PATTERN

THE FIELDS ARE REFERENCED TO THE PATTERN COORDINATE SYSTEM

THETA	PHI	E-THETA		PHASE	UNNORMALIZED MAGNITUDE	UNNORMALIZED DB GAIN	NORMALIZED MAGNITUDE	NORMALIZED DB
0.00000	0.00000	.11978E 0	.30201E 0	68.36569	.32489E 0	12.21073	1.00000	.00000
10.00000	0.00000	.19477E 0	.22402E 0	48.99642	.29685E 0	11.42668	.91369	-.78404
20.00000	0.00000	.21204E 0	.12119E 0	29.75002	.24423E 0	9.73201	.75173	-2.47872
30.00000	0.00000	.16859E 0	.28407E -1	9.56312	.17396E 0	6.63195	.52621	-5.57678
40.00000	0.00000	.62231E -1	-.96053E -2	-8.77428	.62968E -1	-2.04172	.19381	-14.25245
50.00000	0.00000	-.31887E -1	.81761E -2	165.61870	.32919E -1	-7.67529	.10132	-19.88602
60.00000	0.00000	-.34359E -1	.91078E -2	165.15967	.35544E -1	-7.00973	.10940	-19.21946
70.00000	0.00000	-.43292E -3	.56361E -3	127.52886	.71068E -3	-40.99057	.00219	-53.20130
80.00000	0.00000	.17606E -2	.15899E -2	42.06536	.23716E -2	-30.52320	.00730	-42.77393
90.00000	0.00000	-.50341E -9	.60370E -9	129.82375	.78605E -9	-160.11505	.00000	-172.32578

Figure 30a. Line printer output for the $E_{\theta p}$ fields of Example 8A.

E-PHI PATTERN

THE FIELDS ARE REFERENCED TO THE PATTERN COORDINATE SYSTEM

THETA	PHI	E-PHI		PHASE	UNNORMALIZED MAGNITUDE	UNNORMALIZED DB GAIN	NORMALIZED MAGNITUDE	NORMALIZED DB
0.00000	0.00000	.69852E-13	.17412E-12	0.00000	.26247E-10	-189.64260	1.00000	-.00000
10.00000	0.00000	.14856E-12	-.39748E-12	0.00000	.26247E-10	-189.64260	1.00000	-.00000
20.00000	0.00000	-.88429E-13	-.11170E-11	0.00000	.26247E-10	-189.64260	1.00000	-.00000
30.00000	0.00000	.46436E-13	.51882E-12	0.00000	.26247E-10	-189.64260	1.00000	-.00000
40.00000	0.00000	-.41612E-12	.42410E-12	0.00000	.26247E-10	-189.64260	1.00000	-.00000
50.00000	0.00000	.11032E-12	-.53052E-13	0.00000	.26247E-10	-189.64260	1.00000	-.00000
60.00000	0.00000	-.15018E-12	.10840E-12	0.00000	.26247E-10	-189.64260	1.00000	-.00000
70.00000	0.00000	.25505E-12	.25645E-12	0.00000	.26247E-10	-189.64260	1.00000	-.00000
80.00000	0.00000	.10424E-12	-.13719E-12	0.00000	.26247E-10	-189.64260	1.00000	-.00000
90.00000	0.00000	.24322E-21	.29045E-21	0.00000	.26247E-10	-189.64260	1.00000	-.00000

Figure 30b. Line printer output for the $E_{\phi p}$ fields of Example 8A.

TOTAL DIRECTIVE GAIN IN DB

THE FIELDS ARE REFERENCED TO THE PATTERN COORDINATE SYSTEM

THETA	PHI	MAJOR	MINOR	TILT ANG	AXIAL RATIO	[illegible]	NORM GAIN
0.00000	0.00000	12.21073	-89.64260	.00000	.00000	12.21073	-.00000
10.00000	0.00000	11.42668	-89.64260	.00000	.00000	11.42668	-.78404
20.00000	0.00000	9.73201	-89.64260	.00000	.00000	9.73201	-2.47872
30.00000	0.00000	6.63395	-89.64260	.00000	.00000	6.63395	-5.57678
40.00000	0.00000	-2.04172	-89.64260	.00000	.00000	-2.04172	-14.25245
50.00000	0.00000	-7.67529	-89.64260	-.00000	.00000	-7.67529	-19.88602
60.00000	0.00000	-7.00873	-89.64260	-.00000	.00000	-7.00873	-19.21946
70.00000	0.00000	-40.99057	-89.64260	.00000	.00000	-40.99057	-53.20130
80.00000	0.00000	-30.52320	-89.64260	.00000	.00000	-30.52320	-42.73393
90.00000	0.00000	-89.64260	-89.64260	0.00000	.03339	-100.00000	-100.00000

Figure 30c. Line printer output for the total directive gain of Example 8A.

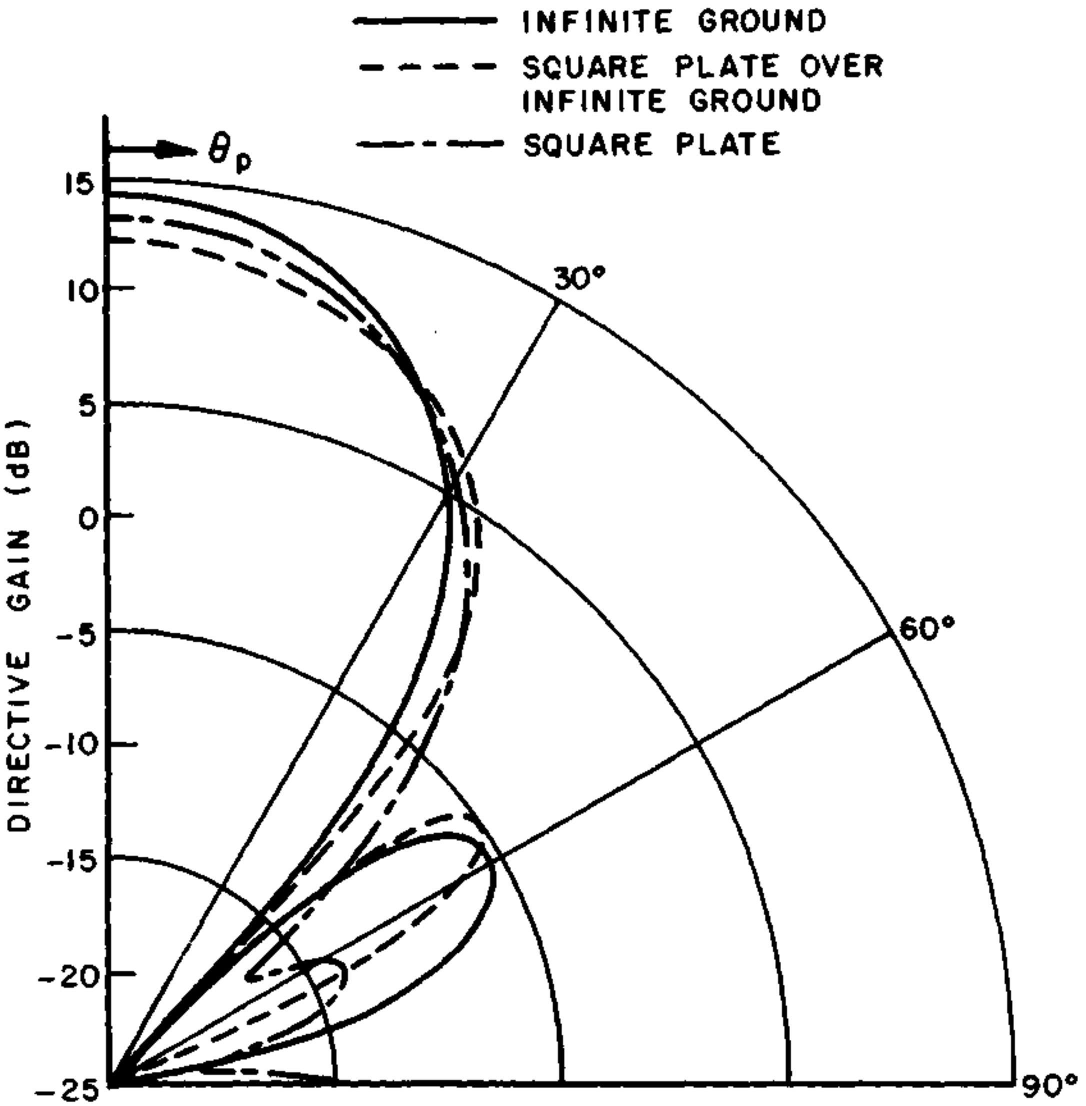

Figure 31a. Comparison of the directive gain of four dipoles over an infinite ground with four dipoles over a square plate over an infinite ground and four dipoles over a square plate alone ($\phi=0^{0}$, vertical polarization).

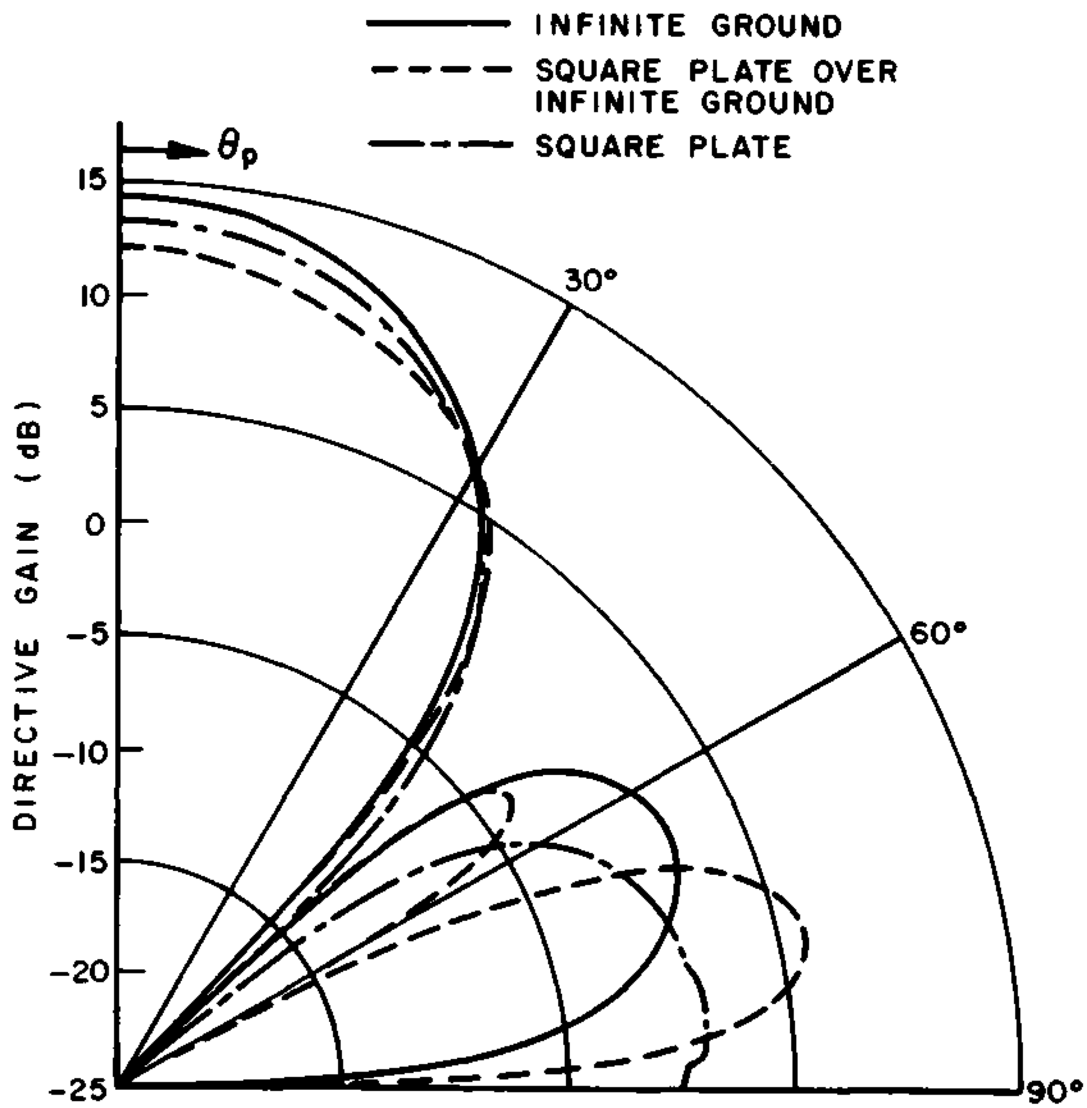

Figure 31b. Comparison of the directive gain of four dipoles over an infinite ground with four dipoles over a square plate over an infinite ground and four dipoles over a square plate alone ($\phi=90°$, horizontal polarization).

Example 8B. Consider the pattern of a set of four electric dipoles in the presence of a square plate over an infinite ground plane as shown in Figure 29. The four dipoles are specified by their analytic representation using the SG: command. This example illustrates the use of the PR: and US: command. The input data is given by

```
CE:    NEC TEST, EXAMPLE 8B.
PD:
0.,0.,90.,0.
F,0.
0,90,1
FR:
0.2998
UN:
3
RG:
150.
GP:
RT:
0.,0.,28.5
0.,0.,90.,0.
PG:
4
25.,-25.,0.
25.,25.,0.
-25.,25.,0.
-25.,-25.,0.
UN:
1
US:
1
PR:
.001535
SG:    SOURCE #1
-.35560,-.35560,.20637
90.,0.,90.,90.
0,0.3048,0.
.005073,82.2
SG:    SOURCE #2
.35560,-.35560,.20637
90.,0.,90.,90.
0,0.3048,0.
.005073,82.2
SG:    SOURCE #3
-.35560,.35560,.20637
90.,0.,90.,90.
0,0.3048,0.
.005073,82.2
SG:    SOURCE #4
.35560,.35560,.20637
90.,0.,90.,90.
0,0.3048,0.
.005073,82.2
XQ:
EN:
```

This example gives approximately the same results as those in Example 8A. The directive gain is within approximately 0.5 dB throughout the entire pattern range. The pattern shape is essentially identical to the one in Figure 30a for the four dipoles over a plate over an infinite ground plane so the pattern is not shown.

Example 9. Consider a combination of three different problems. The first problem is the plate test of Example 1A. The second problem is the cylinder test of Example 4A, and the third example is the plate and cylinder test of Example 6. This example illustrates the use of the NX: command in defining entirely different problems in the same input set. This is a handy example that can be used for the initial start up test for the code on a new computer system, since the plate and cylinder are tested separately and in combination with one another in the same input set. The input data is given by

```
CM:   MULTIPLE TEST EXAMPLE
CE:   PLATE TEST, EXAMPLE 1A.
UN:
3
FR:
8.0
PD:
0.,0.,90.,0.
1,90.
0,180,10
PG:
4
0.,3.5,3.5
0.,-3.5,3.5
0.,-3.5,-3.5
0.,3.5,-3.5
SG:
5.12,0.,0.
0.,0.,90.,0.
0.,.5,0.
1.,0.
XQ:
NX:
CE:   CYLINDER TEST, EXAMPLE 4A.
FR:
9.94
PD:
0.,0.,90.,0.
1,90.
90,270,10
SG:
0.,0.15,0.
90.,0.,180.,0.
0,0.5,0.
1.,0.
CG:
0.1,0.1
```

```
-Ø.11,9Ø.,Ø.11,9Ø.
XQ*
NX*
CE*    PLATE AND CYLINDER TEST, EXAMPLE 6.
PD*
Ø.,Ø.,9Ø.,Ø.
1,9Ø.
9Ø,27Ø,1Ø
UN*
3
FR*
4.
SG*
Ø.,5.625,Ø.
9Ø.,Ø.,Ø.,Ø.
Ø,Ø.566,Ø.Ø
1.,Ø.
PG*
4
5.,Ø.,5.
5.,Ø.,-5.
-5.,Ø.,-5.
-5.,Ø.,5.
RT*
Ø.,12.3125,-Ø.125
Ø.,Ø.,9Ø.,Ø.
CG*
1.25,1.25
-8.5,9Ø.,8.5,9Ø.
XQ*
EN*
```

The line printer output and the graphical representation of the fields for each of the three examples above are given in their respective example sections. The line printer output of the first execution is given in Figure 12 and the plotted output is given in Figure 13a. The line printer output of the second execution is given in Figure 19 and the plotted output is given in Figure 20a. The line printer output of the last execution is given in Figure 25 and the plotted output is given in Figure 26d.

APPENDIX I

The following is a listing of a polar plot subroutine which can be used to generate the polar patterns given in Chapter VI. Note that this code refers to two subroutines "PLOTS" and "PLOT" which must be added by the system or operator. The definitions of these routines are given in the comments associated with the code.

```
      SUBROUTINE POLPLT(ET,RP,IPLT,IPHS,IDM)
C!!!
C!!!  THIS ROUTINE IS USED TO PLOT THE RESULTS IN TERMS OF A
C!!!  POLAR PLOT. THE CALL TO SUBROUTINE "PLOTS" IS USED TO INITIALIZE
C!!!  THE PLOTTER. THE CALLS TO THE SUBROUTINE "PLOT" ARE USED TO
C!!!  DRAW THE DATA AS FOLLOWS:
C!!!
C!!!        CALL PLOT(X,Y,N)
C!!!
C!!!        X,Y=COORDINATES OF THE NEW PLOT POINT.
C!!!
C!!!        N=2     PEN IS DOWN MOVING TO THE NEW POINT.
C!!!        N=3     PEN IS UP MOVING TO THE NEW POINT.
C!!!        N=999   BUFFER USED TO STORE PLOT DATA IS EMPTIED TO PLOTTER
C!!!
C!!!        N<0     IMPLIES ORIGIN SHIFT TO THE NEW POINT.
C!!!        N>0     IMPLIES NO ORIGIN SHIFT AFTER MOVING TO NEW POINT.
C!!!
      COMPLEX ET(IDM)
      DIMENSION IBUF(100)
      DATA PI,TPI,DPR/3.14159265,6.2831853,57.29577958/
      EMX=0.
      DO 101 IP=0,360,IPHS
      I=IP+1
      EM=CABS(ET(I))
      IF(EM.GT.EMX) EMX=EM
 101  CONTINUE
      CALL PLOTS(IBUF,100,3)
      CALL PLOT(4.25,5.5,-3)
C *** POLAR GRID ***
      DO 110 I=1,4
      RG=RP*I/4.
      CALL PLOT(RG,0.,3)
      DO 110 J=0,360,2
      ANG=J/DPR
      XX=RG*COS(ANG)
      YY=RG*SIN(ANG)
 110  CALL PLOT(XX,YY,2)
      DO 112 I=1,6
```

```
      ANG=(I-1)*PI/6.
      ANGS=ANG+PI
      ANGF=ANG
      IF(I.EQ.2*(I/2)) GO TO 111
      ANGS=ANG
      ANGF=ANG+PI
  111 CONTINUE
      XX=RP*COS(ANGS)
      YY=RP*SIN(ANGS)
      CALL PLOT(XX,YY,3)
      XX=RP*COS(ANGF)
      YY=RP*SIN(ANGF)
  112 CALL PLOT(XX,YY,2)
C *** PATTERN PLOT ***
      DO 120 IP=0,360,IPHS
      I=IP+1
      ETM=CABS(ET(I))/EMX
      IF(IPLT-2) 121,122,123
  121 RD=RP*ETM
      GO TO 125
  122 RD=RP*ETM*ETM
      GO TO 125
  123 IF(ETM.LT.0.01) ETM=0.01
      RD=20.*ALOG10(ETM)
      IF(RD.LT.-40.) RD=-40.
      RD=RP*(RD+40.)/40.
  125 CONTINUE
      ANG=IP/DPR
      XX=RD*SIN(ANG)
      YY=RD*COS(ANG)
      IPEN=2
      IF(I.EQ.1) IPEN=3
  120 CALL PLOT(XX,YY,IPEN)
      CALL PLOT(4.25,-5.5,-3)
  130 CONTINUE
      CALL PLOT(0.,0.,999)
      RETURN
      END
```

REFERENCES

1. R. J. Marhefka, "Analysis of Aircraft Wing-Mounted Antenna Patterns," Report 2902-25, June 1976, The Ohio State University ElectroScience Laboratory, Department of Electrical Engineering; prepared under Grant No. NGL 36-008-138 for National Aeronautics and Space Administration.

2. W. D. Burnside, M. C. Gilreath, R. J. Marhefka, and C. L. Yu, "A Study of KC-135 Aircraft Antenna Patterns," IEEE Trans. on Antennas and Propagation, Vol. AP-23, No. 3, May 1975, pp. 309-316.

3. C. L. Yu, W. D. Burnside and M. C. Gilreath, "Volumetric Pattern Analysis of Airborne Antennas," IEEE Trans. on Antennas and Propagation, Vol. AP-26, No. 5, September 1978, pp. 636-641.

4. R. G. Kouyoumjian and P. H. Pathak, "A Uniform Geometrical Theory of Diffraction for an Edge in a Perfectly-Conducting Surface," Proc. IEEE, Vol. 62, November 1974, pp. 1448-1461.

5. R. G. Kouyoumjian, "The Geometrical Theory of Diffraction and Its Applications," Numerical and Asymptotic Techniques in Electromagnetics, edited by R. Mittra, Spring-Verlag, New York, 1975.

6. P. H. Pathak, W. D. Burnside and R. J. Marhefka, "A Uniform GTD Analysis of the Diffraction of Electromagnetic Waves by a Smooth Convex Surface," submitted for publication to IEEE Trans. on Antennas and Propagation. (Also Report 784583-4, April 1979, The Ohio State University ElectroScience Laboratory, Department of Electrical Engineering; prepared under Contract No. N62269-76-C-0554 for Naval Air Development Center.

7. G. J. Burke and A. J. Poggio, "Numerical Electromagnetic Code (NEC) - Method of Moments," NOSC/TD 116, July 1977, Naval Ocean Systems Center, San Diego, California 92152.

8. F. W. Schmidt and R. J. Marhefka, "Numerical Electromagnetic Code (NEC) - Basic Scattering Code, Part II: Code Manual," Report 784508-14, September 1979, The Ohio State University ElectroScience Laboratory, Department of Electrical Engineering; prepared under Contract No. N00123-76-C-1371 for Naval Regional Procurement Office.

9. C. H. Walter, Traveling Wave Antennas, Dover Publications, Inc., New York, 1979, pp. 15-16.

10. J. D. Kraus, Antennas, McGraw Hill Book Company, Inc., New York, 1950, pp. 464-477.

11. H. Bach, "Pattern Measurements of High Frequency Satellite-Mounted Antennas," Electromagnetic Institute, Technical University of Denmark, R154, January 1976.

ATE
LMED
8